Dana et al. *Swiss Journal of Geosciences* (2023) 116:18
https://doi.org/10.1186/s00015-023-00445-0

SGG SGS sc | nat
Swiss Journal of Geosciences

ORIGINAL PAPER Open Access

Structural and metamorphic evolution of a subducted passive margin: insights from the Briançonnais nappes of the Western Alps (Ubaye–Maira valleys, France–Italy)

Davide Dana[1], Salvatore Iaccarino[1*], Stefan M. Schmid[2], Alessandro Petroccia[1] and André Michard[3]

Abstract

This contribution analyses the structural architecture and tectono-metamorphic evolution of Briançonnais units in the southern French-Italian Western Alps. The studied area extends from a virtually non-metamorphic area adjacent to the Helvetic-Dauphinois External Domain in the west to the Monviso-Queyras ocean-derived units in the east, where metamorphism increases up to eclogite-facies. Mapping at the scale 1:10.000 of a mountainous part of the Ubaye-Maira transect was performed, which portrays in detail the Briançonnais units over ~ 100 km^2. The lithologies include meta-andesite, meta-siliciclastics, marbles, turbiditic calcschists and flysch whose age spans from Late Carboniferous to Eocene. Metamorphism is low-grade greenschist-facies in the west but reaches the blueschist-facies to the east. Structures related to four phases of deformation are identified. The first two generations of structures (D1–D2), related to the original top-to-the-west nappe stacking, are associated with conditions close to the peak of Alpine metamorphism. Previous tectonic surfaces are transposed by the dominant deformation structures (D3), developed under retrograde/decompression conditions. This D3 corresponds to a backfolding and back-thrusting event with a top-to-the-E transport. A fourth phase (D4) developed during late low-grade metamorphic conditions and deforms the previous surfaces by locally developing a crenulation cleavage, followed by brittle tectonics. An updated metamorphic map is presented, backed on published estimates and new thermometric data obtained by Raman Spectroscopy of Carbonaceous Material (RSCM). The T_{RSCM} values range from ~ 295 °C to > 350 °C, moving from the most external Briançonnais unit to the internal Queyras "Schistes Lustrés" units. Suspected Upper Cretaceous palaeofaults have been documented, allowing us to group the classic Aiguille de Mary and Ceillac (sub-) units into a single tectonic unit, here referred to as Maurin unit. The palaeogeographical reconstruction of the evolution of the studied transect highlights the importance of the Marinet and Maurin axial units in the feeding of the Late Cretaceous-Eocene breccias deposited on the more internal Acceglio-type units.

Keywords Western Alps, Briançonnais, Passive margin, Structural analysis, HP-LT metamorphism, RSCM, Exhumation, Backthrusting

Editorial handling: Jean-Luc Epard

*Correspondence:
Salvatore Iaccarino
salvatore.iaccarino@unito.it
Full list of author information is available at the end of the article

1 Introduction

The Western Alps (Fig. 1a), formed by a stack of oceanic and continental units derived from the European and Adriatic plates (Schmid et al., 2004; Handy et al., 2010; Pfiffner, 2014). The close association of ophiolites and continent-derived units, and the widespread occurrence of high pressure (HP)–low temperature (LT) metamorphism, including ultra-high-pressure (UHP) metamorphism in continental slices (Chopin; 1984; Goffé and Chopin, 1986), make the Western Alps one of the most studied sectors of the Alps. They provide a natural laboratory for understanding processes related to subduction and mountain building. The Briançonnais units, widespread in the axial zone of the Western Alps (Debelmas & Kerckhove, 1980; Sartori et al., 2006; Bergomi et al., 2017), derive from the Briançonnais terrane or microcontinent that in the Jurassic formed the distal margin of Europe toward the Piemonte-Liguria Ocean (Lemoine et al., 1986). In Early Cretaceous times, the Briançonnais micro-continent became separated from Europe by the opening of the narrow Valais Ocean (Frisch, 1979; Stampfli, 1993; Schmid et al., 2004; Loprieno et al., 2011). During the Late Cretaceous-Paleogene, Africa-Europe convergence triggered the subduction of the Piemonte-Ligurian lithosphere and of the European distal margin. In the northern part of the Western Alps, the Briançonnais-derived internal units largely consist of basement and cover nappes, such as the Great St. Bernard nappe system (e.g., Thélin et al., 1993; Pantet et al., 2020). In the southern parts of the Western Alps a multitude of often small tectonic units or "nappes", dominantly consisting of detached Permian to Cenozoic cover slices, forms the external parts of the Briançonnais-derived units (Fig. 1b), whereas large basement complexes such as the Dora-Maira and Gran Paradiso massifs, dominantly consisting of upper crustal basement slices, form the internal parts (Tricart, 1980; Platt et al., 1989; Schmid et al., 2017; Michard et al., 2022). The Classic Briançonnais units of the southern Western Alps were extensively studied in the 1950s–80s (e.g., Debelmas, 1955; Gidon, 1958; Galli, 1964; Barféty, 1965; Gaillet, 1976; Lefèvre, 1982; Deville, 1987), while subsequently they were only the subject of occasional studies (e.g., Schwartz et al., 2000; Michard et al., 2004, 2022; Dumont et al., 2022). The available literature on these units mainly focused on their stratigraphy, whereas only few studies provided an up-to-date analysis of their structural architecture and tectono-metamorphic evolution.

In order to fill this gap, we undertook the study of the Aiguille de Chambeyron-Denti di Maniglia massif, a high-elevation area of the Ubaye–Maira transect in the French-Italian border area (red box in Fig. 1b). The area includes all types of Briançonnais units cropping out between the internal ocean-derived Queyras Schistes Lustrés and the external Helminthoid Flysch units (Figs. 1b, 2; Kerckove et al., 1984; Michard et al., 2004). Our major aim is to present new structural observations at different scales and geothermometry results based on the Raman Spectroscopy of Carbonaceous Material (RSCM), accompanied by a new geological-structural map at the scale of 1: 15,000 of the Aiguille de Chambeyron massif (Additional file 1). Our new data combined with those from literature allow us to discuss both the structural evolution and initial paleogeographic relationships between Briançonnais-derived and ocean-derived units, highlighting their common subduction-exhumation dynamics.

2 Geological setting

2.1 Overall structure of the South-Western Alps

The Western Alps (Fig. 1a) embrace several paleogeographic-tectonic domains going from west to east, i.e., from the external of the orogenic arc towards its interior (Dal Piaz et al., 2003; Dal Piaz, 2010; Schmid et al., 2004; Handy et al., 2010; Steck et al., 2015). The external Helvetic–Dauphinois–Provençal tectonic units derive from the proximal part of the former European passive margin. These include pre-Mesozoic basement rocks exposed in the External Crystalline Massifs (Pelvoux and Argentera in the south Western Alps, Fig. 1b) and a largely detached and folded Permo-Triassic to Neogene cover (Dumont et al., 2012; Bellahsen et al., 2014). There, Alpine metamorphism only reaches sub-greenschist to greenschist facies conditions (Bousquet et al., 2008), dated from c. 35–30 Ma to 17–10 Ma (Lemoine et al., 2000; Bellanger et al., 2014). The more internal, so-called Penninic units include the classic Briançonnais units derived from the distal European s.l. margin, and the ophiolite-bearing "Schistes Lustrés" units, derived from the Piemonte-Liguria branch of Alpine Tethys (Escher et al., 1988; Handy et al., 2010). An out-of-sequence thrust of early Oligocene age (34–31 Ma), the Penninic Front (Ceriani et al., 2001; Simon-Labric et al., 2009; Schmid et al., 2017), separates the hanging-wall Subbriançonnais and Briançonnais units from those of the Helvetic–Dauphinois domain in the footwall. In the Embrunais–Ubaye and Maritimes Alps the footwall of this out-of-sequence thrust also embraces slices detached at the end of the Eocene from the Subbriançonnais and Briançonnais domains and overlying oceanic non-metamorphic Helminthoid Flysch Units (Fig. 1b). Part of the Penninic Front was reactivated as an extensional fault during the Pliocene (Bilau et al., 2021) or even earlier (Sue & Tricart, 2003).

According to current paleogeographical reconstructions, the Briançonnais s.l. paleogeographic domain (grouping together Briançonnais s.s., Pre-Piemonte and

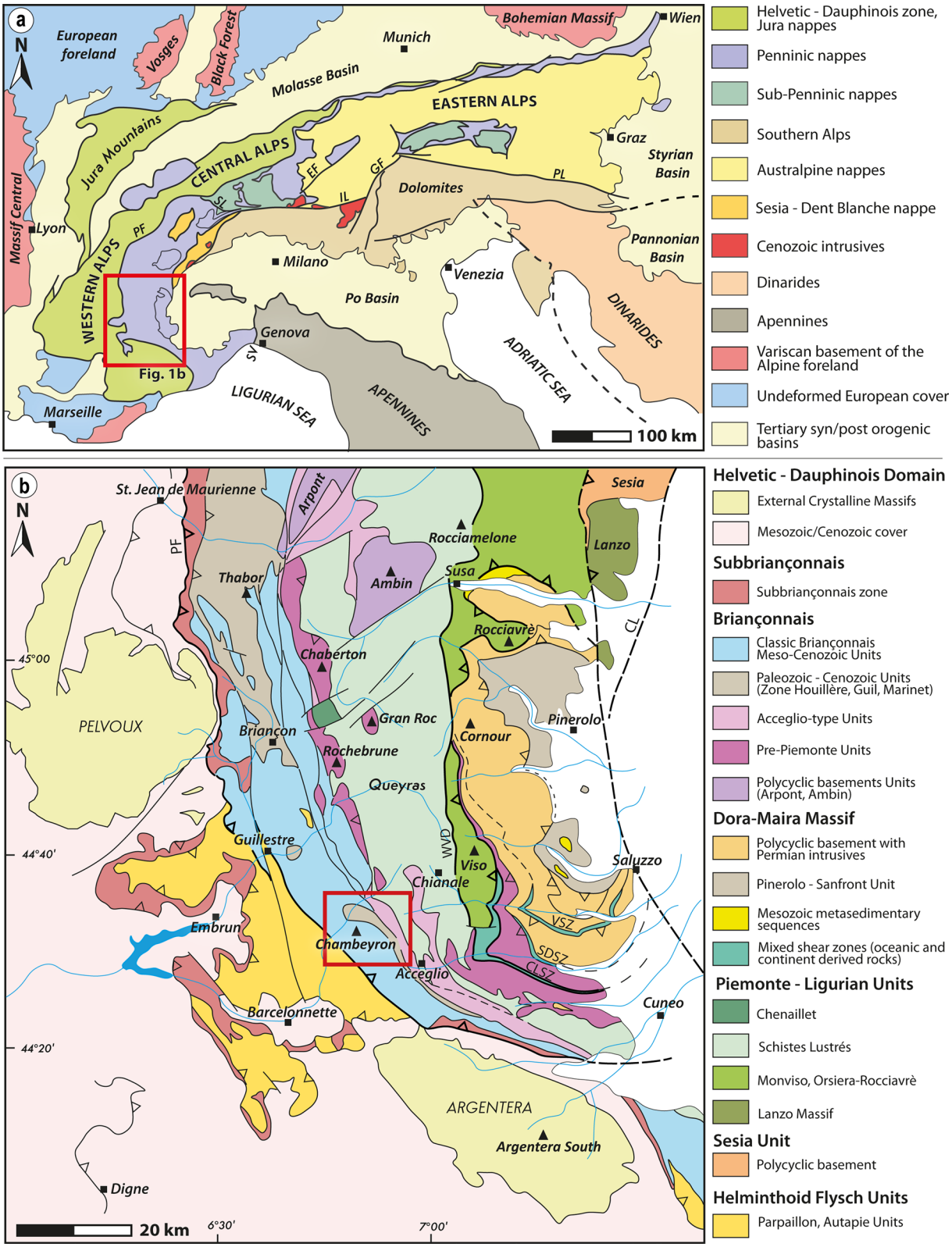

Fig. 1 **a** Tectonic map of the Alps (modified after Schmid et al., 2004). *EF* Engadine Fault, *IL* Insubric Line, *GF* Giudicarie Fault, *PF* Penninic Front, *PL* Periadriatic Line, *SL* Rhône–Simplon Line, *SV* Sestri-Voltaggio line. **b** Tectonic map of the South-Western Alps (modified after Ballèvre et al., 2020 and Michard et al., 2022). Framed: Study area (Fig. 3). *CLSZ* Cima Lubin Shear Zone, *SDSZ* San Damiano Shear Zone, *VSZ* Valmala Shear Zone, *WVD* West Viso Detachment, *PF* Penninic Front. Red box indicates the study area

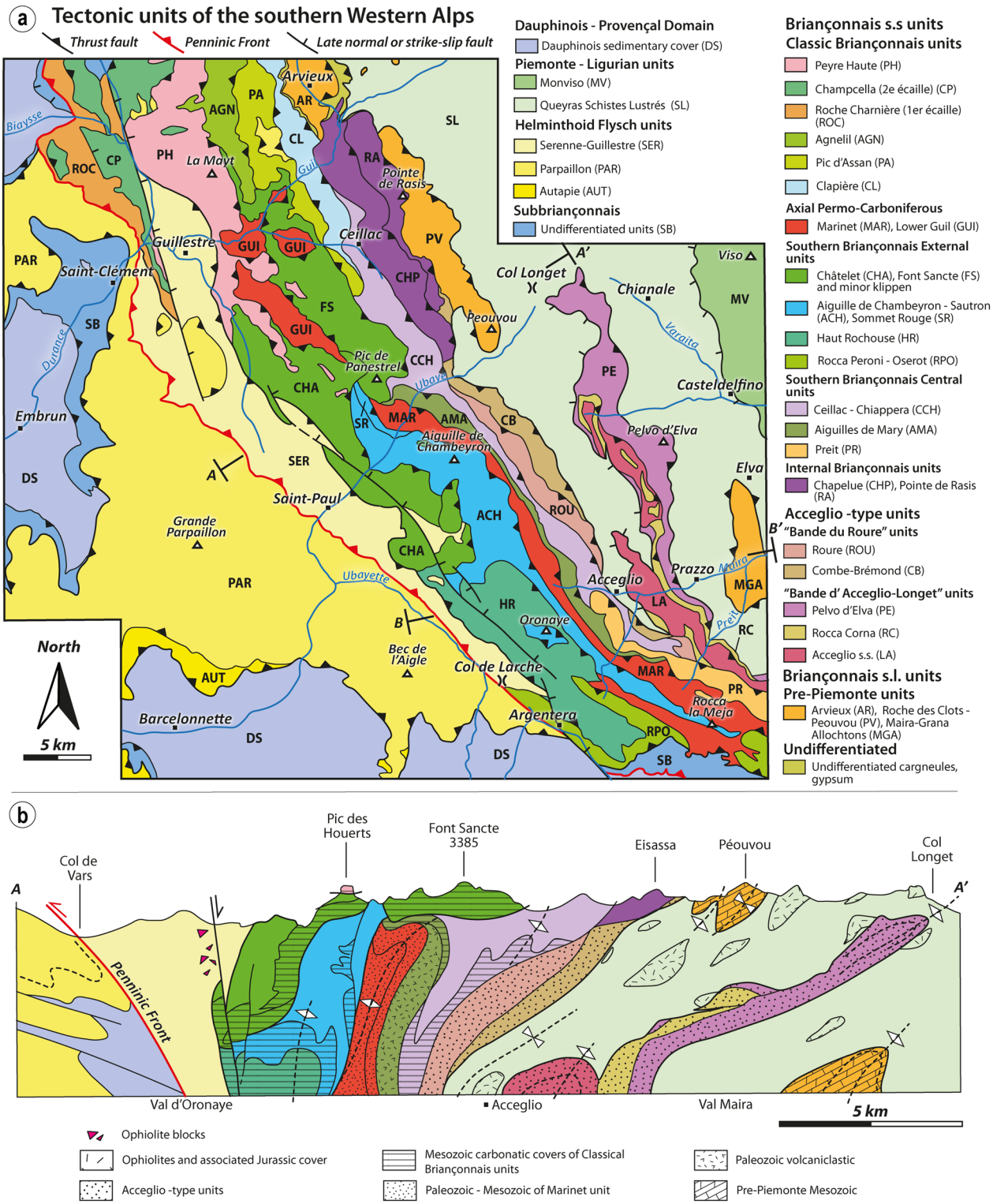

Fig. 2 **a** Compilation of the main tectonic units of the southern French–Italian Alps based on Debelmas & Lemoine (1966); Malaroda et al. (1970); Tricart (1980); Gidon et al., (1994, 1977); Barféty et al. (1995); Claudel (1999); Michard et al., (2004, 2022); Kerckhove et al. (2005). The main features of some of the tectonic units are given in Table 1. Further details are found in Additional file 2. **b** Schematic cross-section of the Ubaye-Maira transect along the NW side of the Ubaye valley, i.e. located immediately north of our working area (modified after Michard et al., 2004). For the location of cross section and related legend see a. Note that the deeper parts of the profile A–A′ were obtained by axial projection of structures cropping out near the surface along the B–B′ profile in **a**

Dora-Maira) had a thinned continental crust loosely connected with the Iberia microplate (Stampfli, 1993; Van Hinsbergen et al., 2020). Before the Alpine orogeny, the thinned crust domain was located between the partially oceanic, Early Cretaceous Valais-Subbriançonnais basin (Escher et al., 1988; Schmid et al., 2004; Loprieno et al., 2011; Beltrando et al., 2012) and the major branch of Alpine Tethys, the Jurassic-Cretaceous Piemonte–Liguria Ocean (Lemoine et al., 1986; Lagabrielle & Cannat, 1990; Agard, 2021). The Briançonnais s.l. domain was shortened and accreted to the proximal European paleomargin during the construction of the orogenic wedge by the end of the Eocene (Frisch, 1979; Tricart, 1980, 1984; Schmid & Kissling, 2000; Handy et al., 2010; Michard et al., 2004).

The outer tectonic units derived from the Briançonnais s.l. form the classic Briançonnais units largely composed of Late Paleozoic and Mesozoic sequences (Fig. 1b). Their northern equivalents are found in the Zone Houillère and the basement-cover nappes of the Grand Saint Bernard Nappe System (Thélin et al., 1993; Sartori et al., 2006, Pantet et al., 2020; Scheiber et al., 2013). Alpine metamorphic peak conditions in these units vary from lower greenschist facies in the most external parts to upper blueschist-facies in the more internal units (Oberhänsli et al., 2004; Bousquet et al., 2008; Lanari et al., 2012).

The most internal tectonic units, derived from the Briançonnais paleomargin form the so-called "Internal Crystalline Massifs", namely the Dora-Maira Massif in the south (Fig. 1b) and the Gran Paradiso and Monte Rosa massifs further north. They consist of basement-dominated units exposed as tectonic windows beneath the ocean-derived units. Since a long time (e.g., Franchi, 1898; Michard, 1967, his fig. C) they are considered to derive from the pre-Triassic basement of the Briançonnais s.l. domain (Ballèvre et al., 2018, 2020; Michard et al., 2022). The lowest, monocyclic units of the Dora-Maira Massif and Gran-Paradiso, the Pinerolo–Sanfront unit and the Money unit, respectively, share many features with the Zone Houillère (Feys, 1954) of the classic Briançonnais (Vialon, 1966); they underwent blueschist-facies Alpine metamorphism (Ballèvre et al., 2018, 2020; Manzotti et al., 2016). The Pinerolo–Sanfront unit is overlain by polycyclic basement and monocyclic orthogneiss units exhibiting Alpine peak metamorphism in eclogite-facies (Vialon, 1966; Borghi et al., 1984; Sandrone et al., 1993; Henry et al., 1993). Two of these units, the Brossasco-Isasca unit (Chopin, 1984) and the Chasteiran unit (Manzotti et al., 2022), in the Dora–Maira Massif have been affected by ultra-high-pressure (UHP) Alpine metamorphism.

The Piemonte–Ligurian Units (Fig. 1b) derive from the main branch of Alpine Tethys and can be subdivided into three different groups (Agard, 2021). The most internal tectonic units, namely the Monviso (Agard et al., 2001; Angiboust et al., 2012; Locatelli et al., 2018) and Orsiera-Rocciavré (Seyrig, 1972; Pognante, 1979) units, exhibit peak metamorphism in eclogite-facies locally with UHP conditions (Gilio et al., 2020; Ghignone et al., 2023). Their equivalents further north are the Zermatt-Saas-type units. The second group, the Queyras Schistes Lustrés, are in a more external tectonic position (Herviou et al., 2022; Schwartz et al., 2007) and characterized by blueschist-facies Alpine metamorphism (Agard, 2021). Their equivalents further north are the Tsaté- (or Combin)-type units (Marthaler & Stampfli, 1989). At the top of the nappe pile, the Chenaillet unit (e.g., Cordey & Bailly, 2007; Manatschal et al., 2011) represents a large ophiolite klippe overlying the Schistes Lustrés units. This unit was regarded as lacking significant Alpine metamorphism, but recent findings of Corno et al. (2023) challenge this view. According to Schmid et al. (2017), the Chenaillet unit klippe occupied an upper plate position in an intra-oceanic subduction settings, together with the early-detached, non-metamorphic Helminthoid Flysch Units (Fig. 1b), mainly consisting of Upper Cretaceous–Paleocene turbidites (Kerckhove, 1969; Kerckhove et al., 1984; Stampfli et al., 1998; Schmid et al., 2017).

The Piemonte-Liguria Ocean was limited to the southeast by the Adria microplate (Handy et al., 2010; van Hinsbergen et al., 2014, 2020), the "African promontory" of Argand (1924). Tectonic units that were part of the Adria paleo-margin are not outcropping in the south Western Alps. The last remnants of the Southern Alps that wedge out southwestward are seen in the strongly tectonized Canavese area located NE of the area of Fig. 1b (Beltrando et al., 2015). However, geophysical evidence clearly shows that the Ivrea geophysical body, representing lower crust and mantle of the Adria plate, is present in the subsurface of the westernmost Po Plain, forming the backbone of the Western Alps (Schmid et al., 2017). The Sesia-Dent Blanche units, wedging out southward in the NE corner of Fig. 1b, are often attributed to the Austroalpine because of their Adria-derived protolith affinity. However, they cannot be considered part of the Austroalpine s.s. since these high-pressure units occupy a lower plate position and are part of the Alpine wedge (Schmid et al., 2004). Thus, the Sesia-Dent Blanche units are regarded as Adria derived extensional allochthons recording blueschist to eclogite-facies Alpine metamorphism (Manzotti et al., 2014, 2018) dated at c. 85–75 Ma (Engi et al., 2018).

2.2 The Briançonnais s.str. and Pre-Piemonte units in the South-Western Alps

From the 50 s'up to the last decades, several authors investigated the numerous, small, and dismembered

Briançonnais units in the southern French-Italian Alps, highlighting their stratigraphic and structural settings (e.g., Debelmas, 1955; Gidon, 1958; Galli, 1964; Barféty, 1965; Lefèvre; 1982; Gaillet, 1976; Leblanc, 1962; Michard & Henry, 1988; Claudel, 1999; Schwartz et al., 2000; Michard et al., 2004). The resulting picture is that of a highly complex system of stacked and re-folded tectonic slices (or nappes) which often can be followed only over short distances along strike (Fig. 2). The main characteristics that define the various units are summarized in Table 1. Details on the stratigraphy, tectonics and along strike correlations of these units are given in the Additional file 2.

Two types of Briançonnais s.str. units (Fig. 2; Table 1) are currently described, the Classic Briançonnais units and the Acceglio-type units. The Pre-Piemonte units that crop out at the eastern border of the latter constitute a third type of units derived from the Briançonnais paleogeographic domain (e.g., Lemoine et al., 1986; Michard et al., 2022). The Classic Briançonnais units are characterized by hundreds of meters thick Triassic carbonate, whereas the Acceglio-type units (also referred to as "Ecailles intermédiaires" or "Ultrabriançonnais") are characterized by the complete or nearly complete absence of Triassic carbonates, generally due to their Jurassic sub-aerial erosion experienced during the Pangea rifting. Other stratigraphical gaps resulted from a Late Cretaceous to Paleocene phase of extension. Middle to early Upper Jurassic beds unconformably overlie the partially eroded Triassic carbonates in the Classic Briançonnais units, and the Lower Triassic (*Werfenian*) quartzites or Upper Permian polygenic conglomeratic quartzites (Verrucano facies) in the Acceglio-type units (Debelmas & Lemoine, 1957; Lemoine, 1960, 1961; Lefèvre & Michard, 1976). Acceglio-type units derive from Early–Middle Jurassic paleogeographical highs, drowned and topped by chaotic breccias during the Late Cretaceous, generally located in a more internal position with respect to the Classic Briançonnais units. The Pre-Piemonte units occur next to and usually east of the Acceglio-type units, hence closer to the Piemonte-Liguria (Schistes Lustrés) units. This accounts for their traditional name (Ellenberger, 1958; Lemoine, 1961, 1964). Their stratigraphy is more basinal than that of the Classic Briançonnais (Michard, 1967; Dumont et al., 1984; Michard et al., 2022, their Fig. 2). Pre-Piemonte units are characterized by thick Middle-Upper Triassic carbonates followed by abundant syn-rift series consisting of chaotic and bedded carbonate breccias, partly dated by Sinemurian and Pliensbachian ammonites (e.g., Michard, 1967). Upper Jurassic and possibly Cretaceous deep-sea deposits are present in the Pre-Piemonte Rochebrune unit southeast of Briançon (Dumont et al., 1984). In terms of paleogeography, we group these units, together with the Acceglio-type units and the Internal Crystalline Massifs (Sect. 2.1), under the heading of "Briançonnais distal margin" (Michard et al., 2022). Accordingly, the paleogeographic setting of the Classic Briançonnais units s.str. is that of the "Briançonnais proximal margin".

3 Study area, methodology and sampling locations

3.1 The mapped area

The Aiguille de Chambeyron–Denti di Maniglia massif (Fig. 3 and Additional file 1) culminates at 3412 m. a.s.l. south of the High Ubaye valley (France) and above the headwaters of the Maira and Varaita rivers (Italy). The highest and westernmost unit of the sector is the Sérenne-Guillestre unit defined by Kerckhove et al. (2005), representing the internal most part of the Helminthoid Flysch Units. The unit dominantly consists of typical lithologies of the "Complexe de base" of the Helminthoid flysch (Kerckhove, 1969), namely black shales and flysch-type shaly series (Late Cretaceous), locally with ophiolitic blocks (Kerckhove, 1969; Kerckhove et al., 2005). In contrast to the major part of the Helminthoid units (Autapie and Parpaillon nappes), emplaced onto the external Dauphinois zone (Merle & Brun, 1984) and hence presently located in the footwall of the Penninic Front, the Sérenne-Guillestre unit represents that portion of the Helminthoid Flysch units which is still located in the hangingwall of the Penninic Front (Fig. 2). Therefore, it is affected by back-folding and backthrusting together with the underlying Briançonnais units (Kerckhove et al., 2005). The emplacement of the Sérenne-Guillestre unit took place during middle to latest Eocene times by top-to-the-northwest movement over Briançonnais, Subbriançonnais and Dauphinois units, as proposed by Merle and Brun (1984) during an early stage of gravitational emplacement of the Parpaillon nappe.

Beneath the Sérenne-Guillestre unit lies the Châtelet unit, the structurally highest and outermost Briançonnais unit in the area, which is a composite nappe consisting of the Châtelet unit s. str. on the one hand and three subunits representing klippen of the same unit further east (Brec de Chambeyron, Aiguille Grande, Pas de Chillol) on the other hand, as well as the Font Sancte subunit found north of the Ubaye, outside of our study area (Figs. 2, 3; Michard and Henry, 1988; Gidon et al., 1994; Kerckhove et al., 2005). Slightly northwest of our study area, the Ubaye valley natural cross-section shows the Châtelet unit backthrust towards the NE and above a SW-dipping nappe stack that includes, from SW to NE, the Aiguille de Chambeyron-Sautron unit, the anticlinally folded Marinet unit, the Aiguilles de Mary and Ceillac-Chiappera units for more than 7 km (Michard &

Table 1 List of units derived from the Briançonnais s.l. paleogeographical domain in the SW Alps (see Figs. 2, 3), including their equivalents in the Guil transect located further north (second column)

Ubaye-Maira transect	Guil transect equivalent	Pre-rift succession	Post-rift succession	Relative tectonic position
ACH Aiguille de Chambeyron–Sautron	–	Middle Triassic carbonates	UJ locally reduced, UC "calcschist" + breccias, Flysch noir	FW = Haut Rochouse, Marinet HW = Châtelet
AMA Aiguilles de Mary	–	Permian, Lower Triassic, Middle–Upper Triassic carbonates and breccia	UC "calcschist" + breccia, Flysch noir	FW = Marinet HW = Ceillac–Chiappera
CB Combe-Brémond (Acceglio type)	–	Permian, Strongly reduced Lower Triassic, Anisian–Ladinian	UJ sandy marble, UC–PC breccia and chlorite marbles	FW = Schistes Lustrés HW = Roure, Chapelue, Pointe de Rasis
CCH Ceillac–Chiappera	CCH Ceillac–Chiappera -	Middle–Upper Triassic carbonates and breccia	Middle–Upper Jurassic limestone, UC "calcschists", Flysch noir	FW = Roure, Chapelue, Combe-Brémond
CHA Châtelet sensu stricto	–	Middle–Upper Triassic carbonate and breccia	Middle–Upper Jurassic limestones, UC "calcschist", Flysch noir	FW = Aiguille de Chambeyron–Sautron HW = Font Sancte, Peyre Haute
CHP Chapelue	CHP Chapelue	Permian, Lower Triassic quartzite, Middle Triassic carbonates	–	FW = Pointe de Rasis, Combe-Brémond HW = Roure, Ceillac–Chiappera, Clapiere
–	CL Clapière	Norian dolostone	UJ limestone, UC calcschist	FW = Ceillac–Chiappera, Chapelue, Arvieux HW = Pic d'Assan
FS Font–Sancte	FS Font–Sancte	Middle–Upper Triassic carbonates and breccia	Middle–Upper Jurassic limestones, UC "calcschists", Flysch noir	FW = Marinet, Aiguilles de Mary, Ceillac -Chiappera, Pic d'Assan, Agnelil, Guil HW = Peyre Haute
HR Haut Rochouse	–	Permian (rhyol. or conglom.), Lower Triassic quartzites, Middle–Upper Triassic carbonates and breccia	Middle–Upper Jurassic limestones, UC "calcschists" Flysch noir	FW = Rocca Peroni–Oserot HW = Aiguillle de Chambeyron–Sautron
MAR Marinet	GUI Nappe inférieure du Guil	Upper Carbonif. (?)-Permian (andesites or conglom.), Lower Triassic quartzite, strongly eroded Triassic carbonate	UJ reduced/lacking, UC + breccia, Flysch noir	FW = ? HW = Font-Sancte
–	PA Pic d'Assan	Middle Triassic carbonates	UJ limestones, UC "calcschists", Flysch noir	FW = Font Sancte HW = Agnelil
PH Peyre Haute (minor klippen)	PH Peyre Haute	Carnian with gypsum and Norian « Hauptdolomit» dolostone	UJ limestones UC "calcschists" Flysch noir	FW = Guil, Font Sancte–Châtelet, Agnelil, Roche Charnière, Champcella HW = ?
–	RA Pointe da Rasis	Middle Triassic dolostones	UJ limestones, UC "calcschists" Flysch noir	FW = Roche des Clots–Péouvou HW = Chapelue
ROU Roure (Acceglio type)	–	Permian conglom., Lower Triassic quartzite	–	FW = Combe-Brémond HW = Ceillac–Chiappera
RPO Rocca Peroni–Oserot	–	Permian rhyol., Lower Triassic quartzite, Middle Triassic carbonates	MJ limestones, UC "calcschists" + breccia, Flysch noir (locally)	FW = Subbriançonnais HW = Haut Rochouse

The list is alphabetically ordered using acronyms as in Fig. 2. Note that syn-rift Rhaetian-Hettangian argillaceous limestone and breccia are present only in the Peyre-Haute unit (not listed in this table). Such syn-rift sediments are also found in the Pre-Piemonte units outside the area of Fig. 3 (Michard et al., 2022). The Cretaceous-Paleocene, pelagic detrital "calcschists" are often labeled "marbres en plaquettes". Additional information is given in Additional file 2.

PC Paleocene, *UC* Upper Cretaceous to lower Paleogene, *UJ* Upper Jurassic, *MJ* Middle Jurassic, *FW/HW* footwall/hanging-wall units.

Henry, 1988, their Fig. 3). In the present work, the latter two units are regarded as sub-units of a single Maurin unit (see Sect. 4.1.3).

The Châtelet, Aiguille de Chambeyron-Sautron, Marinet and Maurin units belong to the Classic Briançonnais. They are separated by the Ceillac backthrust from a pair of Acceglio-type units, the Roure and Combe-Brémond units (Fig. 3). These units form the most internal part of the "Briançonnais Fan" *auctoris*, being backthrusted onto the Queyras Schistes Lustrés. Their internal folding is consistent with their position at the southwestern limb of a synclinorium cored by the Schistes Lustrés and whose northeastern limb is exposed in the Acceglio-Longet band (Fig. 2; Michard et al., 2022, their Fig. 6).

3.2 Methods and sampling

A geological map at the scale of 1:15,000 (Additional file 1) was realized starting from new surveys at the scale of 1:10,000, and where needed, 1:5,000. To map the Quaternary formations and less accessible locations, the interpretation of satellite images was used. Structural orientation data were collected using both digital instruments and traditional compass; they were organized in a database and used to construct the geological map in a GIS environment. In the map we adopted the use of the Geological Map of Italy project guidelines (ISPRA, 2022). For the definition of the main formations adopted in the geological map, we relied on Gidon et al. (1994), although with modifications that are discussed in Sect. 6.

Approximately 50 oriented samples were collected for both microtectonic studies and characterization of metamorphic grade based on mineral assemblages (Additional file 3: Table S1). Microtectonic analyses of 32 samples were particularly crucial for inferring the kinematics along the tectonic contacts (Fig. 3, cross-section A, B). We applied Raman Spectroscopy of Carbonaceous Material (Beyssac et al., 2002a, b; Lahfid et al., 2010) to estimate the maximum temperatures ($Tmax = T_{RSCM}$) of metamorphism for 18 samples selected according to their richness in carbonaceous material (see sub-Sect. 5.2).

4 Structural analysis

4.1 Large-scale structure of the tectono-stratigraphic units

The overall structure of the study area has been presented above (Sect. 3.1; Fig. 3). In the following, the Briançonnais tectono-stratigraphic units, their mutual contacts and major structural elements are presented at the outcrop scale.

4.1.1 External units

The external Châtelet and Aiguille de Chambeyron–Sautron units consist of Triassic–Eocene formations detached along Lower Triassic evaporites (Fig. 4). Their stratigraphy differs from the Carnian upward. In the Châtelet unit, Carnian dolomitic meta-breccias are followed by Middle-Upper Jurassic dark marbles and Upper Cretaceous-Paleocene, more or less clastic calcschists, the so-called "marbres en plaquettes". In the Aiguille de Chambeyron–Sautron unit, Middle Triassic carbonates are unconformably overlain by the "Marbres de Guillestre", i.e. Oxfordian-Kimmeridgian nodular marbles that show a reduced thickness. The thickness of the "marbres en plaquettes" in this unit apparently exceeds 500 m, likely due to tectonic doubling, but nevertheless contrasting with their restricted thickness (c. 50 m) in the Châtelet unit. In the Aiguille de Chambeyron–Sautron unit Kerckhove et al. (2005) have noted the local unconformity of the "marbres en plaquettes" over the Triassic rocks; this was observed north of the mapped area in a tectonic slice referred to as the Sommet Rouge subunit (Michard & Henry, 1988). The top of the stratigraphic sequence of both these external Briançonnais units is made up of "Flysch noir" turbidites (Bartonian to early Priabonian; Barféty et al., 1992; Kerckhove et al., 2005) outside of the studied area.

4.1.2 Backthrust klippes derived from the Châtelet unit

The Brec de Chambeyron (BREC) and the Aiguille Grande (AG) klippes overlie the Aiguille de Chambeyron–Sautron unit, while the Pas de Chillol (PDC) klippe overlies the Aiguille de Mary subunit. All three testify to the intense backthrusting event along flat-lying thrust fault (Fig. 3, and Additional file 1). Except for the BREC klippe, which presents a complete Middle Triassic–Paleocene stratigraphic sequence comparable to that of the Châtelet unit, the remaining two are erosional remnants entirely composed of Middle Triassic dolomitic marbles. They are correlated with the Châtelet unit only according to their tectonic position and their similar low-grade metamorphic evolution (Sect. 5.).

(See figure on next page.)

Fig. 3 Tectonic sketch map (**a**) and structural profile (**b**) of the study area based on this work (see detail geological map in Additional file 1) and modifying Gidon et al. (1994); Michard et al. (2004) and Kerckhove et al. (2005). The black stars indicate the observation points of Figs. 6 and 7. *φBRE* Brec de Chambeyron basal thrust, *φHOU* Col des Houerts fault/backthrust, *φCHI* Chillol thrust, *φCEI* Ceillac fault/backthrust, *φCDC* Colle di Ciabriera backthrust, *φSL* Schistes Lustrés thrust, *BREC* Brec de Chambeyron klippe, *AG* Aiguille Grande klippe, *PDC* Pas de Chillol klippe, *BDT* Bassa di Terrarossa klippe

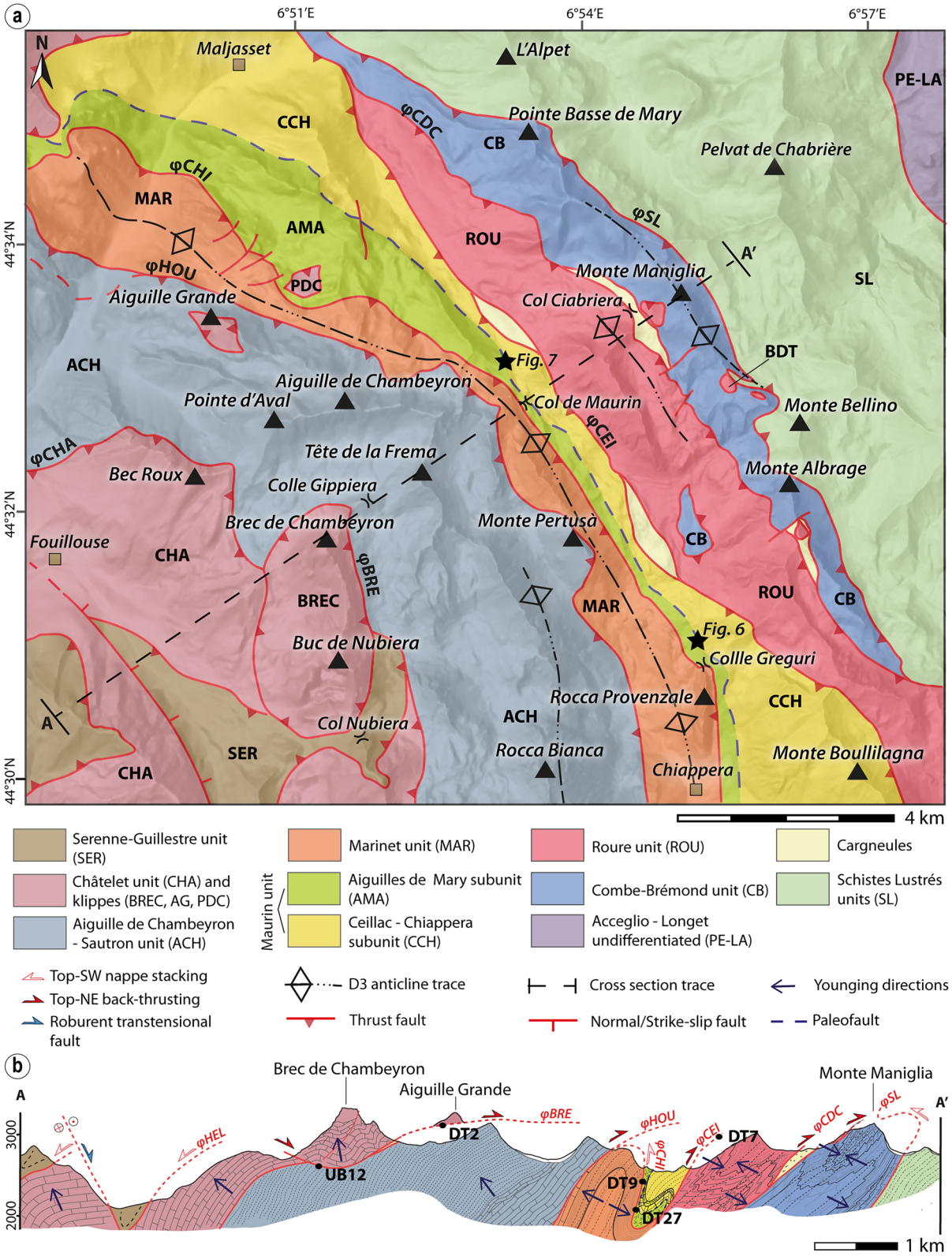

Fig. 3 (See legend on previous page.)

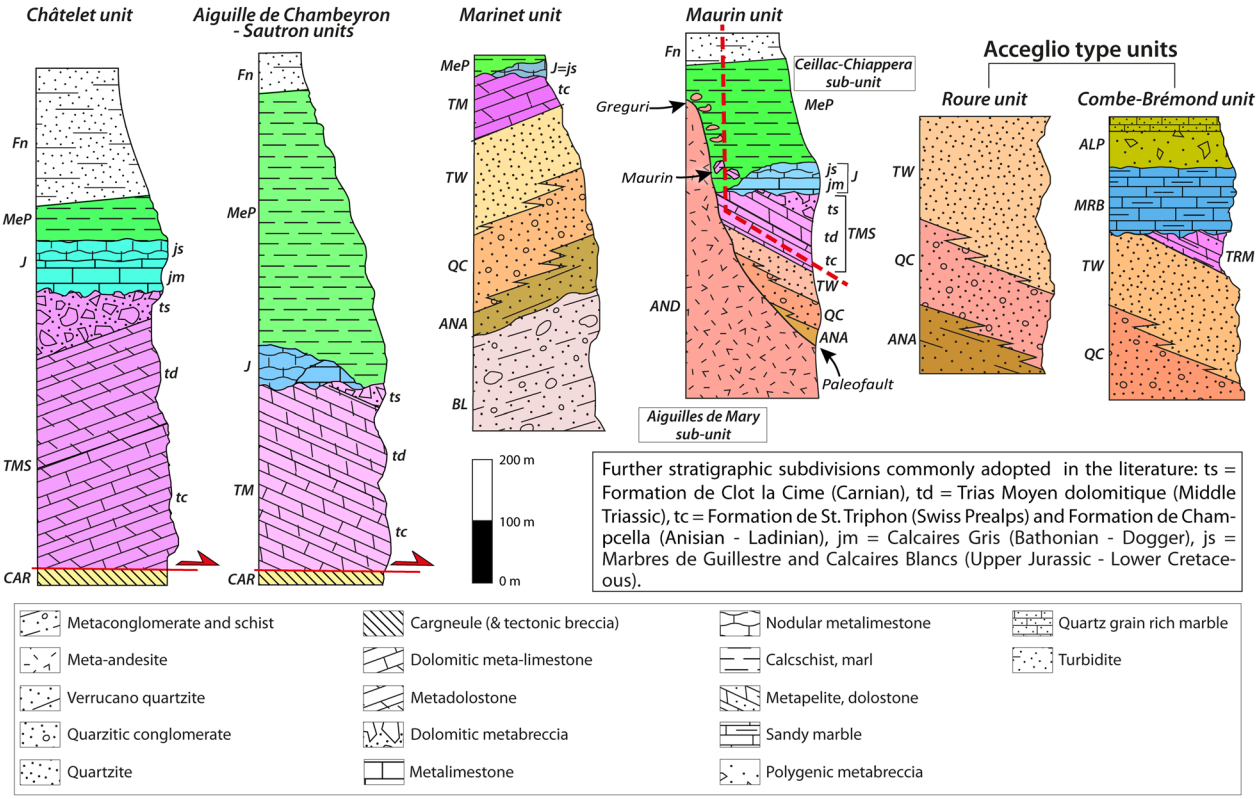

Fig. 4 Stratigraphic columns of the studied units. Colors as in the geological map (Additional file 1). Stratigraphy of the individual units are based on Michard & Henry (1988) and Gidon et al. (1994), except for the Maurin unit defined in this work. The latter combines the former Aiguilles de Mary and Ceillac-Chiappera units, now labeled sub-units. See text for details. *Fn* "Flysch noir" (Lutetian ?—early Priabonian); *ALP* Série de la Bergerie de l'Alpet (Upper Cretaceous–lower Paleogene); *MeP* "marbres en plaquettes" (detrital calcschist, Upper Cretaceous–lower Paleogene), *MRB* Sandy marble (Upper Jurassic-Cretaceous), *Jm/Js* Middle-Upper Jurassic marble, *TMS* Middle-Upper Triassic dolomitic marbles, breccia and dolostone; *TM* Middle Triassic dolostone and dolomitic marbles, *TRM* metapelite and dolostone (Anisian-Ladinian ?), *CAR* cargneule and tectonic breccia; *TW* tabular quartzite (Lower Triassic "Werfenian"), *QC* Quarzitic conglomerate (Lower Triassic–Upper Permian), *ANA* "Verrucano" quartzite (Upper Permian), *AND* meta-volcanite, mainly andesite (Permian), *BL* meta-conglomerate and schist (Upper Carboniferous ?)

From a structural point of view the AG klippe is affected by a west facing fold truncated at the base by the D3 backthrust, in the footwall a series of complicated superposed folds part of the Aiguille de Chambeyron–Sautron unit are observed. In contrast, the PDC klippe internal structure is difficult to understand due to the intense brittle fracturing observed in the outcrops.

The BREC klippe is affected by a west-verging major fold truncated by the basal thrust contact, as can be observed south of this klippe (Col Nubiera area). There, the klippe is separated from the Aiguille de Chambeyron–Sautron unit by a few meters of cargneule and breccia, and, a sliver of dark reddish pelite typical for the Sérenne-Guillestre unit (Fig. 5a). At the base of the Ladinian marbles of the klippe, an increase in strain intensity is observed, indicating a fault zone. Macroscopically, no clear ductile kinematic indicators were observed along the contact. However, calcite steps and slickensides are observed, consistent with a markedly brittle component of top-to-the-NE kinematics. This observation points to late-stage backthrust emplacement of the BREC klippe. A Cretaceous paleofault has been recognized in the southern part of the BREC klippe (J.P. Bouillin, personal comm., 2022), near the Buc de Nubiera peak (Fig. 5b). Along this paleoscarp, it is possible to recognize paleokarst imprints in the Upper Jurassic marbles, filled by Upper Cretaceous-Paleocene "marbres en plaquettes" with Jurassic blocks.

4.1.3 The Marinet unit and the newly defined Maurin unit

The Marinet and Maurin units are the axial units of the "Briançonnais Fan" (Fig. 3b). Both are characterized by siliciclastic deposits of Carboniferous to Early Triassic age and quite restricted Middle Triassic-Jurassic deposits (Fig. 4). The Col des Houerts thrust fault is a first-order tectonic boundary between the two external units and the underlying central units. This contact, often highlighted by cargneules, reveals top-to-the-NE

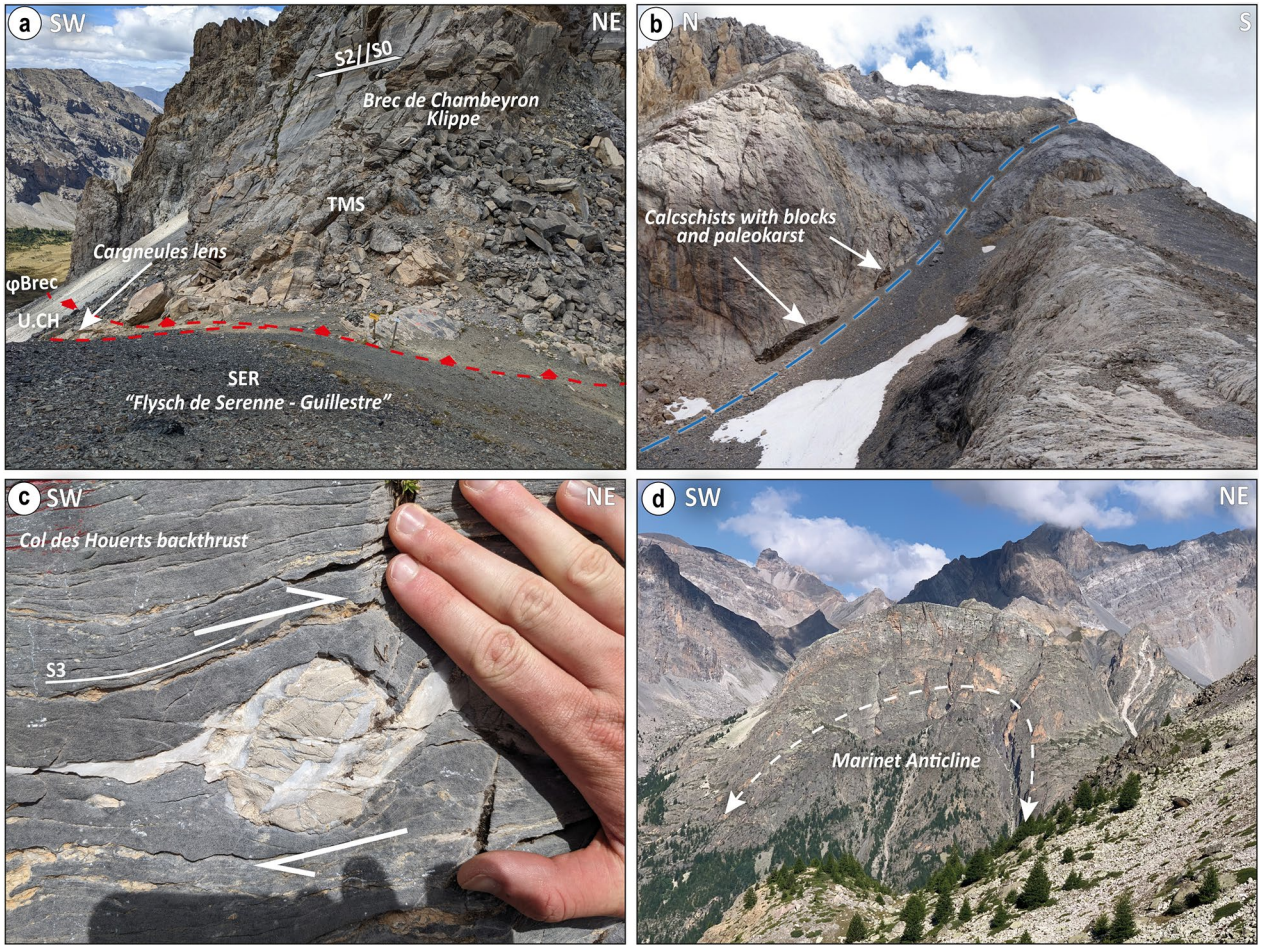

Fig. 5 **a** Relationships between Sérenne-Guillestre unit and Brec de Chambeyron klippe at Col Nubiera (Fig. 3, 44°30′22.0″N 6°51′33.5″E); **b** Paleofault trace (blue line dipping N) in the Brec de Chambeyron klippe (courtesy of J.P Bouillin, 2022); Upper Cretaceous to early Paleogene calcschists including Jurassic blocks marks the fault scarp; **c** Ductile kinematic indicator (dolostone delta porphyroclast) indicating top-to-NE sense of shear along the Col des Houerts backthrust calc-mylonites, developed in Triassic marble; **d** Natural cross-section of the Marinet anticline as seen from the southern slope of the Ubaye valley. The high cliffs and peaks in the background belong to the Châtelet-Font-Sancte nappe. *SER* Flysch de Serenne-Guillestre, *TMS* Middle–Upper Triassic limestone, *φBrec* Brec de Chambeyron thrust

backthrust kinematics in calc-mylonites (Fig. 5c), and it carries the Aiguille de Chambeyron-Sautron unit above the Marinet unit. The latter is folded into a tight, northeastward-reclined anticline, bounded to the northeast by the Chillol thrust (Fig. 3b). The Upper Carboniferous (?) "Conglomérats de la Blachière" (Gidon, 1958; Gidon et al., 1994) are grey-greenish quartzitic metaconglomerates similar to those described in the Zone Houillère. They are followed upward by wine-colored arenaceous schist, probably deriving from volcanoclastites, and by a thick, Permian–Lower Triassic siliciclastic sequence. Rare carbonate cover relicts are observed mainly in the Italian (SE) part of the Marinet unit, involving 10–50 m-thick Middle Triassic, a few meters of Upper Jurassic nodular marbles and 10–15 m of Upper Cretaceous-Paleocene "marbres en plaquettes".

The Marinet unit is structurally overlain by the "Aiguilles de Mary unit" of Michard & Henry (1988), hereafter defined as sub-unit of the Maurin unit, through the Chillol thrust (Fig. 3), which is folded around the Marinet anticline (Fig. 5d). No clear kinematic indicators along the Chillol thrust were observed in the field. However, thin sections of oriented samples (DT9, DT27) taken along this contact reveal original top-to-the-SW sense of shear (see sub-Sect. 4.3.2). Thus, the Aiguilles de Mary sub-unit was anticlinally folded together with the Marinet unit during top-NE backfolding.

Based on new field data, we define the Maurin unit (Fig. 4) by grouping together the Classic Aiguilles de Mary and Ceillac-Chiappera sub-units (Gidon, 1962; Michard & Henry, 1988; Gidon et al., 1994). The Aiguilles de Mary (AMA) sub-unit, made of an Upper Permian to Eocene sequence (Fig. 4) is characterized by thick meta-andesites (Lonchampt, 1962). Meta-volcanites are followed by Permian siliciclastic formations and by a relatively thin carbonate cover (Middle Triassic–lower Paleogene). The thin carbonate cover includes Upper Triassic (Carnian) dolomitic meta-breccia directly in contact with few meters of "marbres en plaquettes" (Upper Cretaceous–lower Paleogene). On the northern side of the Ubaye valley, at the Tête du Sanglier, west of our study area, the Flysch noir overlies c. 10 m of "marbres en plaquettes", which in turn onlap onto 2 m of Triassic meta-limestone of Aiguilles de Mary unit (AMA) (Gidon et al., 1994).

Further northeast, the Ceillac–Chiappera (CCH) subunit (Fig. 4), in contrast to the other axial units, is detached along a sole of cargneules (Gidon et al., 1994) at the base of the Middle Triassic marbles and Carnian (?) dolomitic breccias. Thin (c. 30–40 m) Middle and Upper Jurassic marbles locally overlie the Triassic sequence. They are in turn topped by up to 200 m-thick "marbres en plaquettes". The alleged boundary between the Ceillac-Chiappera and Aiguilles de Mary subunits is frequently represented by a band of "marbres en plaquettes", which seems common to both subunits, or by a direct supposedly tectonic contact of the Permian meta-volcanics of the Aiguille de Mary subunit with the "calcschists" of the Ceillac-Chiappera subunit. In the following we describe two key outcrop areas suggesting that the "marbres en plaquettes" belong to one and the same tectonic unit, sealing a paleo-fault and hence either transgressing Permian andesites (footwall of the paleo-fault) or Triassic–Jurassic beds (hanging-wall of the paleo-faults, Fig. 4).

Near Colle Greguri pass (SE part of Figs. 3 and 6a) the contact between andesites (formerly AMA unit) and underlying "marbres en plaquettes" (formerly CCH) turned out to be an overturned stratigraphical contact since we observed a thin layer of reworked andesitic material interbedded within the calcschist formation in the contact area (Fig. 6b, c). In places arenitic layers of andesite detritus are monomineralic and mimic meta-andesites. Under the microscope, the detrital material typically consists of feldspar and altered mafic minerals within a calcite-rich matrix. Hence this is an overturned unconformable contact between metavolcanic basement and transgressing "marbres en plaquettes" rather than an Alpine tectonic thrust. The entire Triassic-Jurassic sequence originally covering the andesites was omitted during normal faulting and the "marbres en plaquettes" directly seal a paeofault scarp. Close to the Mt. Eighier summit (Fig. 6a) the same band of detrital calcschists stratigraphically overlies Jurassic beds in a normal position (Fig. 6a, d). A syncline is hosted here in the calcschists overlying the zone of imbrication near the Ceillac Fault (Fig. 6d).

In addition, systematic occurrences of Triassic dolomitic clasts, embedded within the basal part of the "marbres en plaquettes", were observed near the Col de Maurin Pass (Fig. 3). Thus, a Late Cretaceous paleofault scarp has been inferred there, formerly juxtaposing detrital calcschist over the Permian meta-andesites (Fig. 7). This paleofault was overturned during the backfolding event, now mimicking an Alpine backthrust.

In the cliffs visible to the west from the pass (Fig. 7a), "marbres en plaquettes" are in direct stratigraphic contact with various Permian to Triassic strata of the Aiguilles de Mary subunit (Fig. 4). The contact between these various formations of the Aiguilles de Mary subunit with the "marbres en plaquettes" was formerly interpreted as a thrust, juxtaposing the Aiguilles de Mary subunit above the "marbres en plaquettes" attributed to the Ceillac-Chiappera subunit. As shown in Fig. 7 we interpret this contact as a Late Cretaceous normal-sense fault that became overturned during D3, based on the following observations:

i. At Col de Maurin, the calcschist formation not only contains detrital beds similar to those described from the Colle Greguri outcrops, but also larger blocks and clasts of dolostone (Fig. 7c, d), which attests for reworking of fragmented Triassic outcrops during the Late Cretaceous-lower Paleogene (cf. Lemoine, 1961);
ii. In the northwestern parts of the cliffs shown in Fig. 7a, i.e., close to Col de Maurin (Fig. 3), the now steeply southwest-dipping contact between the Late Cretaceous "marbres en plaquettes" and the Middle Triassic carbonates, Lower Triassic and Permian quartzites and meta-arkoses is interpreted as the paleofault whose upper part formed a submarine scarp and was the source of the reworked clasts (dolostone and quartz grains).

It is worth noting that Gidon et al. (1994) also admitted a possible stratigraphic contact between the "marbres en plaquettes" and meta-andesites along the Col de Maurin pass, judging such a situation to be exceptional in the Briançonnais domain. In summary, these observations support the idea of a single Maurin Alpine tectonic unit, that we subdivide into two subunits separated by an important paleofault.

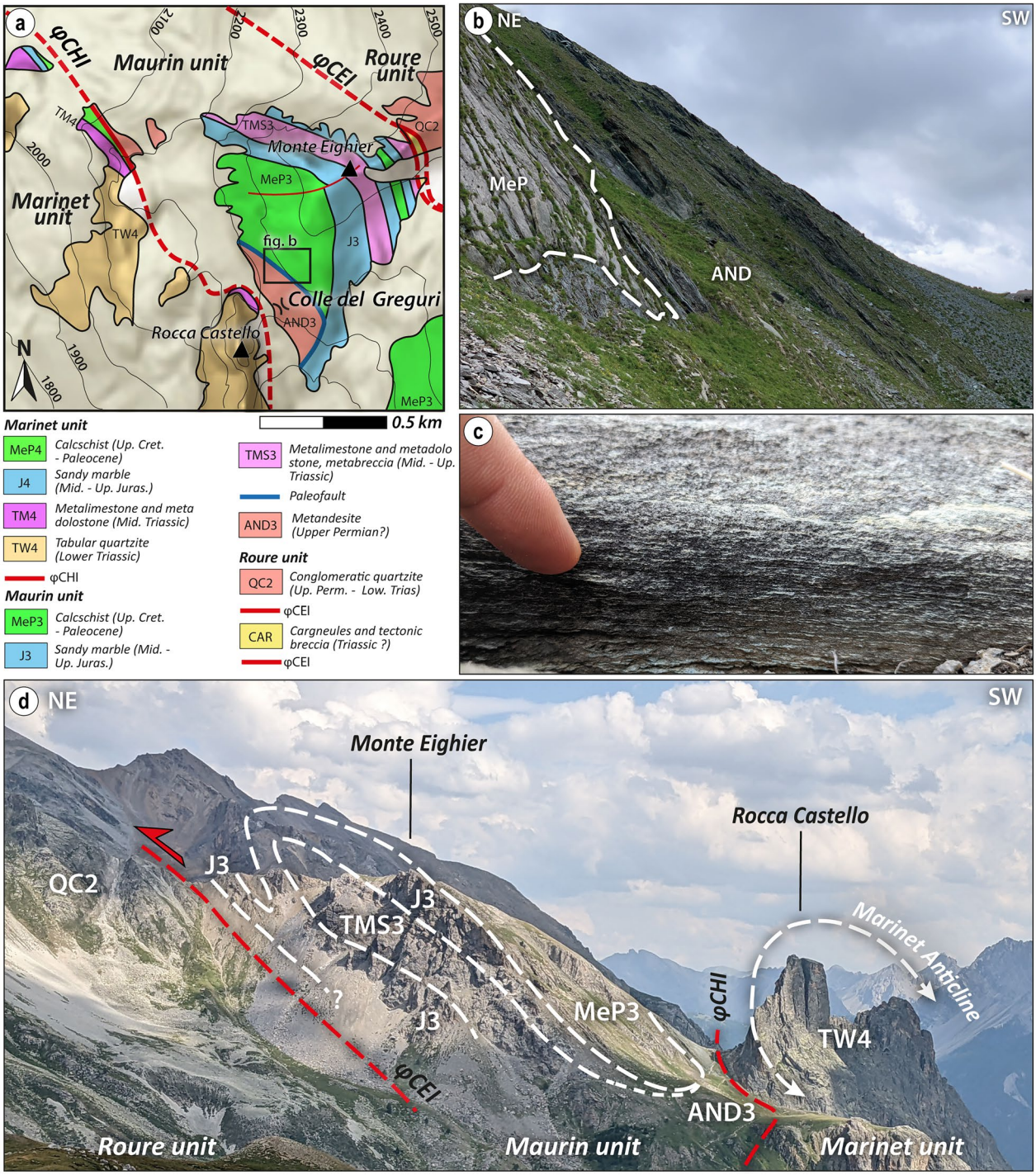

Fig. 6 Colle Greguri outcrop. **a** Simplified geological map; **b** View of the contact between metandesite (AND) and "Marbres en Plaquettes" (MeP) calcschist, note the interbedding of thin layers of limestone (white) and andesitic sand (dark) at the overturned base of the "Marbres en Plaquettes"; **c** Fine lamination between andesite layers and calcite layers, in a distal turbidite, at the base of "Marbres en Plaquettes". View is orthogonal to the layering; **d** Panorama on Colle Greguri and Rocca Castello–Provenzale group from Col de Maurin. The main stratigraphic and tectonic contacts are traced to highlight the syncline in the "marbres en plaquettes" calcschist. *MeP* "marbres en plaquettes" calcschist (Upper Cretaceous—early Paleogene), *J* Jurassic Marble, *TMS* Middle–Upper Triassic meta-limestone and meta-dolostone, *TW* Tabular quartzite (Lower Triassic), *QC2* conglomeratic quartzite (Roure unit); *AND* metavolcanite/metandesite (Upper Permian), *φCEI* = Ceillac backthrust

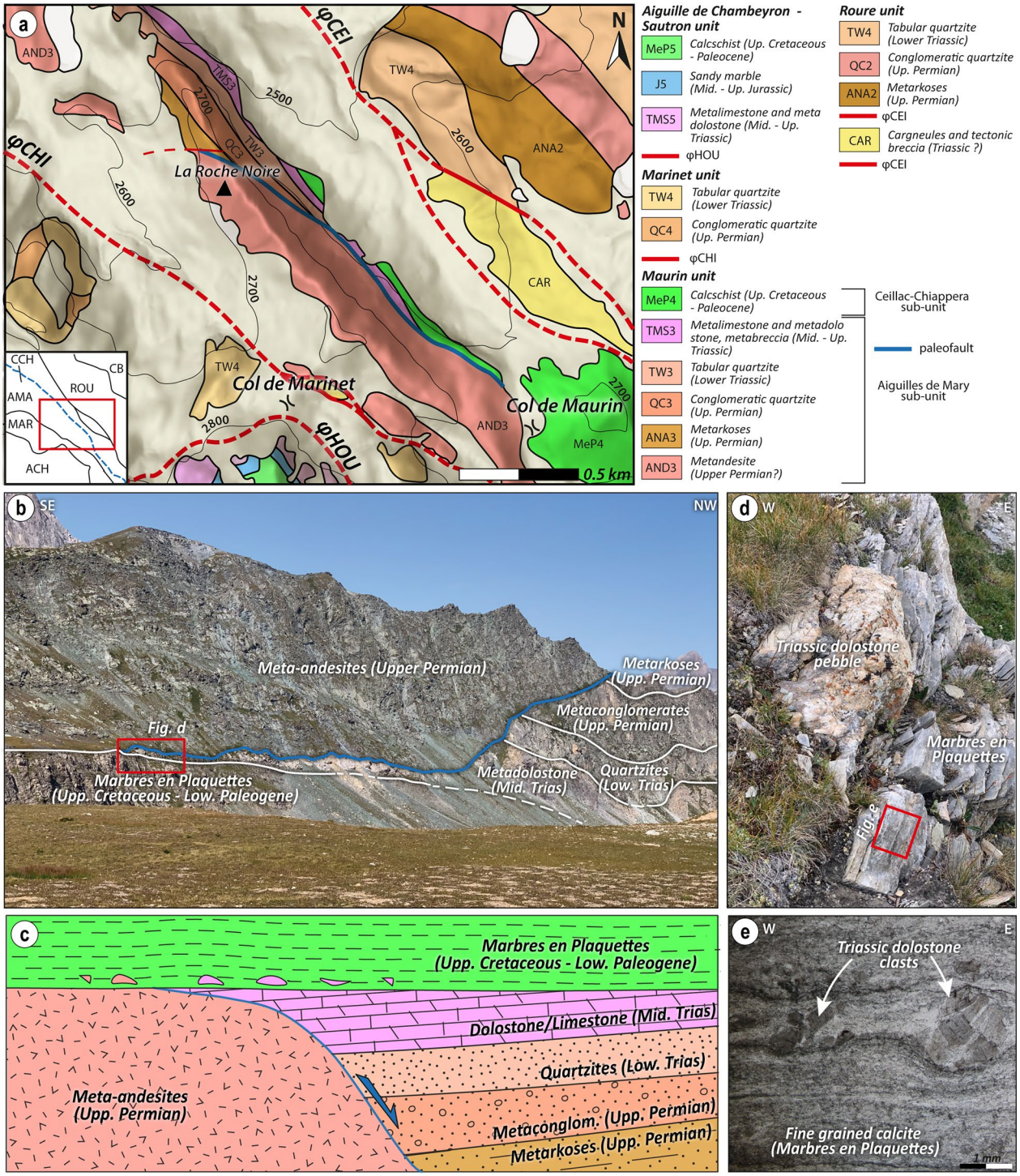

Fig. 7 Col de Maurin outcrops. **a** Simplified geological map of the Col de Maurin area (see Additional file 1); **b** Interpreted panorama, blue line marks the trace of a suspected paleofault interpreted to be located between the steeply SW-dipping and overturned Permian meta-andesite (AMA sub-unit) and younger formations (CCH sub-unit); **c** Proposed schematic reconstruction of the original tectono-stratigraphic setting by simple rotation of the overturned sequence seen in Fig. 7a including the suspected Late Cretaceous fault, into an upright position; **d** Triassic dolostone pebbles and clasts the stratigraphic base of the "*marbres en plaquettes*" (see b for the location of this outcrop), **e** micrograph showing dolostone clasts embedded in the fine grained calcite and detrital quartz matrix of the Upper Cretaceous–Paleocene "*marbres en plaquettes*"

The Ceillac backthrust (ϕCEI, Fig. 3), at the base of the Maurin unit, marks the boundary of the Classic Briançonnais backthrust over the paleogeographically more internal Acceglio-type units. This tectonic contact is marked by cargneules and tectonic breccias or by an increase of strain within the sheared rocks near the contact. No clear kinematic indicators were observed at the mesoscale. However, at the microscopic scale, calc-mylonites close to the contact (e.g., DT7) indicate backthrusting kinematics (Sect. 4.3.2).

4.1.4 Acceglio-type units

These particular types of Briançonnais units are, from top to bottom, the Roure and Combe-Brémond units, separated from each other by the Col de Ciabriera backthrust (Fig. 3). Along this SW-dipping fault, cargneule and tectonic breccias are observed. Mesoscale duplexes in the adjacent quartzites are compatible with a top-to-NE sense of shear.

The Roure unit only consists of Permian siliciclastic sequences and Lower Triassic bedded quartzites. In the Combe-Brémond unit, some Middle Triassic metadolostones with interbedded metapelites are locally preserved beneath the unconformable Upper Jurassic marbles (Fig. 4). Detrital Late Cretaceous-Paleocene chlorite calcschists ("marbres chloriteux") overlie through phosphatic hard-grounds the Jurassic marbles (Debelmas and Lemoine, 1957; Le Guernic, 1967). Furthermore, south of Ubaye River, the Combe-Brémond inverted stratigraphic sequence ends with the "Série de la Bergerie de l'Alpet" (Le Guernic, 1966), which mainly consists of polygenic metabreccias whose reworked elements vary in size from millimeters to tens of meters (olistoliths). The lithologies of the reworked blocks is that of the formations of the Classic Briançonnais. Upward the breccia is followed by gray, quartz rich marbles (Fig. 4). Sometimes the strongly metamorphosed breccia is rich enough in sand-sized clasts of quartzite, micaschist and/or metavolcanics to mimic a micaschist of the basement (Permian?). Such lithologies were commonly labeled "*Permien reconstitué*" ("restored Permian") by Lemoine (1967). Their breccia nature can be deciphered as soon as scattered dolostone clasts also appear in the outcrops. An Upper Cretaceous–Eocene age has been proposed by Le Guernic (1966) for this series. Olistolithic breccia formations associated with detrital calcschists are well known in the Western Alps and are regarded as a common feature of the Acceglio-type units (Dumont et al., 2022; Michard et al., 2022).

Some outcrops of Combe-Brémond Upper Jurassic marble are observed in the Maurin valley (Additional file 1). We noted that these outcrops are sandwiched between *Verrucano-type* conglomeratic quartzites of the Roure unit at the roof and bedded fine-grained quartzite (*Werfenian*) belonging to the Combe-Brémond unit at their base. A tectonic contact, probably the deeper part of the Col de Ciabriera backthrust (ϕCDC), separates these marbles from the structurally higher Roure unit. This can be seen in a small marble outcrop that forms a tectonic window of the Combe-Brémond unit within the Roure unit (Fig. 3, south-west of Monte Albrage). Further to the east, the older tectonic contact between the Combe-Brémond and the underlying ophiolite bearing Queyras Schistes Lustrés units is folded together with the two juxtaposed units in the southwestern limb of a large post-nappe synclinorium of Schistes Lustrés linking the Acceglio-type units of our working area with the Acceglio-Longet units (Michard et al., 2022, their Fig. 6).

4.2 Macro- and mesoscale structures and phases of deformation

Structures referred to four phases of deformation (D1–D2–D3–D4) were recognized, whereby the D3 structures, related to backfolding and backthrusting, are the dominant at the meso- and regional scale. Figure 8 shows a summary stereonet diagram for each of the structural elements described below.

The S1 foliations represent the very rarely preserved records of the D1 phase, transposing the original S0 bedding. In turn, S1 also appears as a folded surface in rarely preserved F2 isoclinal folds (Fig. 9a) formed during the D2 phase. Where D2 is associated with a S2 crenulation cleavage, records of S1 are also seen within microlithons. It is often unclear whether D1 should be considered as a stand-alone event or, more likely, as the beginning stage of progressive deformation, culminating in D2. In most places the D2 phase is associated with a S2 foliation that is axial-planar to F2 folds completely transposing the previous S1 foliation (Fig. 8a). The F2 folds generally have an isoclinal to very tight geometry and their axes are reoriented by the later F3 folds forming a great circle distribution (Fig. 8b). Based on large scale considerations (Michard et al., 2022) we associate the formation of F2 folds with original nappe stacking during older westward thrusting, developed under ductile conditions as highlighted by some kinematic indicators at the microscale preserved along tectonic contacts (e.g., Aiguille Grande basal thrust and Chillol thrust). Low-strain domains can occasionally be observed where relics of the pre-D3 deformation phases are preserved in competent lithologies. An exceptional case is represented by metric F2 folds (Fig. 9b) in the Vallon de Chillol (Additional file 1), located in the hinge zone of the D3 Marinet Anticline. In the D3 folds of Monte Pertusà (Fig. 3) the folded S2 is clearly seen as a crenulation cleavage with relicts of S1 in the microlithons (Fig. 9c, d). However, in the majority of outcrops it is difficult to clearly distinguish between S1 and S2 foliations.

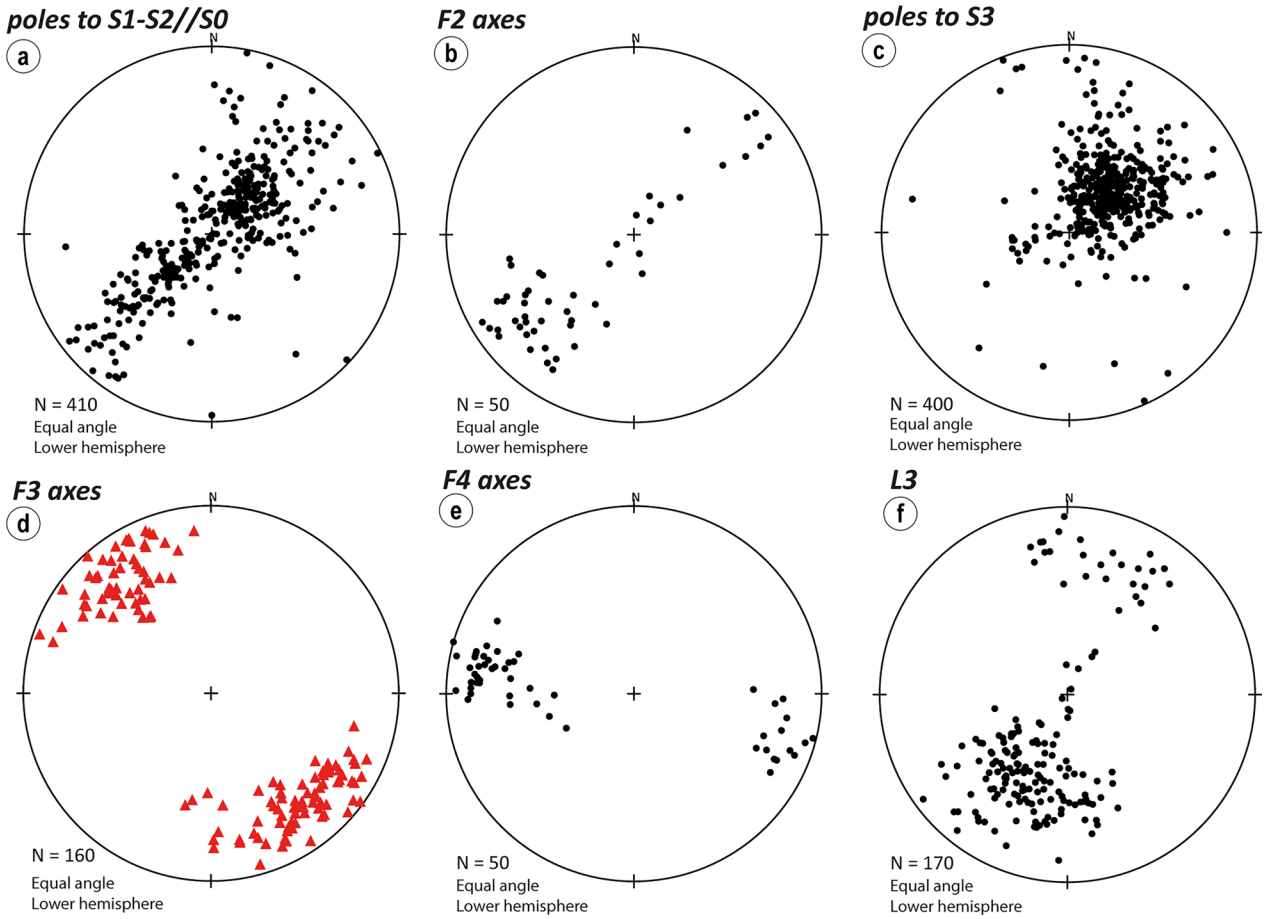

Fig. 8 Cumulative stereographic projection (lower hemisphere, Wulff net) of the measured structural elements. See text for more details

D3 deformation dominates the overall structure along the transect at all scales. Large-scale, decametric to kilometric F3 folds deform previous foliations and develop a new axial plane foliation S3, striking NW–SE and dipping to the WSW (Fig. 8c). F3 folds face eastward, and hence are referred to as backfolds. F3 fold axes are oriented NW–SE (Fig. 8d) and, although locally undulated by the effect of the later D4 phase, have a slight tendency to dip toward SE by a few degrees. The tight Marinet anticline is the most striking large-scale F3 fold of the area, an anticline already reported by Franchi (1898). Its hinge is continuously exposed over more than 16 km along strike in the studied transect (Fig. 3) and recognized over ~ 40 km at the regional scale (Fig. 2). The tight normal and reverse limbs of this fold demand a detachment below the folded, Permian–Triassic competent succession (Fig. 5c). Interestingly tightening decreases to the north as is seen in the famous Guil windows (see Fig. 2).

In the Roure and Combe-Brémond units F3 folding is accompanied by parasitic folds. Their geometry is highly disharmonic (particularly in the Monte Maniglia area), due to strong contrasts in competency between quartz-rich lithologies and marbles. The S3 foliation commonly forms a cleavage fan (Fig. 9e). A stretching lineation, L3, in association with the S3 foliation, is also developed, striking SSW-NNE and commonly plunging SSW (Fig. 6f). Folding during the D3 deformation was accompanied by the first stages of backthrusting. Backthrusting likely outlasted the end of F3 backfolding as is highlighted by the presence of discrete thrust planes below far travelled backthrusts-forming klippes such as the Aiguille Grande klippe (Fig. 3). These thrusts overlay and crosscut earlier F3 folds at the map scale (see the Geological-structural map in Additional file 1 and related cross-sections). One of the best examples is represented by the Bassa di Terrarossa klippe (Fig. 10a). This klippe, formed by the Roure unit, is even backthrust above the folded contact between the Combe-Brémond and Queyras Schistes Lustrés units. Commonly, the Acceglio-type Roure and Combe-Brémond units are folded together with the Queyras Schistes Lustrés, forming a large D3 syncline. This demonstrates that D3 folding postdated D2

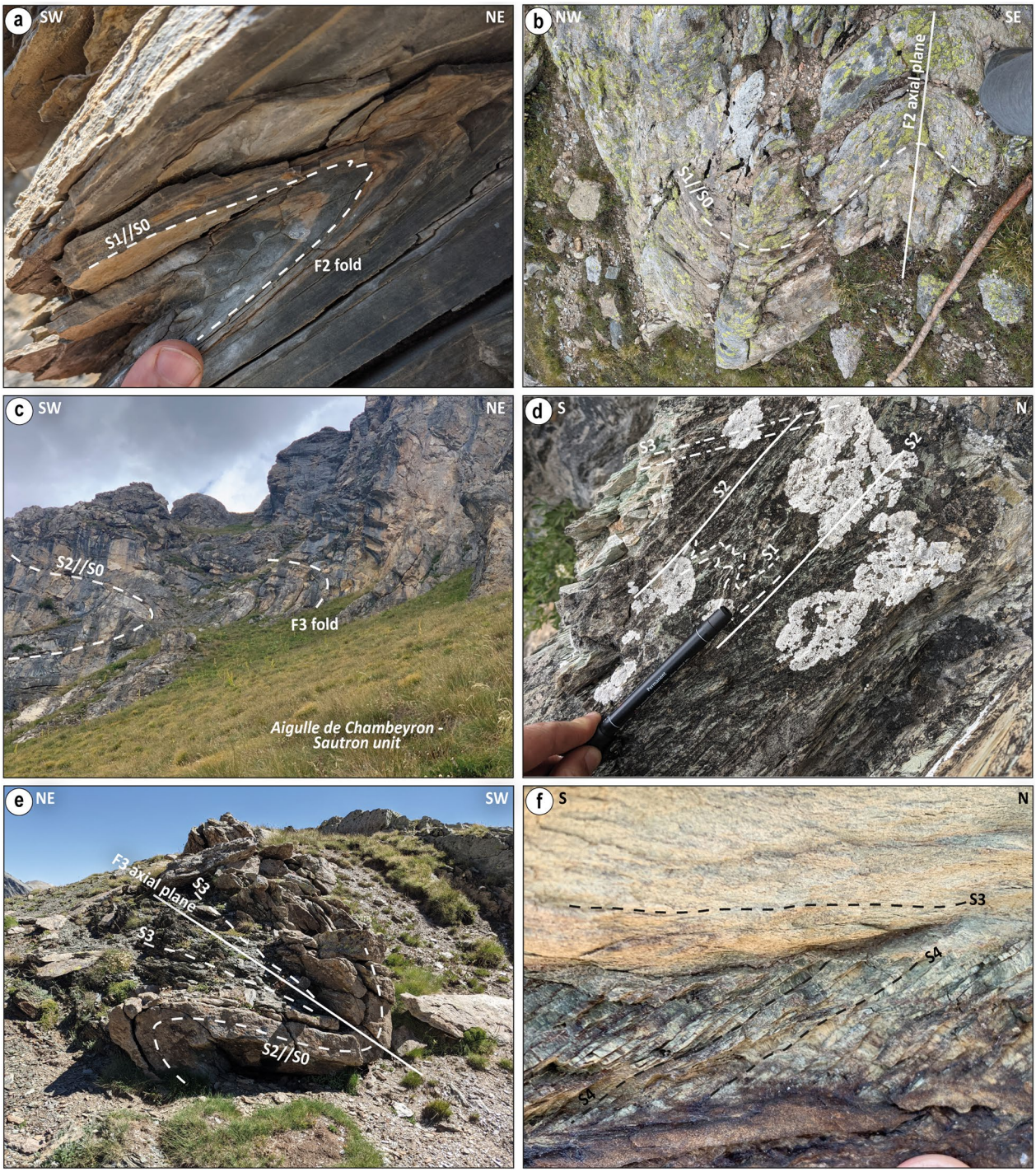

Fig. 9 Mesoscale structures. **a** F2 fold in meta-limestone of the Ceillac-Chiappera subunit, a folded S1//S0 surface is recognizable; **b** Vallon de Chillol quartzite, an old S1//S0 foliation folded by an open F2 fold. The F2 fold axis is verticalized by subsequent F3 folding; **c** F3 minor folds in the Middle Triassic low-grade marbles of the Aiguille de Chambeyron unit; Fig. 7d is taken in the hinge of one of these folds; **d** S2 crenulation cleavage in a F3 hinge (white patches are lichens); **e** Minor F3 parasitic fold of Monte Maniglia D3 syncline in the Combe-Brémond unit; S3 foliation describes a cleavage fan with respect to the fold axial plane; **f** S4 foliation developed locally in a fine grained quartz–phyllite level (Roure unit)

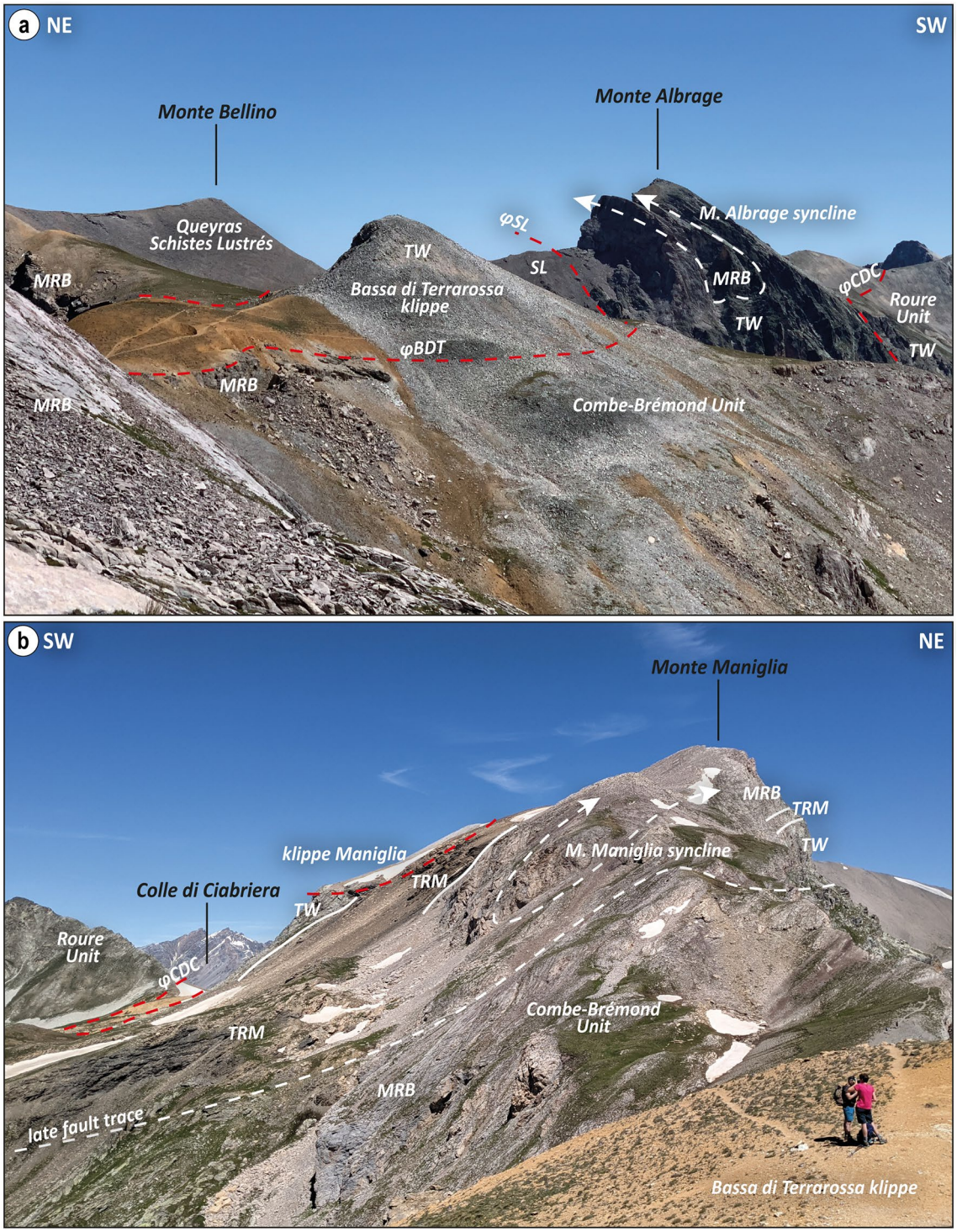

Fig. 10 Klippes and large D3 folds in the Combe-Brémond and Roure units. **a** Interpreted panorama on Bassa di Terrarossa klippe. This klippe overlies the contact between Roure unit and Queyras Schistes Lustrés. Another D3 syncline is visible in the background on Monte Albrage northern wall; **b** Interpreted panorama of Monte Maniglia from Bassa di Terrarossa; the D3 syncline and the backthrust klippe are highlighted. *MRB* Upper Jurassic Combe-Brémond marbles, *TRM* Ladinian-Anisian meta-dolostone and metapelite, *TW* Lower Triassic quartzite, *SL* Schistes Lustrés calcschist, *φCDC* Colle di Ciabriera backthrust, *φBDT* Bassa di Terrarossa backthrust; *φSL* Schistes Lustrés thrust

nappe stacking. Another interesting backthrust klippe, derived from the Roure Unit, is present on the western side of Monte Maniglia (Combe-Brémond unit), where the klippe cuts the normal limb of the D3 Maniglia syncline (Fig. 10b). The D3 phase is associated with decompression and retrograde metamorphic conditions.

A late D4 phase is weakly developed and tends to cause undulations of F3 folds axes and related S3 axial plane foliation. D4 folds are upright open folds whose axes are oriented ESE-WNW (Fig. 6e). Locally, in incompetent lithologies, D4 develops a S4 crenulation cleavage, striking ESE-WNW and dipping toward the S (Fig. 9f). This phase occurred under very low-grade metamorphic conditions heralding high structural levels.

Post-metamorphic brittle faulting with strike-slip, transtensional to extensional kinematics are mostly oriented ENE-WSW and frequently exhibit several generations of slickensides.

4.3 Microstructures and related mineralogy

4.3.1 Microstructures and relationships between deformation and metamorphism

The S3 foliation acquires a different feature in function of metamorphic grade and lithology of the unit within which it develops. It tends to transpose all previous foliations, especially in weak lithologies, such as the "marbres en plaquettes", where it is often the only visible foliation. Generally, the S3 foliation can be classified as a crenulation cleavage, or in some circumstances, as a disjunctive cleavage (Passchier & Trouw, 2005). In the more competent lithologies, S3 has a strong pressure-solution component whereas in soft lithologies it is formed by greenschist-facies platy minerals (white mica, chlorite). In the more external units (Châtelet, Aiguille de Chambeyron) the role of pressure-solution is greater and S3 develops with a disjunctive foliation or a spaced cleavage morphology. In the Marinet unit, greenschist-facies recrystallization assumes a greater role, and S3 is usually a crenulation cleavage, with preserved S2 relics in microlithons. S3 hardly developed in coarse-grained siliceous lithologies and often only develops in fine-grained beds rich in phyllosilicates.

In the units that have reached blueschist facies conditions (Maurin unit, Roure and Combe-Brémond units) S3 may occur as a disjunctive foliation or, in carbonate lithologies, as a penetrative foliation (Fig. 11a–c); it is generally associated with retrograde mineral growth (Michard et al., 2004). The S2 foliation also tends to transpose the earlier surfaces (S0, S1) and exhibits different morphologies in thin section, depending on the lithology and metamorphic grade (Fig. 11d). S2 is particularly well-defined in the higher metamorphic grade units, by phyllosilicate (white mica and chlorite) preferred orientation. Thus, S2 probably developed close to peak temperature metamorphic conditions. S2 is often preserved as a continuous, fine or disjunctive foliation in microlithons of the S3 foliation. On a few occasions, S2 is a crenulation cleavage, and hence relicts of S1 can be recognized in the hinges of the F2 microfolds (Fig. 11e). S1 transposes the sedimentary layering (Fig. 9a) and thus represents a surface parallel or sub-parallel to the lithological contacts (S0), probably developed during the prograde-to peak stages of metamorphism. An observation in the Roure blueschist-facies unit supports this proposal: the growth of quartz-carpholite fibers in composite veins accreted by a crack-seal mechanism (Ramsay, 1980) suggests a progressive deformation context (Fig. 11f). In these veins, quartz fibers are often dynamically recrystallized within this blueschist-facies unit by the bulging mechanism (Stipp et al., 2002a, b), hence after the growth of the carpholite fibers. This suggests that the carpholite fibers probably predate the D2 event associated with quartz recrystallization during D2. This interpretation in agreement with that of Michard et al. (2004) in the Ceillac-Chiappera subunit, where the carpholite fibers are boudinaged along a "P2-3" foliation (corresponding to S2 in the present work) and folded by F3 folds.

Mineral assemblages formed during D2 peak temperature conditions are: white mica and chlorite in the Châtelet unit s.l., white mica (phengite, according to Michard et al., 2004) in the Aiguille de Chambeyron unit, phengite and chlorite in the Marinet unit. Lawsonite (reported by Lonchampt, 1962), albite and epidote are found in the

(See figure on next page.)

Fig. 11 Deformation features at the microscale. **a** S3 disjunctive foliation developed in the Aiguille de Mary unit metandesite associated to growth of chlorite and white mica (sample DT17); **b** S3 disjunctive foliation in the Combe-Brémond Upper Jurassic marble (sample DT30); **c** S3 continous fine foliation developed in Combe-Brémond Upper Cretaceous marble (sample DT13); **d** Feldspar porphyroclast enveloped by S2 foliation in the Aiguilles de Mary metandesite. This foliation is associated with the growth of white mica and chlorite (sample DT18); **e** F2 folds in the sample of Fig. 10d; the S2 crenulation cleavage is parallel to the axial plane of the folds that deform the previous S1 foliation (sample DT18); **f** Quartz-carpholite composite vein, in the Roure unit; note how the quartz is affected by bulging after the carpholite grow (sample DT16); **g** Plagioclase crystal approximately parallel to the fine S3 foliation of a "*Série de la Bergerie de l'Alpet*" marble; note also the development of grain boundary migration (GBM) in calcite (sample DT33); **h** Selective S3 foliation developed in a Permian quartz-schist and subsequently deformed by D4 folds associated with a S4 spaced cleavage (sample DT23)

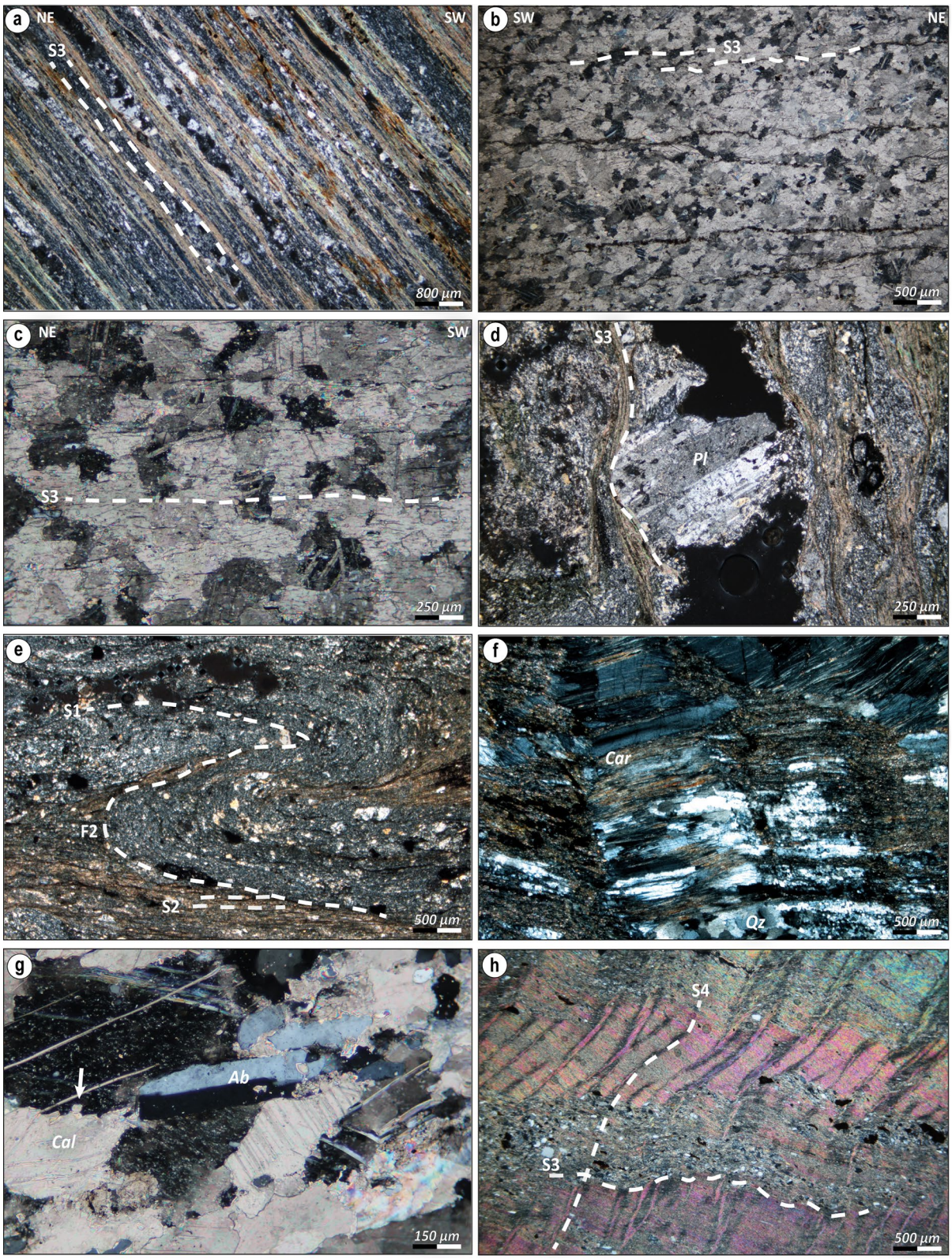

Fig. 11 (See legend on previous page.)

Aiguilles de Mary meta-volcanites. In the Ceillac–Chiappera, Roure and Combe-Brémond units, characterized by the successive growth of carpholite-quartz and albite (Fig. 11f, g), white mica and chlorite assemblages partly replace carpholite suggesting that carpholite might have grown already during D1. The D4 phase (Fig. 11h), particularly well preserved in weak levels (metapelites and calcschists), develops a crenulation cleavage, S4 (Fig. 9f) with no mineral recrystallization associated.

4.3.2 Deformation mechanisms and kinematics

We mainly focused on deformation mechanisms in quartz and calcite that provide useful information on the conditions of deformation, particularly the associated temperatures (Passchier & Trouw, 2005 with references). Feldspar, if present, invariably exhibits brittle deformation behavior, and only growth of albite does occur. Mica typically has a strong shape preferred orientation and frequently grows along foliations. Detrital micas are particularly frequent in lower metamorphic grade samples (e.g., Châtelet unit) and in siliciclastic lithologies (e.g., Verrucano quartzite).

Calcite is generally twinned in lower metamorphic grade units (Fig. 12a). Type I–II twins observed in the Châtelet unit allow for inferring temperatures of about 250–300 °C during deformation (Ferril et al., 2004). In the Aiguille de Chambeyron unit type II-III twins are observed, indicating somewhat higher temperatures of about 300 °C during deformation ("deformation T"); some dynamically recrystallized grains are locally observed (Passchier & Trouw, 2005). The occurrence of twinned dolomite crystals could even indicate deformation conditions >300 °C (Barber & Wenk, 2001). Dynamic recrystallization in calcite plays a prominent role in higher-grade units. Spectacular examples of dynamically recrystallized calcite (Schmid et al., 1981, 1987) are observed in marbles of the Combe-Brémond unit, associated with type IV twins. These deformation mechanisms indicate deformation conditions near at or around 350 °C, i.e., close to temperature peak conditions determined with RSCM. Calcite, defining the S3 foliation, often manifests dynamic recrystallization compatible with temperatures above 300 °C during the D3 event in the Combe-Brémond unit. In some samples from the blueschist-facies units, calcite crystals exhibit a particular "elongated column" shape (Fig. 12c) oriented at a high angle to the macroscopically visible main foliation. According to Brady et al. (2004), Whitney et al. (2014), Gerogiannis et al. (2021) this shape could be interpreted as related to elongate calcite pseudomorphs on former aragonite that were deformed later on during D3. Dynamic recrystallization of calcite fibers is another possibility.

Concerning quartz microstructures, undulose extinction, deformation lamellae, and fractured grains are common in the Marinet unit. This is compatible with deformation temperatures below 350 °C (Stipp et al., 2002a, b; Law et al., 2014). In the Roure unit the bulging I (BLG_I) regime indicating ca. 310 °C (Stipp et al., 2002a) has frequently been observed (Fig. 12d). The recrystallized volume fraction of quartz grains increases approaching the Colle di Ciabriera backthrust (ϕCDC, Fig. 3) highlighting a strain gradient. More intense quartz recrystallization (BLG_{II} regime of Stipp et al., 2002a) is observed in the Combe-Brémond unit where a preferred Shape Preferred Orientation (SPO) and a Lattice Preferred Orientation (LPO) (Fig. 12e) are present. These deformation mechanisms indicate temperatures around 350–370 °C (Stipp et al., 2002a).

Penetrative ductile deformation along D3 tectonic contacts within the more internal units tends to be localized within marble, and is associated with the formation of calc-mylonites suitable for inferring sense of shearing. The calc-mylonite found along the Ceillac fault shows a clear top-to-the-NE sense of shear, inferred from the development of an oblique grain shape foliation (Sb; Fig. 12f) that operated at temperatures >300°C.

Two samples of calc-mylonites (DT8, DT2), interpreted to be a part of the Châtelet unit (see also Gidon et al., 1994, and Gidon, 1958) were taken in Ladinian marbles at a short distance from above the basal thrust of Aiguille Grande klippe that formed during D3 backthrusting. In the field, this basal thrust appears as a brittle tectonic contact, characterized by the presence of cargneule and tectonic breccia, slickenlines

(See figure on next page.)

Fig. 12 Microstructural features. **a** Calcite type I-II twins in the Châtelet unit (sample DT1); **b** Dynamic recrystallization on S3 foliation of calcite in the Combe-Brémond unit (sample DT30); **c** Partially recrystallized calcite crystals with an elongated shape, interpreted as calcite pseudomorphs on aragonite (sample DT14); **d** Dynamic recrystallization of quartz grains by "bulging" I (BLG_1) mechanism (sample DT21); **e** SPO and LPO developed in quartz-rich schists at a short distance from Schistes Lustrés thrust contact, recrystallized by "bulging" (BLG_{II}; sample DT33); **f** Ceillac backthrust calc-mylonite (sample DT7); the oblique foliation in respect to S3 indicated by the calcite grain shape (S_b) suggests a top-to-the-NE sense of shear; **g** Aiguille Grande base thrust indicating a top-to-the-SW sense of shear, inferred from the oblique foliation of calcite (Sb), (sample DT8); **h** Chillol thrust folded D2 mylonitic quartzite (sample DT9); an apparent top-to-the-NE sense of shear is inferred from S-C fabric (corresponding to a restored top-to-the SW kinematic in pre-D3 geometry)

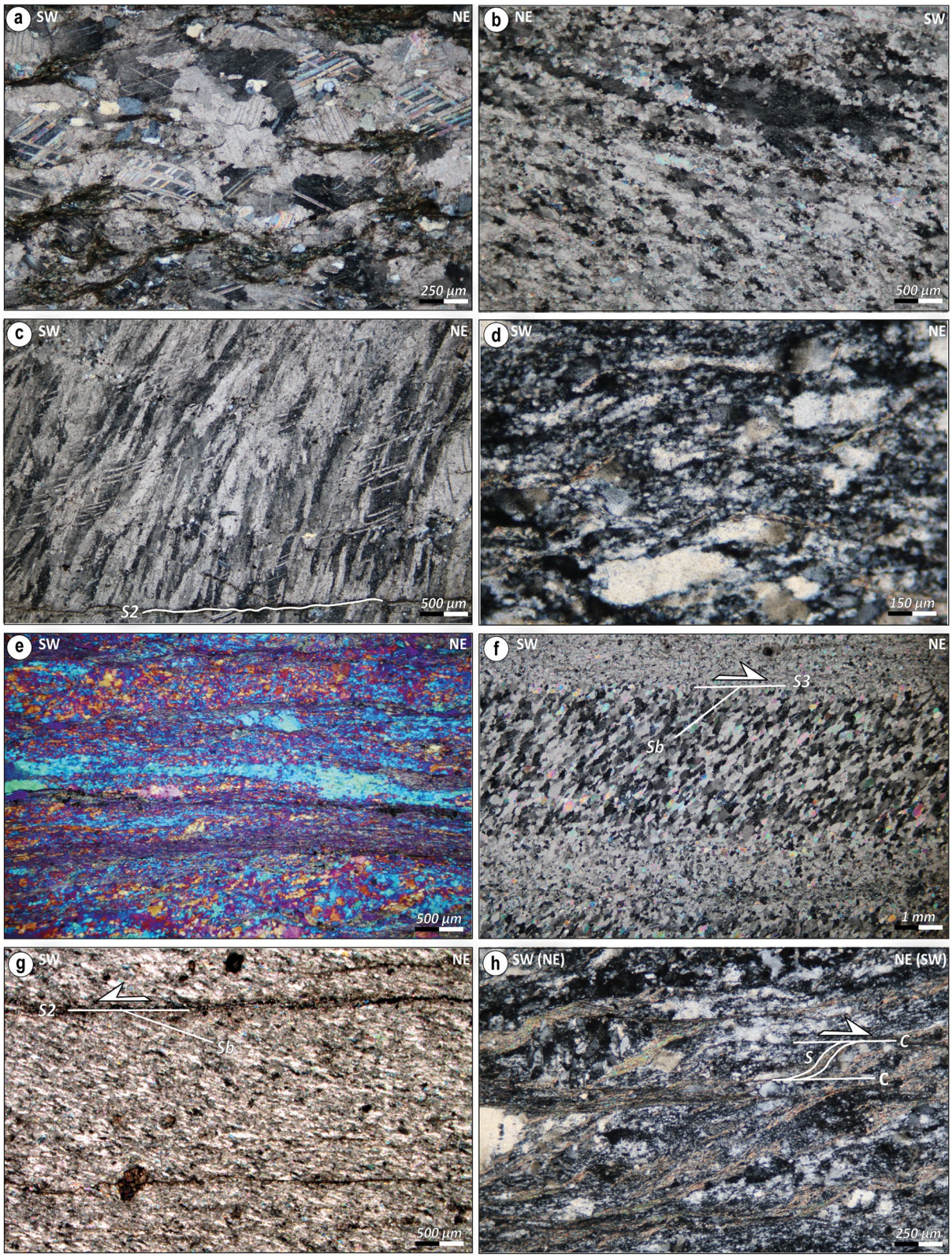

Fig. 12 (See legend on previous page.)

and calcite steps that indicate a top-to-the-NE shear sense (D3 backthrusting phase). However, only a few meters above the brittle contact, the above mentioned oriented calc-mylonite samples (DT8, DT2) yielded kinematic indicators that clearly suggest an opposite, i.e., top-to-the-W, sense of shear (Fig. 12g) such as an oblique foliation (Sb, Fig. 12g) defined by the SPO of calcite grains. A possible interpretation of this puzzling finding could be that a brittle late-D3 reactivation occurred along an earlier D2 (or D1–D2?) ductile contact by inversion of previous top-to-the-W kinematics, destroying the earlier calc-mylonites only preserved within the calc-mylonites immediately above the thrust fault itself.

The tectonic contact between the Marinet and Aiguilles de Mary units, referred as *Chillol thrust* (Fig. 3), later folded during D3, was investigated by oriented sampling of mylonitic quartzite and metavolcanics at two different places (Vallon de Chillol and near Colle Greguri). At both locations the oriented samples (DT9, DT27) are characterized by an intense mylonitic foliation associated to the growth of white mica and chlorite, folded by D3 and so attributed S2. This S2 foliation and associated lineation were re-oriented during D3 folding and hence presently dip to the WSW. Hence, the presently recognized top-to-the-NE D2 kinematics (see Fig. 12h) have to be restored. Since the investigated samples come from the overturned NE limb of the Marinet anticline, the restored D2 kinematics would indicate syn-D2 top-to-the-SW shear after rotation caused by D3 folding.

In summary, the temperature conditions during backthrusting (D3 phase) were high enough to allow for dynamic recrystallization in calcite and for the formation of calc-mylonites. Later on this D3 deformation continued under more brittle conditions, partly along the same backthrusts. Since dynamic recrystallization associated with the S3 foliation is widespread in the blueschist-facies units (see chapter metamorphism), the temperature difference between the earlier D1/D2 events (broadly coincident with the metamorphic peak) and those prevailing during the early stages of D3 must have been relatively small.

5 Metamorphism: review of existing data and new data

5.1 Overview

The progressive increase of Alpine peak metamorphic conditions, going from the external greenschist-facies units towards the internal blueschist-facies units was recognized since years in the Briançonnais-derived units (Oberhänsli et al., 2004; Bousquet et al., 2008; Michard et al., 2022). In our study area, metamorphic conditions were estimated for each unit by Gidon et al. (1994) and Michard et al. (2004); their converging results are summarized in Table 2.

Michard et al. (2004) noted the presence of carpholite fibers in the Maljasset and Alpet outcrops (Ceillac–Chiappera subunit and Combe-Brémond unit, respectively) and suggested cooling during decompression. In the case of the Acceglio–Longet units (Fig. 2), Schwartz et al. (2000) suggested a heating episode reaching about 465 ± 25 °C at the beginning of the decompression. Note that these authors classified peak metamorphism of the Pelvo d'Elva unit (part of the Acceglio–Longet, Fig. 2) to reach eclogite-facies, which is controversial, as the garnet of the studied material are possibly inherited from pre-Alpine metamorphism (Lefèvre and Michard, 1976). Michard et al. (2004), instead, propose peak P–T conditions at about 13 kbar–430 °C and an alternative decompression pathway with decreasing T. Agard et al., (2000, 2002) proposed similar clockwise pathways for the Queyras Schistes Lustrés. The age of the onset of metamorphism in the Briançonnais units, predating D2, is poorly constrained since no really consistent radiometric age data are yet available. The age of the youngest sediments involved by Alpine deformation only provide an upper time limit. According to Barféty et al. (1992; 1995) the stratigraphic base of the youngest sediments, i.e., the Flysch noir, is Lower Bartonian (c. 41–39.5 Ma), these sediments being followed by an olistostrome of unknown age that are in turn overlain by large-scale submarine slides, providing the only available constraint of the onset of deformation in the most external part of the Briançonnais. Consequently, an age interval between some 40–37 Ma for the onset of metamorphism is no more than a best guess. In the Dora-Maira massif, UHP metamorphism was dated at ~ 35 Ma (Gebauer et al., 1997; Rubatto and Hermann, 2001; Xiong et al., 2021). The overlying HP units show a trend of peak metamorphic ages younging downwards in the nappe stack, from ~ 40 to ~ 33 Ma (Bonnet et al., 2022). Therefore, the leading edge of the former Briançonnais passive margin became deeply subducted between about 40 to 33 Ma.

5.2 New TRSCM results

The Raman Spectroscopy of Carbonaceous Material (RSCM) allows calculating maximum temperatures (T_{RSCM} or Tmax) for samples containing CM with a precision generally better than 50 °C regarding absolute temperature estimates, but is more sensitive to relative temperature differences over the range 200–650 °C (Beyssac et al., 2002a, b; Lahfid et al., 2010). Details on the analytical method can be found in Delchini et al. (2016). During the last decades, RSCM geothermometry

Table 2 Metamorphism of the studied units (from west to east) after Gidon et al. (1994) and Michard et al. (2004)

Tectonic Units	Gidon et al. (1994)			Michard et al. (2004)		
	Metamorphic facies	P–T estimate	Mineral assemblages	Metamorphic facies	P–T estimate	Mineral assemblages
Sérenne-Guillestre	Anchizone	T < 300 °C	Ilt	Chl-Pumpellyite	–	Chl, Ms, Qz
Châtelet and Brec	Low-grade greenschist	T 300 °C, P = 1–3 kbar	Ms, Chl	Low-grade greenschist	–	Chl, Ms, Qz
Aiguille de Chambeyron-Sautron	Low-grade greenschist	T 300 °C, P = 1–3 kbar	Ms, Chl	Low-grade greenschist	T = 310 °C, P = 6 kbar	Ph, Ab, Qz
Marinet	Low-grade, intermediate-pressure metamorphism	T 300 °C, P = 3–6 kbar	Lws, Ph, Pg, Car	High pressure greenschist	T = 330 °C, P = 7 kbar	Ph, Chl, Ab, Qz
Aiguilles de Mary s.l	Low-grade, intermediate-pressure metamorphism	T 300 °C, P = 3–6 kbar	Lws, Ph, Pg, Car	Low grade blueschist	–	Lws, Ch, Ab, Ep
Ceillac–Chiappera	Blueschist lacking significant overprint in greenschist	T = 300–350 °C, P = 8–12 kbar	Car, Lws, Arg	Blueschist lacking significant overprint in greenschist	T < 350 °C, P = 10 kbar	Car, Ph
Roure	Blueschist partially overprinted by intermediate grade greenschist	T = 300–350 °C, P = 8–12 kbar	Car, Chl, Pg; Ph	Blueschist lacking significant overprint in greenschist	T < 350 °C, P = 11 kbar	Car, Ph
Combe–Brémond	Blueschist partially overprinted by intermediate grade greenschist	T = 300–350 °C, P = 8–12 kbar	Car, Chl, Pg; Ph	Blueschist partially overprinted by intermediate grade greenschist	T < 350 °C, P = 11 kbar	Car, Ph
Schistes lustrés (La Blave)	Blueschist partially overprinted by intermediate grade greenschist	T = 300–350 °C, P = 8–12 kbar	Gln, Lws, Phe, Jd	Blueschist to high-grade blueschist, partially overprinted by greenschist facies	T = 370 °C. P = 13 kbar	Gln, Lws, Car

Mineral abbreviations after Whitney & Evans (2010)

was widely used to decipher the thermal evolution of the internal Western Alps (Beyssac et al., 2002a; Gerber, 2008; Gabalda et al., 2009; Plunder et al., 2012; Negro et al., 2013; Angiboust et al., 2012, 2014; Schwartz et al., 2013; Lanari et al., 2012; Herviou et al., 2022; Michard et al., 2022). We applied the RSCM geothermometer to 18 samples selected according to their richness in carbonaceous material. The results are summarized in Fig. 13, sample list and other information are available in Additional file 3.

In the Sérenne-Guillestre unit, sample UB15 (black pelite) yielded 312.2 ± 21.4 °C. In the most external Châtelet unit, two samples from the Triassic marbles yield temperatures between 294 ± 7.9 (sample DT1) and 306.3 ± 9.5 °C (sample UB17). Two samples from the Brec de Chambeyron klippe (part of the Châtelet unit) yield a T_{RSCM} value of 301.8 ± 14.6 °C in Upper Jurassic beds (sample UB13) and 315.9 ± 11.5 °C for collected in Middle Triassic marbles (sample UB16). Two samples from the Triassic marbles of the Aiguille Grande klippe (frontal part of the Châtelet unit) yield 332 ± 7.8 °C (sample DT2) and 332.3 ± 4.7 °C (sample UB10), respectively. In the slightly more internal Aiguille de Chambeyron–Sautron units, calcschist sample DT10 yields 317 ± 16 °C. Two samples from the Marinet unit, collected in Middle Triassic beds, DT9 and DT39, yielded significantly higher 329.6 ± 11.8 and 335.3 ± 9.6 °C, respectively. Four samples have been collected in the Maurin unit. The Aiguilles de Mary sub-unit shows 333 ± 18 °C in Upper Triassic metabreccia (sample DT15), while sample DT3 from the same sub-unit further to the south yields a similar value of 329 ± 17 °C. Very similar values, namely 327 ± 19.2 and 339 ± 8.2 °C were measured in calcschist and marble (samples DT14 and DT7) in the Ceillac–Chiappera sub-unit. Sample DT6 from the tectonic window of the Combe-Brémond unit yielded 341 ± 8.5 °C. Also, the other three samples from the Combe-Brémond unit, namely samples DT5, DT13 and DT12, yielded slightly higher values ranging between 340 ± 8.7 °C and 346 ± 5.4°.

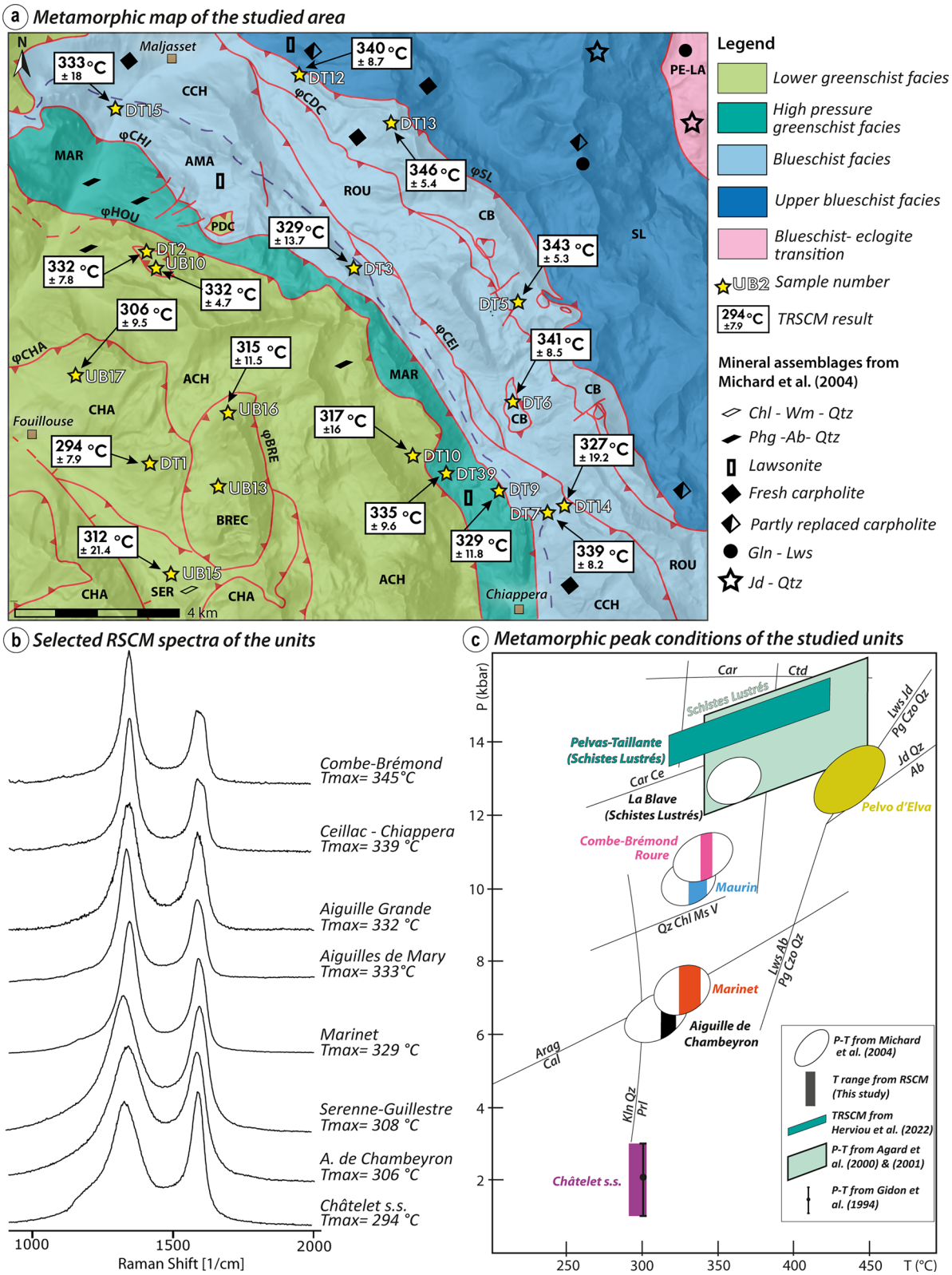

Fig. 13 Metamorphism of the studied units. **a** Metamorphic map of the studied area according to our new data and Michard et al. (2004) data. Metamorphic facies according to Bousquet et al. (2008); **b** Selected Raman Spectra and corresponding T_{RSCM} (Tmax in b) for selected units; **c** Metamorphic peak conditions for the studied Briançonnais units (this work), the nearby Schistes Lustrés (from Herviou et al., 2022, Agard et al., 2000, 2001) and the Pelvo d'Elva unit (Michard et al., 2004). Abbreviations of units and tectonic contacts as in Fig. 3

6 Discussion

6.1 Tectonometamorphic evolution of the Ubaye–Maira Briançonnais

6.1.1 Deformation history

At different scales we recognized structures referred to four successive deformation phases labeled D1 to D4 in the Briançonnais units of the Ubaye–Maira valleys. D1 produced a S1 foliation subparallel or parallel to the original bedding S0 and became folded by rarely observed F2 folds. It is not clear whether this D1 phase has to be considered a stand-alone event in the area. Michard et al. (2022) argued for the case of the more internal Briançonnais units that their D1 coincides with peak pressure conditions; similar conclusions were also reached by Sanità et al. (2022a) south of our study area. F2 folds are tight to isoclinal and transpose S1 into an S2 foliation. We associate D2 deformation with original nappe stacking. Following Michard et al. (2022) who observed an identical D1-D3 deformation history, we associate D2 to nappe stacking with buoyant uplift and/or extrusion of nappe bodies within the subduction channel. The minor F2 folds are in turn folded by major F3 folds. Despite this pervasive overprint, some large west facing F2 folds are preserved in the Brec de Chambeyron klippe (Fig. 14a, b). The D3 phase, associated with backfolding and backthrusting is the dominating deformation event seen in the field at all scales, wiping out much of the older structures. On a large-scale, relicts of the original D2 nappe stacking event are very rarely preserved and inferred from kinematic indicators and refolded D2 nappe contacts as was demonstrated in the case of the subsequently backfolded Chillol thrust (Fig. 3). D3 is associated with retrograde/decompression metamorphic conditions. The D4 phase leads to undulations of the F3 fold axes and their axial plane foliations S3 and forms broadly E–W trending folds (Fig. 6e) indicating N–S shortening, possibly associated with late-stage oroclinal bending in the Western Alps. The D4 phase occurred under late- to post-metamorphic conditions and is followed by brittle tectonics.

A comparison between the deformation phases proposed by previous authors for neighboring areas with those we recognized in the present work is shown in Additional file 3. Deformation phases proposed by the previous authors are broadly consistent with our scheme and that of Michard et al. (2022). The main potential differences concern the following points:

1) The D1 event proposed here was also postulated by, for example, Caron et al. (1973), Platt (1989) and Tricart (1980). Relic, prograde foliations are recognized, sometimes labeled "D1" (Agard et al., 2001), which preserved their D1 phase, which corresponds to our D2 phase; this is also the case in the works on the Acceglio-Longet units (Lefèvre & Michard, 1976; Caby, 1996). We propose to relate D1 to subduction that predates nappe stacking.
2) D2 is associated with roughly west-directed tectonic transport in our study area. However, in view of the fact that D3 deformation is very intense on all scales, the exact direction of nappe transport during D2 can no longer be reliably inferred in a simple way due to (a) strong re-orientation of D2 structures by syn-D3 shearing and (b) oroclinal bending. At a large scale some authors (e.g., Choukroune et al., 1986; Schmid et al., 2017; Dumont et al., 2022) postulate initial top N to NW transport during early stages nappe stacking in the Western Alps that can possibly no more be seen in our area due to serious D3 overprint and later oroclinal bending in the Miocene. Nevertheless, we disagree with the reconstruction of the early top-N-NW thrusting by Dumont et al. (2022) who identified isoclinal folds (their "D1", our D1/D2) at the Bergerie de l'Alpet cliff (boundary of the Combe-Brémond unit with the underlying Queyras Schistes Lustrés), associated to nappe emplacement, deformed by a later deformation phase (their "D2", our D3). Their analysis is based on deriving shear senses using the asymmetry of folds, which is known to be far from being a reliable kinematic indicator (e.g., Fossen, 2016). At this same place we documented how the folded surface is already a tectonic surface and we interpreted these asymmetric folds as minor parasitic folds, associated with a large D3 antiform with the Combe-Brémond "Verrucano" in its core; this large fold also affects the contact with the Queyras Schistes Lustrés (Fig. 3b, Additional file 1).
3) The backfolding/backthrusting D3 deformation event under weakly retrograde conditions was also indicated as D3 by Platt et al. (1989) and Tricart (1980). However, this event is differently numbered by different authors. D3 corresponds to D2–D3 of Michard et al. (2004). Conversely, in the nomenclature proposed by Dumont et al. (2022), backfolding and backthrusting are labeled D2 and corresponds to the sum of events D2 and D3 of Tricart (1980). Such nomenclatural problems make comparisons amongst different authors difficult. However, NE-directed backthrusting and backfolding (E-directed further north) was recognized by all previous authors. However, the intensity of D3 deformation was often grossly underestimated.
4) Significance age and nature of the D4 event are not clear amongst authors. D4 is either not mentioned or often associated with strike-slip and late normal faulting as discussed by Michard et al. (2004), Lefèvre & Michard (1976) and Carminati & Gosso (2000).

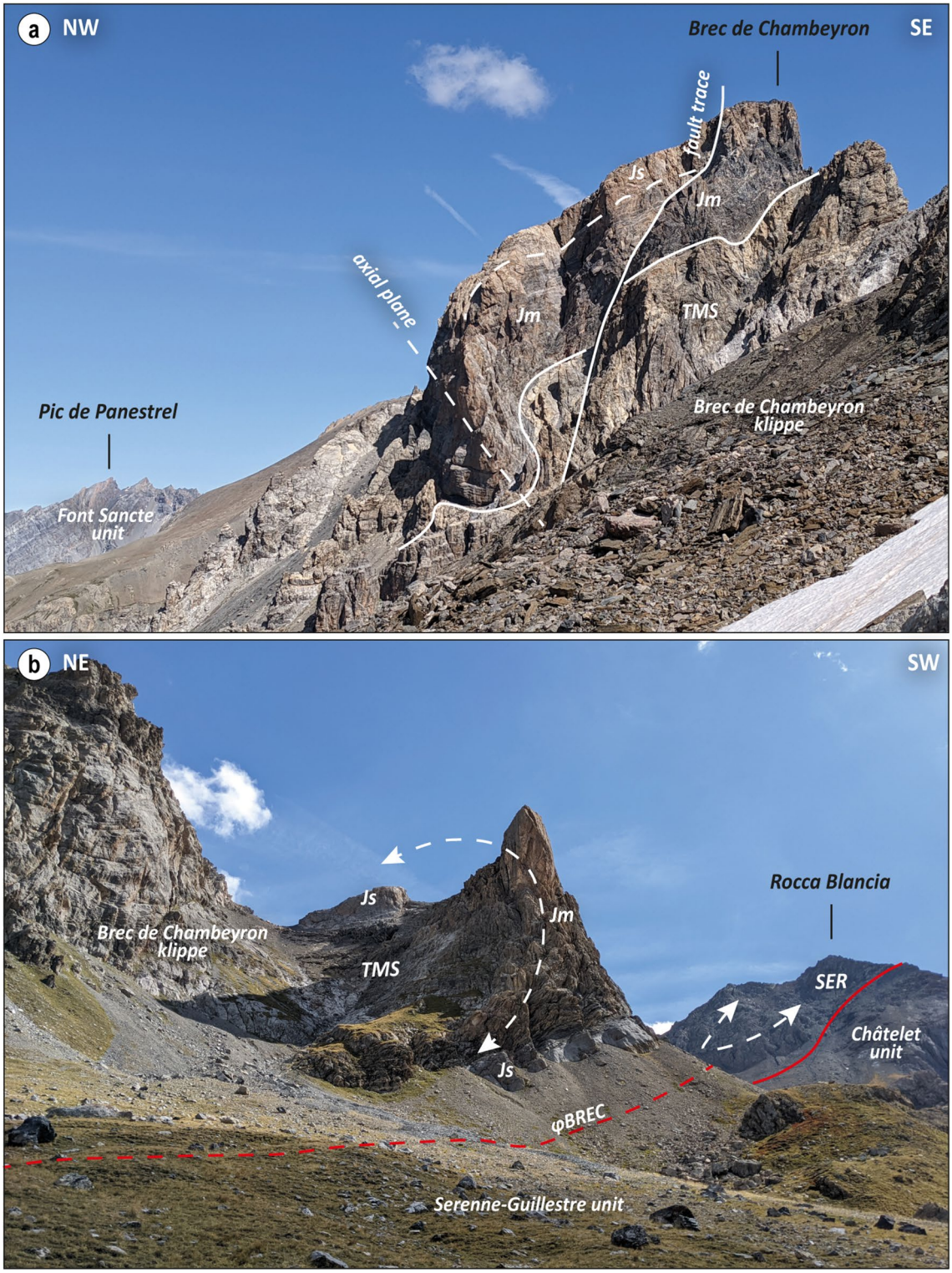

Fig. 14 Interpreted panoramas illustrating preserved F2 folds. **a** Brec de Chambeyron southern wall, Middle–Upper Triassic (TMS) and Middle (Jm)—Upper Jurassic (Js) limestone are folded by a series of W-facing folds. In the background the highest peaks of the Font Sancte unit are visible; **b** Le Massour (southern peak of the Brec de Chambeyron klippe) seen from Vallon de Plate Lombarde. Major F2 W-facing major fold affecting Middle–Upper Triassic (TMS) and Middle (Jm) and Upper Jurassic (Js) beds. On the right, in the background the Helminthoid flysch Serenne-Guillestre unit (SER) tectonically overlies the Châtelet unit

Late-stage normal faulting is still going on today, as witnessed by the Ubaye Valley recent seismicity (Sue et al., 2007).

6.1.2 Metamorphism and deformation temperatures of the Ubaye–Maira units

Now we discuss the metamorphic peak temperatures obtained through the RSCM geothermometer with available P–T data from the literature (Fig. 13a–c). The P–T conditions derived from mineral parageneses indicate that also pressure increases from west to east, namely starting from 294 ± 7.9 °C/1–3 kbar in the Châtelet Unit, to 346 ± 5.4 °C/11 kbar in the Combe-Brémond unit, up to around 370 °C/13 kbar in the Schistes Lustrés further east. The temperatures derived from the RSCM geothermometer are in general compatible with these PT conditions taken from the literature. Only the sample from the Sérenne-Guillestre unit shows a higher peak temperature with respect to the estimations of Gidon et al. (1994). Lanari (2009) presented a transect of metamorphic peak temperatures determined by the RSCM method in the Guil Valley (see location in Fig. 2). Although they used the RSCM calibration of Beyssac et al. (2002a), the results obtained by Lanari (2009) are well comparable to those proposed for our transect.

Comparison of the RSCM temperature data with temperature estimates based on the mechanism of dynamic recrystallization in quartz (Sect. 4.3.2) suggests that syn-D3 deformation occurred under temperature conditions close to those reached during the metamorphic peak acquired at an earlier stage. Dynamically recrystallized calcite also indicates temperatures above 300 °C (Bestmann & Prior, 2003) in almost all units. Calcite recrystallisation becomes increasingly more intense from west to east, sometimes reaching a sub-grain rotation (SGR) regime (Passchier & Trouw, 2005) in the blueschist-facies units.

In the calcite-aragonite phase transition diagram, the peak P–T data of the Maurin, Roure and Combe–Brémond blueschist-facies units plot into the aragonite stability field (Fig. 13c). This is consistent with the inferred microstructures described above (Sect. 4.3.2) in the low strain domains of the blueschist-facies units (Fig. 12c).

6.1.3 Relationships between the Briançonnais s.s. and the ocean-derived units

The studied Briançonnais units are delimited by oceanic-derived units to both sides: the Helminthoid Flysch nappe to the west and the Queyras Schistes Lustrés to the east (Fig. 3). However, the relationships between these two groups of ocean-derived units and the Briançonnais paleomargin units are very different. Concerning the eastern contact, we showed that D3 phase back folding affected the Acceglio-type units and Queyras Schistes Lustrés likewise. In fact, the tectonic contact between the two became overturned during D3 folding. If restored by rotation around the D3 fold axis this restores to a west-directed thrust of the Queyras unit over the Briançonnais related to subduction and nappe stacking (D1–D2).

The relationships of the Briançonnais units with the Helminthoid Flysch units in the west are more complex, as tectonic slices of the Helminthoid Flysch nappe stack (Sérenne-Guillestre unit) are sandwiched between Briançonnais units and cut by a late-stage normal fault. An example of this is seen at Col Nubiera (see map of Fig. 3), where a slice of the Sérenne-Guillestre unit is sandwiched between tectonic slices of the Châtelet unit (Brec de Chambeyron klippe on top and main body of the Châtelet unit below). This implies that both D2 fore- and D3 back-thrusting affected a pre-existing assembly of Helminthoid Flysch nappe (Sérenne-Guillestre unit) thrust upon the Briançonnais (Châtelet unit) during an earlier event. We propose that this early phase of thrusting of the Helminthoid Flysch nappe occurred over not yet substantially deformed and not yet detached Briançonnais units (i.e., before our D2), at least what the most external unit (Châtelet unit) is concerned. This same early phase post-dates the end of sedimentation in the Helminthoid basin (Paleocene to perhaps earliest Eocene according to Kerckhove 1969). This confirms the inference that pre-D2 thrusting must have formed during very early stages of west-directed emplacement of the Helminthoid Flysch nappe in the early Eocene. Note, however, that final west/southwest-directed emplacement of the Embrunais-Ubaye nappe stack over the Dauphinois occurred much later, in Oligocene times (Kerckhove et al. 1969; Tricart 1984; Merle & Brun, 1984). Note that similar relationship between Helminthoid Flysch and Briançonnais units are also observed in the Ligurian Alps (Sanità et al., 2022b).

6.2 Evolution of Haute Ubaye–Maira Briançonnais palaeomargin

Tectonic units observed today may represent only a small portion of the palaeomargin, preserved from erosion and escaping subduction dynamics such as tectonic erosion and recycling in the mantle. Furthermore, deciphering the provenance and thrusting sequence of the nappes simply on the basis of their geometrical expression, metamorphic grade and structural relationships involves simplifying assumptions (e.g., Platt et al., 1986; Dumont

et al., 2022). A correct paleogeographic restoration also needs to proceed by intermediate steps by successive retro-deformation (e.g., Laubscher, 1988, 1991; Schmid & Kissling, 2000). We are aware of these serious limitations when proposing a tectonic and stratigraphic evolution of the Briançonnais paleomargin in the Haute Ubaye–Maira transect (Fig. 15). The proposed paleogeographic reconstructions in 2D are oriented approximately NW–SE, consistent with the kinematics assumed for subduction (Michard et al., 2004, 2022; Tricart and Schwartz, 2006).

6.2.1 Upper Triassic (c. 210 Ma)

During this period the passive margin was not yet structured into horsts and graben (Fig. 15a). An extensive carbonate platform developed over the Permian–Lower Triassic siliciclastic successions. The Middle Triassic carbonate platform consists of three transgressive–regressive cycles and comprises shallow subtidal carbonates and dolomitic mudstones (Mégard-Galli & Baud, 1977; Lualdi, 1985; Lemoine et al., 1986; Decarlis et al., 2013). Instead, the Norian carbonate platform was mainly built in a tidal flat environment (Mégard-Galli, 1972a). According to Lemoine et al. (1986) an aborted Carnian rifting stage, with evidence of synsedimentary extensional tectonics (Mégard-Galli, 1972b), separates the deposition of the Middle Triassic and Norian carbonates. The partial or total absence of Triassic formations in most of the future tectonic units is due to their subsequent erosion during later rifting processes. The drawing of Fig. 15a is based on extrapolating the thickness from adjoining areas (as shown in Fig. 15b and c, e.g., Peyre-Haute and Pre-Piemonte units) where the Triassic cover has been eroded (e.g., Marinet, Roure and Combe-Brémond units). Furthermore, the few active faults in this context are placed in correspondence with the rifting faults. It is assumed that these are the same faults that will reactivate over time (Bonini et al., 2010).

6.2.2 Middle Jurassic (c. 167 Ma)

The rifting stages of the Briançonnais passive margin related to the opening of Alpine Tethys had opposite effects in the Pre-Piemonte and Classic Briançonnais units (Fig. 15b). During the drowning of the Pre-Piemonte units, large thicknesses of breccias were produced while the Classic Briançonnais units became uplifted, producing a prolonged gap in the sedimentary record, sometimes with karst and red soils (Baud & Mégard-Galli, 1975; Claudel & Dumont, 1999; Decarlis et al.,

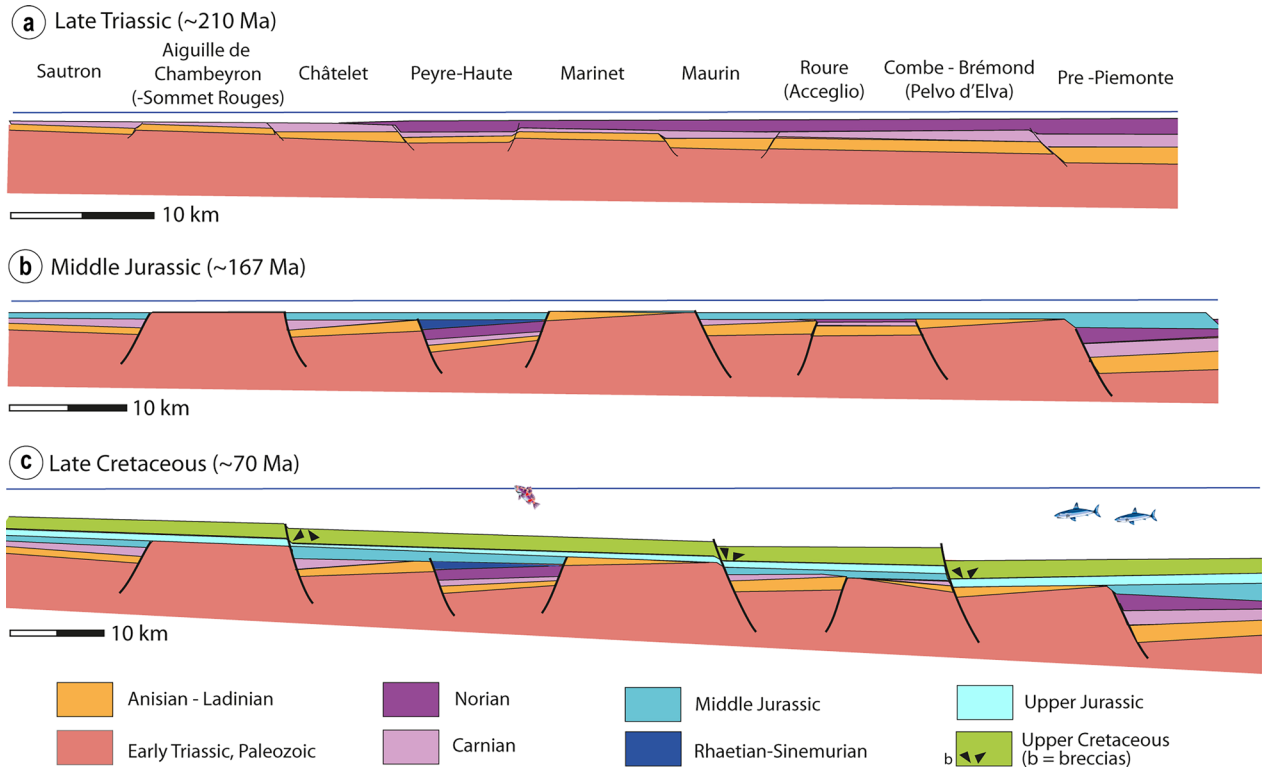

Fig. 15 Proposed restoration of the paleogeographic evolution of the studied Briançonnais area. **a** Late Triassic (~ 210 Ma), pre-rift stage; **b** Middle Jurassic (~ 167 Ma), by the end of the rifting stage; **c** Late Cretaceous (~ 70 Ma), extensional faulting highlighted by tectono-sedimentary breccias (black triangles)

2013). Note, however, that very substantial gaps were also produced much later on during Late Cretaceous to early Paleogene extension. The Lower Liassic is often not represented where such later extension prevailed but it was likely deposited in the syn-rift context over a large part of the Briançonnais s.l. domain from the Châtelet unit to the Pre-Piemonte. In the Pre-Piemonte units, large thicknesses of Liassic formations did accumulate ("Rhétien-Hettangien and Lias Prépiémontais"; Michard, 1967; Dumont, 1984; Michard et al., 2022).

In the Classic Briançonnais and Acceglio-type units to the west, the uplift of the margin is at a maximum during the Aalenian-Bajocian; it results in the erosion of Liassic deposits and part of the Triassic on the crests of tilted blocks with sub-aerial formation of Bathonian bauxite and coal (Faure & Mégard-Galli, 1988). Subsidence increases as Rosso Ammonitico is deposited in the form of "Marbres de Guillestre" (Faure-Muret & Fallot, 1955). Stratigraphic successions evolved differently in the different blocks created during the rifting evolution. Starting from the more external unit, we recognize: (1) Sautron: Dogger formations discordant on Upper Triassic dolostones; (2) Aiguille de Chambeyron: no Dogger formations preserved, the Jurassic transgression is Oxfordian in age ("Marbres de Guillestre" and "Calcaires Gris"); (3) Châtelet–Font Sancte: similar to the Sautron block, except that Triassic formations were thicker before their partial erosion; (4) Peyre Haute: residual presence of Rhaetian, Hettangian, Sinemurian syn-rift formations (Tricart et al., 1988); (5) Marinet: this block must have represent a high, since the Triassic formations are very reduced and Dogger formations are lacking beneath a few meters of Oxfordian "Marbres de Guillestre"; (6) Maurin: compared to the Marinet, this block was less elevated as it shows Dogger and Upper Jurassic formations; (7) Roure: at this time this block must have still carried Triassic dolostones in order to be able to feed the Alpet-Longet breccias of the Combe-Brémond unit during the Late Cretaceous. Whereas no relic of post-Lower Triassic beds have been found in the mapped part of Roure unit, some do exist in the Acceglio unit, which represents the eastern equivalent of the Roure unit (Fig. 2; Lefèvre, 1968; Lefèvre & Michard, 1976); (8) Combe-Brémond and Pelvo d'Elva units: a transgression of Jurassic sandy marbles on the Permo-Triassic siliciclastic sequence is observed, most of the Triassic formations have been reworked into the Pre-Piemonte breccias during the Liassic period; (9) The Pre-Piemonte units contain a poorly defined calcareous-detrital, turbiditic Dogger formation with radiolarites known as "Formation Détritique Rousse" (Lemoine et al., 1978; Dumont, 1984).

6.2.3 Upper Cretaceous (c. 70 Ma)—Paleocene

By this time the Briançonnais domain was a deeply submerged continental margin divided in persisting basins and highs by normal faults inherited from mid-Jurassic rifting (Lemoine et al., 1986). During the Late Cretaceous-Paleocene, the Briançonnais passive margin is affected by an extensional event well-recorded throughout the Classic Briançonnais and Acceglio-type units of the Western and Ligurian Alps by large paleofault scarps and polygenic coarse breccia with olistoliths (Blanchet, 1934; Tissot, 1955; Bourbon et al., 1977; Jaillard, 1988; Michard and Henry, 1988; Gidon et al., 1994; Barféty et al., 1995; Claudel et al., 1997; Michard and Martinotti, 2002; Tricart & Schwartz 2003; Bertok et al., 2012; Tavani et al., 2018; Michard et al., 2022). Upper Cretaceous–lower Paleogene calcareous-argillaceous muds (the future calcschists) likely covered the entire passive margin (Fig. 15c). Their thickness varies between the different blocks and many interstratified breccias associated with paleofaults (see Fig. 5b and Sect. 4.1.3) point to extensional re-activation of inherited normal faults. In our study area and nearby outcrops, the stratigraphic records of this surprisingly strong extensional event are numerous. In the "Brèches de la Magdeleine", Blanchet (1934) observed at the bottom of the "marbres en plaquettes" of his "nappe II" (now Brèches de la Madeleine, in the Lower Guil unit; Fig. 2) the presence of pebbles of radiolarite, Tithonian limestones with *Calpionella alpina*, and of interbedded layers of "marbres en plaquettes". Other outcrops of "Brèches de la Madeleine" were described by Gidon (1962) to both sides of the Ubaye valley. This author noted the presence of blocks of Triassic limestones 10 to 20 m in size. At the nearby Col du Longet, Upper Cretaceous–lower Paleogene mega-breccias have been again described recently (Michard et al., 2022; Dumont et al., 2022). A last example of breccias related to the Late Cretaceous-Paleocene extension event is the occurrence of the polygenic mega-breccia at the Bergerie de l'Alpet (Fig. 16) found in the overturned strata at the front of the Combe-Brémond unit (SE of Maljasset village, Fig. 3). This breccia frequently shows a chaotic mix of different components embedded in a quartz-micaceous matrix ("Permien reconstitué"; Lemoine, 1961), evolving towards a finer-grained carbonate-rich facies and finally to a sandy gray marble (Le Guernic, 1967). In line with Michard et al., (2004, 2022), we interpret this sequence as the stratigraphic sequence of the Acceglio-type overturned Combe-Brémond unit, sourced from moderately uplifted Classic Briançonnais units.

Different explanations have been proposed to have caused this Late Cretaceous to early Paleogene extensional event. Bending of the subducting lithosphere and slab pull could be the main causes of this renewed, late

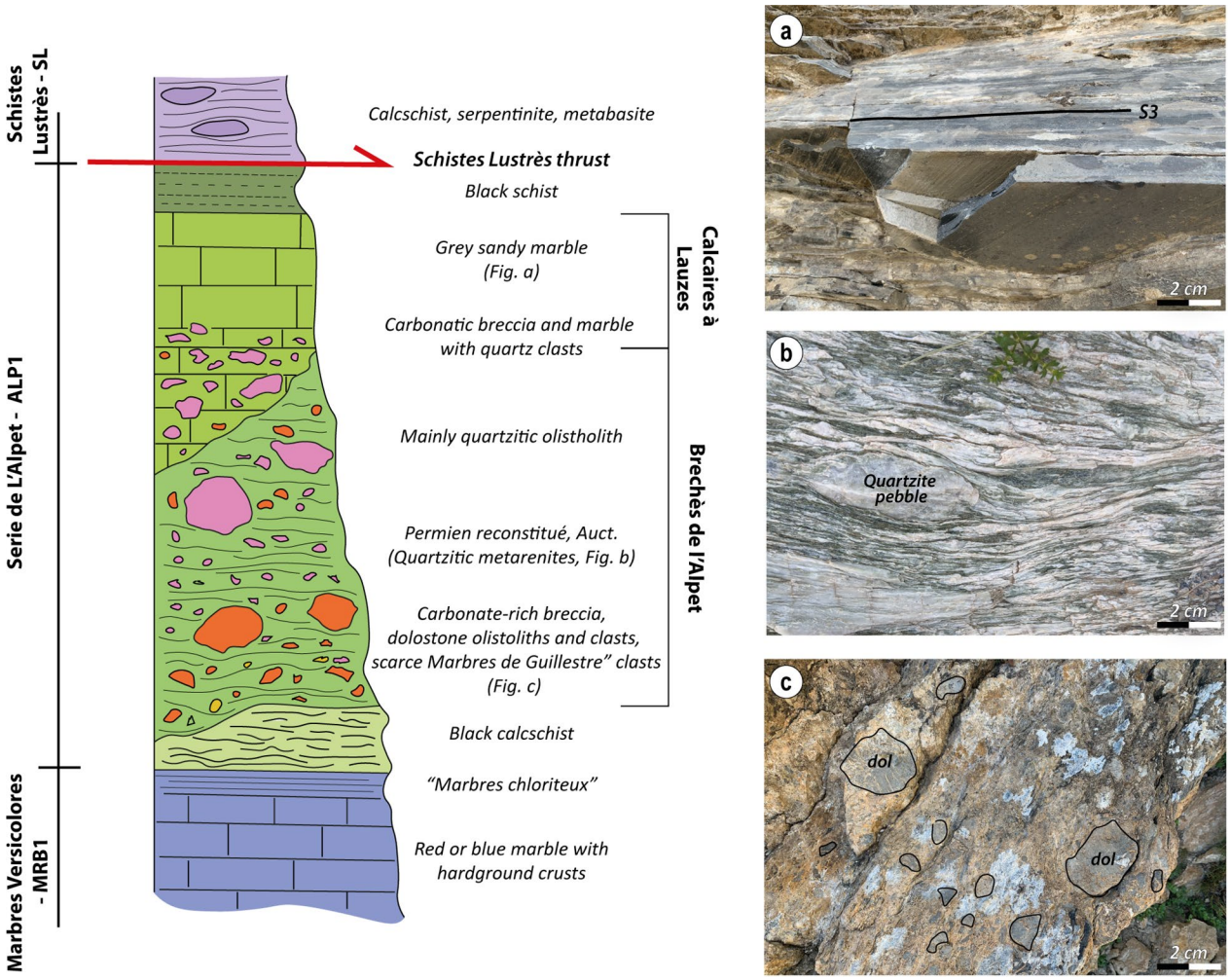

Fig. 16 Simplified stratigraphic column of the "*Série de la Bergerie de L'Alpet*" (Le Guernic, 1966; and this work). The succession is represented as observed and mapped in the type locality (see Additional file 1, where it is overturned and affected by blueschist-facies metamorphism). Thickness and heterometry of the breccia undergo strong lateral variations. The distinction between the black schists belonging to the "*Série de la Bergerie de l'Alpet*" and those referable to the Schistes Lustrés nappe is often hard in the field where serpentinite lenses are missing in the thrust contact. The black calcschist layer following the "*Marbres Chloriteux*" is compared by Le Guernic (1966) to the Eocene Flysch Noir. Three lithotypes are showed in the pictures on the right: **a** Grey sandy marble = "*Calcaires à Lauzes*"; **b** Quarzitic meta-arenite = "*Permien reconstitué*" (Lemoine, 1961); **c** Carbonate-rich breccia with millimetric to decametric dolostone clasts

extension of the Briançonnais passive margin (e.g., Michard et al., 2022, 2023). However, this question remains open and calls for future investigations.

6.2.4 Eocene (c. 45–40 Ma)

During the Bartonian to early Priabonian (Barféty et al., 1992; Kerckhove et al., 2005), "Flysch noir" was deposited in the Briançonnais s.str. units (Fig. 17a), whereas in other cases, "Flysch noir" sedimentation may have already initiated during the Lutetian (Blanchet, 1934; Debelmas, 1955; Gidon, 1962). A few tens to several hundred meters of dark pelites and siliceous sandstones are interpreted to represent terrigenous turbidite sequences deposited beneath the calcite-compensation depth (CCD) in a deep trench that formed after a long period of pelagic sedimentation above the CCD (Kerckhove et al., 2005). Although theoretically deposited in all the Classic Briançonnais units these deposits are only occasionally preserved, mainly north of the studied area. In general, the Eocene rests conformably on the "marbres en plaquettes", particularly in the Peyre Haute and Lower Guil units (Kerckhove et al., 2005; Fig. 2). In the Aiguille de Chambeyron unit, the upper strata of the "marbres en plaquettes" yielded nummulites of Middle to Upper Eocene age (Gidon, 1958), which allows the attribution of the "Flysch noir" to the Bartonian-Priabonian, in the absence

of more precise paleontological data (Gidon et al., 1994; Kerckhove et al., 2005). It is uncertain whether the deposition of the "Flysch noir" also took place in the Acceglio-type units. Le Guernic (1966) interpreted some dark schist levels at the top of the Combe-Brémond unit as corresponding to "Flysch noir", but these units may have already entered the subduction zone at about 45 Ma ago.

6.3 Subduction and exhumation dynamics along the studied transect

After Alpine Tethys became consumed by subduction, also the Briançonnais passive margin started to subduct below the Adria upper plate. During this process, and the subsequent exhumation, individual Briançonnais units became detached from the subducting slab and stacked at various depths (Platt et al., 1989; Michard et al., 2004, 2022). The Classic Briançonnais units, characterized by more complete carbonate sequences and rich in potential decollement levels, likely detached more easily from their underpinnings and remained in a more superficial position. The Acceglio-type units, instead, with minor carbonate cover, would have encountered more difficulties in the process due to the lack of potential detachment levels eroded during Jurassic or Late Cretaceous extension and differential uplift (Ballèvre et al., 2020).

According to Michard et al. (2004), the decoupling process occurred once a critical temperature, allowing for ductile deformation, was reached. For instance, where quartz-rich lithotypes are involved (Roure and Combe-Brémond units), this detachment process may have occurred at around the 300 °C isotherm (corresponding to around 30 km under blueschist facies conditions), i.e., at temperatures close to the ductile–brittle transition of quartz (Stipp & Kunze, 2008; Law, 2014). In Fig. 17b, we show the proposed position of the studied Briançonnais units in the subduction channel. In this qualitative reconstruction, it is assumed that the detachment occurred when each unit reached peak metamorphic conditions. In Fig. 17b, the different units are shown detached and partly stacked during top-to-the-NW thrusting, connected to the D1–D2 deformation phases. We assume that the Briançonnais units were decoupled from their former crustal underpinnings and accreted to the hangingwall of the subduction channel while the decoupled continental basement continued to be underthrust, experiencing higher metamorphic conditions (up to UHP conditions, Chopin, 1984; Manzotti et al., 2022). This subducted continental crust, once exhumed, probably formed the Dora-Maira Massif basement complexes (Michard et al., 1993; Ballèvre et al., 2020). This hypothesis also offers an explanation as to why preserved Mesozoic cover is rarely observed in the Dora-Maira Massif except for rare slices, mainly Lower Triassic quartzites (Michard, 1967), Triassic marbles and Cretaceous calcschists (Marthaler et al., 1986), frequently pinched along major shear zones (Michard et al., 2022). The subsequent step during the exhumation process (Fig. 17c), our D3 event, involves the formation of the orogenic wedge with the stacking of the different units, their refolding and rotation, with the development of backfolds and backthrusts that accommodate wedge shortening. The D3 event is coeval with the fore-thrusting along the Penninic Front (PF) and with extension in the uppermost part of the wedge (Fig. 17c; Bucher et al., 2004; Simon-Labric et al., 2009; Schmid et al., 2017; Michard et al., 2022). The subsequent deformation phase D4, developed under late metamorphic conditions and can be interpreted as linked to the rotation of the orogenic arc of the Western Alps, causing shortening in a N–S direction (Laubscher, 1996; Thomas et al., 1999; Collombet et al., 2002). Late-stage extension in the upper part of the wedge represents the final step of the exhumation process, corresponding to extensional collapse of the wedge and its simultaneous erosion (Tricart & Sue, 2006; Sue et al., 2007).

(See figure on next page.)

Fig. 17 Tectonic evolution of the former Briançonnais passive margin around our study area during Alpine orogeny. During stage (**a**), the External Briançonnais margin (affected by late extension during the Late Cretaceous–Paleocene) is not affected yet by the orogenic deformation, which is limited to the eastern part of the lower plate (Piemonte-Liguria oceanic crust and distal Briançonnais margin). Conversely, stages (**b**) and (**c**) correspond to the tectonic phases D1–D2 and D3 described in this work, respectively. **a** Middle–Late Eocene (45–40 Ma). The External Briançonnais domain is approaching the subduction interface; in continuation of the Late Cretaceous–Paleocene extension, syn-sedimentary extension possibly related to crossing of the forebulge takes place (modified and adapted after Bonnet et al. (2022), Michard and Martinotti (2002), Michard et al. (2022). Note that deposition of "Flysch noir" above the more distal Briançonnais units is uncertain). **b** In the Late Eocene (c. 35 Ma), the Briançonnais units are decoupled and stacked in the subduction channel and in the trench domain (D1–D2 in this study). The overlying accretionary wedge consists of Helminthoid Flysch in its upper/external part and of metamorphic Schistes Lustrés units in its deepest/internal parts (modified after Michard et al., 2004). **c** In the Latest Eocene to Early Oligocene (c. 35–30 Ma) backfolding and backthrusting affected the Briançonnais units (D3 in this study) in the internal part of the wedge (modified after Michard et al., 2004). This internal-ward deformation is nearly coeval with the fore thrusting along the Penninic Front (PF) and with extension in the uppermost part of the wedge (see Bucher et al., 2004, Simon-Labric et al., 2009, Schmid et al., 2017 and Michard et al., 2022). The Helminthoid Flysch nappes, in the footwall of the Penninic Front, are emplaced onto the "Grès d'Annot" basin, dragging slivers of Subbriançonnais and Briançonnais units at their base (Kerckhove, 1969). The Sérenne-Guillestre unit represents that part of the Helminthoid Flysch nappes that remained in the hanging-wall of Penninic Front

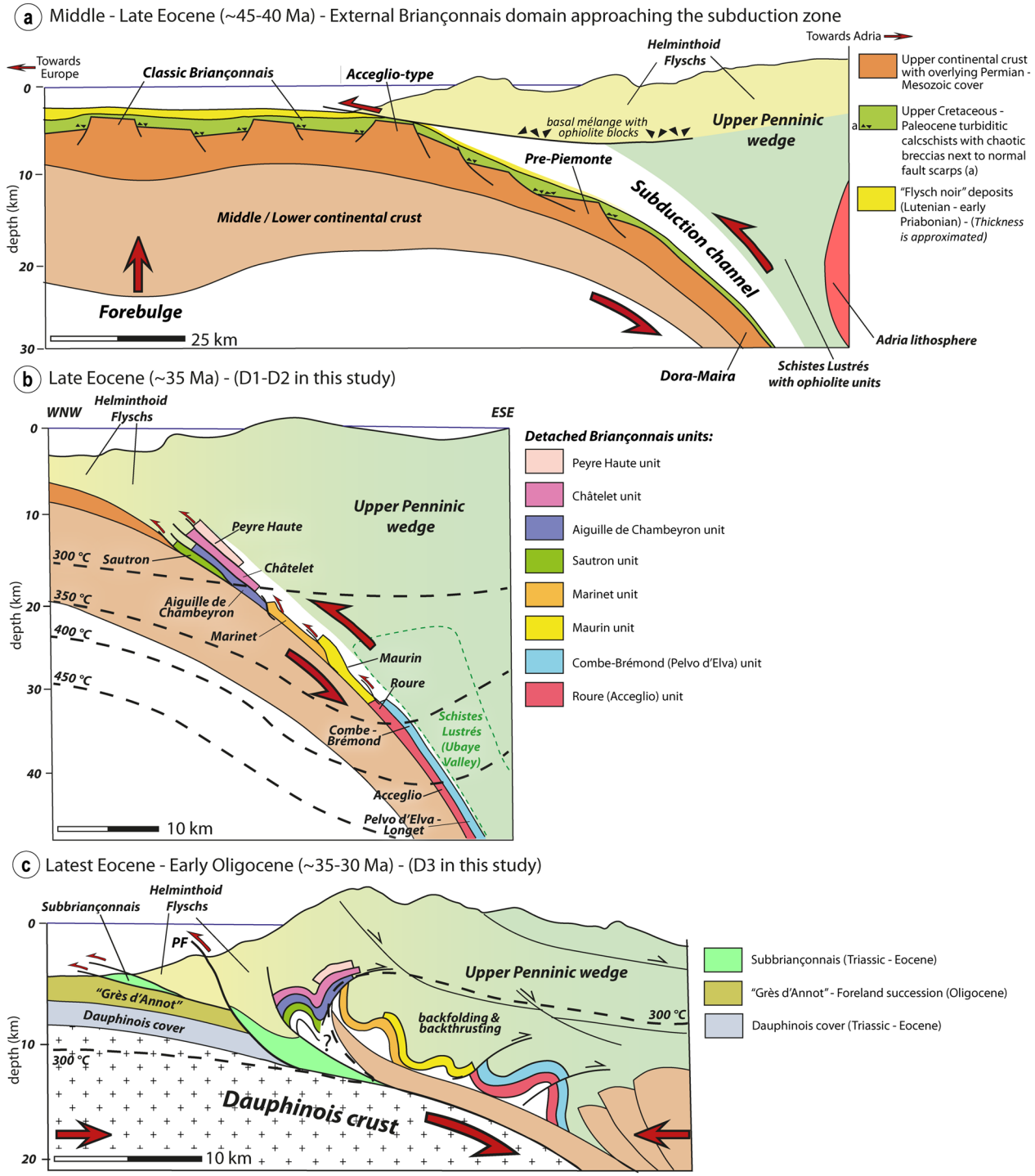

Fig. 17 (See legend on previous page.)

7 Conclusions

We conclude that:

(1) Structures referred to four deformation phases have been recognized. D1-D2 are related to the original fore-thrusting and folding during nappe emplacement and are pervasively overprinted by intense D3 backfolding and backthrusting, associated with greenschist facies recrystallization and linked to the exhumation process.

(2) Metamorphic peak conditions for the studied Briançonnais derived units reached during D1–D2 increase from west to east from greenschist to blueschist facies conditions. Peak thermal conditions were determined by RSCM geothermometry: T_{RSCM} values range from c. 295 °C up to c. 350 °C moving from the most external to the innermost Briançonnais units.
(3) Polygenic chaotic breccia (*Série de la Bergerie de l'Alpet* breccias), as well as several observed paleofaults testify an important late extensional event of Late Cretaceous to Paleocene age associated with the deposition of the "marbres en plaquettes". One of these Late Cretaceous paleo-fault separated the Aiguilles de Mary and Ceillac-Chiappera subunits in our study area. Hence, we propose to group these two subunits into a major Alpine tectonic unit, referred to as Maurin unit.
(4) Folded pre-D3 tectonic contacts have been recognized and after restoration reveal a top-to-the-W sense of shear, preserved in low D3 strain domains.
(5) In general, top-to-the-NE kinematics, associated with D3 backfolding and backthrusting is the dominant deformation event whose intensity is frequently underestimated.

Supplementary Information

The online version contains supplementary material available at https://doi.org/10.1186/s00015-023-00445-0.

Additional file 1: Geological-Structural Map of the Aiguille de Chambeyron-Dents de Maniglia Massif (France, Italy).

Additional file 2: Remarks regarding the definition of the Briançonnais s.l. units in the southern French-Italian Alps. **Fig. S1**. Simplified stratigraphy of the different unit types studied in this work (modified from Michard et al., 2022). **Fig. S2.** Structural map of the south Western Alps tectonic units based on Debelmas & Lemoine (1966); Malaroda et al. (1970); Tricart (1980); Gidon et al. (1994, 1975); Barféty et al. (1995); Claudel (1999); Michard et al. (2004, 2022); Kerckhove et al. (2005)

Additional file 3: Sample list, metamorphism and deformation phases in the High Ubaye–Maira valleys. **Table S1.** Location and main features of key-selected samples studied for microstructural analysis. Only the samples discussed in this paper are reported. The samples used for Raman spectroscopy of carbonaceous material are listed in Table S2. **Table S2.** Result of RSCM thermometry performed on the listed samples. Number of spectra (N), mean RA1 ratio (Lahfid et al., 2010) for N spectra with corresponding standard deviation (Stand. Dev.), and calculated temperature with standard error (SE). **Table S3.** The tectono-metamorphic evolution of the classic Briançonnais and adjoining units: comparing our results with ten earlier publications. The most significant differences are highlighted here and discussed in the main text.

Acknowledgements
We warmly thank Jean-Pierre Bouillin for sharing with us useful information on the geology of the area and Marco Vignolo who accompanied one of us (DD) during part of the geological mapping. Chiara Montomoli and Rodolfo Carosi (Unito) are thanked for their suggestions on the early drafts of the attached geological map. Giancarlo Molli and Michel Ballèvre are thanked for their revisions that greatly helped to improve the manuscript. We also thank Jean-Luc Epard for editorial handling of this paper.

Author contributions
DD, SI carried out geological mapping guided by the advice of AM, who investigated the area in the '70-'80, and by SMS who detected suspected paleofaults. DD, SI and SMS took the samples. DD and SI performed the microtectonics study (with precious insights from SMS) and acquired the microscope images. DD acquired the RSCM spectra with the supervision of AP, and with the help of SI interpreted the RSCM data. The paper has been written by DD, SI, AM and SMS; the figures drawn by DD (SMS contributed significantly to Figs. 2 and 3, AM to Figs. 4 and 15, AM, SMS and SI to Fig. 17). All the authors read and approved the final manuscript.

Funding
The field work has been done on their own salary by the Authors.

Availability of data and materials
All data generated or analysed during this study are included in this article and its Additional files.

Declarations

Competing interests
The authors declare that they have no competing interests.

Author details
[1]Dipartimento di Scienze Della Terra, Università di Torino, via Valperga Caluso 35, 10125 Turin, Italy. [2]Institut für Geophysik, ETH-Zürich, Sonneggstr. 5, 8092 Zurich, Switzerland. [3]Université Paris-Saclay, 10 rue des Jeûneurs, 75002 Paris, France.

Received: 23 May 2023 Accepted: 5 October 2023
Published online: 21 November 2023

References

Agard, P. (2021). Subduction of oceanic lithosphere in the Alps: selective and archetypal from (slow-spreading) oceans. *Earth Science Reviews*. https://doi.org/10.1016/j.earscirev.2021.103517
Agard, P., Goffé, B., Touret, J. L., & Vidal, O. (2000). Retrograde mineral and fluid evolution in high-pressure metapelites (Schistes lustrés unit, Western Alps). *Contributions to Mineralogy and Petrology, 140*, 296–315.
Agard, P., Jolivet, L., & Goffe, B. (2001). Tectonometamorphic evolution of the Schistes Lustrés Complex; implications for the exhumation of HP and UHP rocks in the Western Alps. *Bulletin de la Société Géologique de France, 172*(5), 617–636.
Agard, P., Monie, P., Jolivet, L., & Goffe, B. (2002). Exhumation of the Schistes Lustrés complex: In situ laser probe $^{40}Ar/^{39}Ar$ constraints and implications for the Western Alps. *Journal of Metamorphic Geology, 20*, 599–618.
Angiboust, S., Glodny, J., Oncken, O., & Chopin, C. (2014). In search of transient subduction interfaces in the Dent Blanche-Sesia Tectonic System (W. Alps). *Lithos, 205*, 298–321. https://doi.org/10.1016/j.lithos.2014.07.001
Angiboust, S., Langdon, R., Agard, P., Waters, D., & Chopin, C. (2012). Eclogitization of the Monviso ophiolite (W. Alps) and implications on subduction dynamics. *Journal of Metamorphic Geology, 30*(1), 37–61. https://doi.org/10.1111/j.1525-1314.2011.00951.x
Argand, E. (1924). La tectonique de l'Asie. *Proceedings of the International Geological Congress, XIII*, 171–372.
Ballèvre, M., Camonin, A., Manzotti, P., & Poujol, M. (2020). A step towards unraveling the paleogeographic attribution of pre-Mesozoic basement complexes in the Western Alps based on U-Pb geochronology of Permian magmatism. *Swiss Jornal of Geoscience*. https://doi.org/10.1186/s00015-020-00367-1
Ballèvre, M., Manzotti, P., & Dal Piaz, G. V. (2018). Pre-Alpine (Variscan) inheritance: A key for the location of the future Valaisan Basin (Western Alps). *Tectonics, 37*(3), 786–817. https://doi.org/10.1002/2017TC004633

Barber, D. J., & Wenk, H. R. (2001). Slip and dislocation behaviour in dolomite. *European Journal of Mineralogy, 13*(2), 221–243.
Barfety, J. (1965). *Etude géologique des environs du Monétier-les-Bains (HA) (Zones subbriançonnaise et briançonnaise)-Alpes françaises*. PhD Thesis. Université de Grenoble.
Barféty, J., Lemoine, M., de Graciansky, P., Tricart, P., & Mercier, D. (1995). *Notice explicative, Carte géologique France (1/50000), feuille Briançon (823)*. BRGM.
Barféty, J. C., Tricart, P., & Jeudy de Grissac, C. (1992). La quatrième-écaille prés de Briançon (Alpes Françaises): un olistostrome précurseur de l'orogenèse pennique éocène. Comptes rendus de l'Académie des sciences. Série 2, Mécanique, Physique, Chimie, Sciences de l'univers, Sciences de la Terre, 314(1), 71-76.
Baud, A., & Mégard-Galli, J. (1975). Modèle d'évolution d'un bassin carbonaté du domaine alpin durant la phase préocéanique: cycles et rythmes dans le Trias de la zone briançonnaise des Alpes occidentales et des Préalpes. In: *Proceeding of the 9th International Sedimentological Congress*, Nice, 5(1), 45–50.
Bellahsen, N., Mouthereau, F., Boutoux, A., Bellanger, M., Lacombe, O., Jolivet, L., & Rolland, Y. (2014). Collision kinematics in the western external Alps. *Tectonics, 33*(6), 1055–1088.
Bellanger, M., Bellahsen, N., Jolivet, L., Baudin, T., Augier, R., & Boutoux, A. (2014). Basement shear zones development and shortening kinematics in the Ecrins Massif. *Western Alps. Tectonics, 33*(2), 84–111. https://doi.org/10.1002/2013TC003294
Beltrando, M., Frasca, G., Compagnoni, R., & Vitale-Brovarone, A. (2012). The Valaisan controversy revisited: Multi-stage folding of a Mesozoic hyperextended margin in the Petit St. Bernard pass area (Western Alps). *Tectonophysics, 579*, 17–36. https://doi.org/10.1016/j.tecto.2012.02.010
Beltrando, M., Stockli, D. F., Decarlis, A., & Manatschal, G. (2015). A crustal-scale view at rift localization along the fossil Adriatic margin of the Alpine Tethys preserved in NW Italy. *Tectonics, 34*(9), 1927–1951.
Bergomi, M. A., Dal Piaz, G. V., Malusà, M. G., Monopoli, B., & Tunesi, A. (2017). The Grand St Bernard-Briançonnais nappe system and the Paleozoic inheritance of the Western Alps unraveled by zircon U-Pb dating. *Tectonics, 36*(12), 2950–2972. https://doi.org/10.1002/2017TC004621
Bertok, C., Martire, L., Perotti, E., d'Atri, A., & Piana, F. (2012). Kilometre-scale palaeoescarpments as evidence for Cretaceous synsedimentary tectonics in the External Briançonnais Domain (Ligurian Alps, Italy). *Sedimentary Geology, 251*, 58–75. https://doi.org/10.1016/j.sedgeo.2012.01.012
Bestmann, M., & Prior, D. J. (2003). Intragranular dynamic recrystallization in naturally deformed calcite marble: Diffusion accommodated grain boundary sliding as a result of subgrain rotation recrystallization. *Journal of Structural Geology, 25*(10), 1597–1613.
Beyssac, O., Goffé, B., Chopin, C., & Rouzaud, J. N. (2002a). Raman spectra of carbonaceous material in metasediments: A new geothermometer. *Journal of Metamorphic Geology, 20*(9), 859–871.
Beyssac, O., Rouzaud, J., Goffé, B., Brunet, F., & Chopin, C. (2002b). Graphitization in a high-pressure, low-temperature metamorphic gradient: A Raman microspectroscopy and HRTEM study. *Contributions to Mineralogy and Petrology, 143*(1), 19–31.
Bilau, A., Rolland, Y., Schwartz, S., Godeau, N., Guihou, A., Deschamps, P., Brigaud, B., Noret, A., Dumont, T., & Gautheron, C. (2021). Extensional reactivation of the Penninic frontal thrust 3 Myr ago as evidenced by U-Pb dating on calcite in fault zone cataclasite. *Solid Earth, 12*, 237–251. https://doi.org/10.5194/se-12-237-2021
Blanchet, F. (1934). *Étude géologique des Montagnes d'Escreins*. PhD Thesis. Université de Grenoble.
Bonini, L., Dallagiovanna, G., & Seno, S. (2010). The role of pre-existing faults in the structural evolution of thrust systems: Insights from the Ligurian Alps (Italy). *Tectonophysics, 480*(1–4), 73–87.
Bonnet, G., Chopin, C., Locatelli, M., Kylander-Clark, A. R., & Hacker, B. R. (2022). Protracted subduction of the European hyperextended margin revealed by rutile U-Pb geochronology across the Dora-Maira Massif (Western Alps). *Tectonics, 41*(4), e2021TC007170.
Borghi, A., Cadoppi, P., Porro, A., Sacchi, R., & Sandrone, R. (1984). Osservazioni geologiche nella Val Germanasca et nella media Val Chisone (Alpi Cozie). *Bollettino-Museo Regionale di Scienze Naturali, 2*(2), 503–530.
Bourbon, M., Caron, J. M., De Graciansky, P. C., Lemoine, M., Megard-Galli, J., & Mercier, D. (1977). Mesozoic evolution of the Western Alps: birth and development of part of the spreading oceanic Tethys and of its European continental margin. In B. Biju-Duval & L. Montadert (Eds.), *Structural History of the Mediterranean basins* (pp. 19–34). Editions Technip Paris.
Bousquet, R., Oberhänsli, R., Goffé, B., Wiederker, M., Koller, F., Schmid, S. M., Schuster, R., Engi, M., Berger, A., & Martinotti, G. (2008). Metamorphism of metasediments at the scale of an orogen: A key to the Tertiary geodynamic evolution of the Alps. *Geological Society of London Special Publications, 298*, 393–411. https://doi.org/10.1144/SP298.18
Brady, J. B., Markley, M. J., Schumacher, J. C., Cheney, J. T., & Bianciardi, G. A. (2004). Aragonite pseudomorphs in high-pressure marbles of Syros, Greece. *Journal of Structural Geology, 26*(1), 3–9.
Bucher, S., Ulardic, C., Bousquet, R., Ceriani, S., Fügenschuh, B., Gouffon, Y., & Schmid, S. M. (2004). Tectonic evolution of the Briançonnais units along a transect (ECORS-CROP) through the Italian-French Western Alps. *Eclogae Geologicae Helvetiae, 97*, 321-345.
Caby, R. (1996). Low-angle extrusion of high-pressure rocks and the balance between outward and inward displacements of Middle Penninic units in the western Alps. *Eclogae Geologicae Helvetiae, 89*(1), 229–268.
Carminati, E., & Gosso, G. (2000). Structural map of a Ligurian Briançonnais cover nappe (Conca delle Carsene, Monte Marguareis, Ligurian Alps, Italy) and explanatory notes. *Memorie Della Società Geologica Italiana, 52*, 93–99.
Caron, J.-M., Schumacher, F., & Tricart, P. (1973). Chronologie et évolution longitudinale des structures dans les Schistes lustrés piémontais des Alpes cottiennes (France et Italie). *Sciences Géologiques Bulletin, 26*, 245–258.
Ceriani, S., Fügenschuh, B., & Schmid, S. M. (2001). Multi-stage thrusting at the "Penninic Front" in the Western Alps between Mont Blanc and Pelvoux massifs. *International Journal of Earth Sciences, 90*(3), 685–702.
Chopin, C. (1984). Coesite and pure pyrope in high-grade blueschists of the Western Alps: A first record and some consequences. *Contribution to Mineralogy and Petrology, 86*, 107–118.
Choukroune, P., Ballèvre, M., Cobbold, P., Gautier, Y., Merle, O., & Vuichard, J. P. (1986). Deformation and motion in the Western Alpine arc. *Tectonics, 5*(2), 215–226.
Claudel, M. (1999). *Reconstitution paléogéographique du domaine briançonnais au Mésozoïque. Ouvertures océaniques et raccourcissements croisés*. PhD Thesis. Université Joseph-Fourier Grenoble.
Claudel, M., & Dumont, T. (1999). A record of multistage continental break-up on the Briançonnais marginal plateau (Western Alps): Early and Middle-Late Jurassic rifting. *Eclogae Geologicae Helvetiae, 92*(1), 45–61.
Claudel, M. E., Dumont, T., & Tricart, P. (1997). Une preuve d'extension contemporaine de l'expansion océanique de la Téthys ligure en Briançonnais: Les failles du Vallon Laugier. *Comptes Rendus de l'académie des Sciences-Series IIA-Earth and Planetary Science, 325*(4), 273–279.
Collombet, M., Thomas, J., Chauvin, A., Tricart, P., Boullin, J., & Gratier, J. P. (2002). Counterclockwise rotation of the western Alps since the Oligocene: New insights from paleomagnetic data. *Tectonics, 21*(4), 14–21. https://doi.org/10.1029/2001TC901016
Cordey, F., & Bailly, A. (2007). Alpine ocean seafloor spreading and onset of pelagic sedimentation: New radiolarian data from the Chenaillet-Montgenèvre ophiolite (French-Italian Alps). *Geodinamica Acta, 20*(3), 131–138. https://doi.org/10.3166/ga.20.131-138
Corno, A., Groppo, C., Borghi, A., Mosca, P., & Gattiglio, M. (2023). To be or not to be Alpine: New petrological constraints on the metamorphism of the Chenaillet Ophiolite (Western Alps). *Journal of Metamorphic Geology*. https://doi.org/10.1111/jmg.12716
D'Atri, A., Piana, F., Barale, L., Bertok, C., & Martire, L. (2016). Geological setting of the southern termination of Western Alps. *International Journal of Earth Sciences, 105*(6), 1831–1858. https://doi.org/10.1007/s00531-015-1277-9
Dal Piaz, G. V. (2010). The Italian Alps: a journey across two centuries of Alpine geology. *Journal of the Virtual Explorer*. https://doi.org/10.3809/jvirtex.2010.00234
Dal Piaz, G. V., Bistacchi, A., & Massironi, M. (2003). Geological outline of the Alps. *Episodes, XXVI*(3), 175–180.
Debelmas, J., & Lemoine, M. (1966). *Carte géologique de la France au 1/50 000, feuille Guillestre (847)*. Service de la Carte géologique de France.
Debelmas, J. (1982). Structure profonde de la Zone Brianconnaise dans la Vallee du Guil (Hautes Alpes). In *Alpes de Savoie*. Elsevier Masson.
Debelmas, J. (1955). *Les zones subbriançonnaise et briançonnaise occidentale entre Vallouise et Guillestre (Hautes-Alpes)*. Imprimerie Nationale.

Debelmas, J., & Kerckhove, C. (1980). Les alpes Franco-Italiennes. *Géologie Alpine, 56*, 21–58.
Debelmas, J., & Lemoine, M. (1957). Calcschistes piémontais et terrain à faciès briançonnais dans les hautes vallées de la Maira et de la Varaita (Alpes cottiennes), Italie. *Compte-rendu sommaire des séances de la Société Géologique de France, 3*(38), 40.
Decarlis, A., Dallagiovanna, G., Lualdi, A., Maino, M., & Seno, S. (2013). Stratigraphic evolution in the Ligurian Alps between Variscan heritages and the Alpine Tethys opening: A review. *Earth-Science Reviews, 125*, 43–68.
Delchini, S., Lahfid, A., Plunder, A., & Michard, A. (2016). Applicability of the RSCM geothermometry approach in a complex tectono-metamorphic context: The Jebilet massif case study (Variscan Belt, Morocco). *Lithos, 256*, 1–12. https://doi.org/10.1016/j.lithos.2016.04.007
Deville, E. (1987). *Etude géologique en Vanoise orientale (Alpes occidentales françaises, Savoie). De la naissance à la structuration d'un secteur de la paléomarge européennee et de l'océan Tethysien: aspects stratigraphiques, pétrographiques et tectoniques*. PhD Thesis. Université de Savoie.
Dumont, T. (1984). Le Rhetien et le Lias inferieur prepiemontais: Enregistrement sedimentaire du passage des carbonates de plate-forme triasiques au Jurassique hemipelagique lors du debut du rifting tethysien. *Géologie Alpine, 60*, 13–25.
Dumont, T., Lemoine, M., & Tricart, P. (1984). Tectonique synsédimentaire triasico-jurassique et rifting téthysien dans l'unité prépiémontaise de Rochebrune au Sud-Est de Briançon. *Bulletin de la Société Géologique de France, 7*(26), 921–933.
Dumont, T., Schwartz, S., Guillot, S., Malusa, M., Jouvent, M., Monié, P., & Verly, A. (2022). Cross-propagation of the western Alpine orogen from early to late deformation stages: Evidence from the Internal Zones and implications for restoration. *Earth-Science Reviews*. https://doi.org/10.1016/j.earscirev.2022.104106
Dumont, T., Schwartz, S., Guillot, S., Simon-Labric, T., Tricart, P., & Jourdan, S. (2012). Structural and sedimentary records of the Oligocene revolution in the Western Alpine arc. *Journal of Geodynamics, 56*, 18–38. https://doi.org/10.1016/j.jog.2011.11.006
Ellenberger, F. (1958). Etude geologique du pays de Vanoise. Memoires du Service de la Carte Geologique de la France, Imprimerie Nationale, Paris, (pp. 561).
Engi, M., Giuntoli, F., Lanari, P., Burn, M., Kunz, B., & Bouvier, A. S. (2018). Pervasive eclogitization due to brittle deformation and rehydration of subducted basement: Effects on continental recycling? *Geochemistry, Geophysics, Geosystems, 19*(3), 865–881.
Escher, A., Masson, H., & Steck, A. (1988). *Coupes géologiques des Alpes occidentales suisses*. Mémoires de géologie.
Faure, J., & Megard-Galli, J. (1988). L'émersion Jurassique en Brianconnais; sédimentation continentale et fracturation distensive. *Bulletin de la Société Géologique de France, 4*, 681–692.
Faure-Muret, A. & Fallot, P. (1955). Sur le Secondaire et le Tertiaire aux abords sud-orientaux du Massif de l'Argentera-Mercantour: Feuille de Saint-Martin-Vésubie, Tende et Vièvе au 50'000. Béranger.
Ferril, D. A., Morris, A. P., Evans, M. A., Burkhard, M., Groshong, J., & Ornasch, C. M. (2004). Calcite twin morphology: A low-temperature deformation geothermometer. *Journal of Structural Geology, 26*(8), 1521–1529.
Feys, R. (1954). *Etude géologique du Carbonifère briançonnais, Hautes Alpes–Alpes françaises*. France: Thèse d'Etat, Université de Paris.
Fossen, H. (2016). *Structural geology* (2nd ed.). Cambridge University Press.
Franchi, S. (1898). Sull'eta mesozoica della zona delle Pietre Verdi nelle Alpi occidentali. *Bollettino del Reale Comitato Geologico d'Italia, 29*, 173–247.
Frisch, W. (1979). Tectonic progradation and plate tectonic evolution of the Alps. *Tectonophysics, 60*(3–4), 121–139.
Gabalda, S., Beyssac, O., Jolivet, L., Agard, P., & Chopin, C. (2009). Thermal structure of a fossil subduction wedge in the Western Alps. *Terra Nova, 21*(1), 28–34. https://doi.org/10.1111/j.1365-3121.2008.00849.x
Gaillet, J. L. (1976). *Géologie structurale de la zone briançonnaise orientale en haut val Grana: Alpes cottiennes méridionales*. Italie (Doctoral dissertation, Université Paris Sud-Paris XI).
Galli, J. (1964). *Etude stratigraphique et tectonique du Monte Boulliagna (Haut Val d'Acceglio, Italie)*. PhD thesis. Université de Paris. https://theses.hal.science/tel-00795404. Accessed 31 July 2023.
Gebauer, D. H. P. S., Schertl, H. P., Brix, M., & Schreyer, W. (1997). 35 Ma old ultrahigh-pressure metamorphism and evidence for very rapid exhumation in the Dora Maira Massif, Western Alps. *Lithos, 41*(1–3), 5–24.
Gerber, W. (2008). *Evolution tectono-metamorphique du Brianconnais interne (Alpes Occidentales, massifs de Vanoise Sud et d'Ambin): comportement du socle et de sa couverture dans un contexte de subduction continentale profonde*. PhD thesis Universite P. & M. Curie, Paris, 1–272. https://tel.archives-ouvertes.fr/tel-00340057. Accessed 31 July 2023.
Gerogiannis, N., Aravadinou, E., Chatzaras, V., & Xypolias, P. (2021). Calcite pseudomorphs after aragonite: A tool to unravel the structural history of high-pressure marbles (Evia Island, Greece). *Journal of Structural Geology, 148*, 104373. https://doi.org/10.1016/j.jsg.2021.104373
Ghignone, S., Scaramuzzo, E., Bruno, M., & Livio, F. A. (2023). A new UHP unit in the Western Alps: First occurrence of coesite from the Monviso Massif (Italy). *American Mineralogist, 108*(7), 1368–1375.
Gidon, M. (1958). *La zone briançonnaise en Haute Ubaye (Basses Alpes) et son prolongement au sud-est - Alpes françaises et italiennes*. Thèse d'Etat, Faculté des Sciences de l'Université de Grenoble, France.
Gidon, M. (1962). La zone brianconnaise en Haute Ubaye (Basses-Alpes) et son prolongement au SE. *Mem. expl. Carte geologique detaillee France,* Ministere Industrie, Paris, pp. 1–272.
Gidon, M., et al. (1977). *Carte geologique de France au 1/50 000, feuille Larche. Notice explicative* (p. 28). Bureau de Recherches Géologiques et Minières.
Gidon, M., Kerckhove, C., Michard, A., Tricart, P., Gotteland, P., Gout, C., Leblanc, D., Lefèvre, R., Le Guernic, J., Megard-Galli, J., & Michel-Noel, G. (1994). *Carte geologique de France 1/50 000, feuille Aiguille de Chambeyron. Notice explicative* (p. 90). Bureau de Recherches Géologiques et Minières.
Gilio, M., Scambelluri, M., Agostini, S., Godard, M., Pettke, T., Agard, P., Locatelli, M., & Angiboust, S. (2020). Fingerprinting and relocating tectonic slices along the plate interface: Evidence from the Lago Superiore unit at Monviso (Western Alps). *Lithos, 352*, 105308. https://doi.org/10.1016/j.lithos.2019.105308
Goffe, B., & Chopin, C. (1986). High-pressure metamorphism in the Western Alps: Zoneography of metapelites, chronology and consequences. *Schweizerische Mineralogische und Petrographische Mitteilungen, 66*(1–2), 41–52.
Handy, M. L., Schmid, S. M., Bousquet, R., Kissling, E., & Bernoulli, D. (2010). Reconciling plate-tectonic reconstructions of Alpine Tethys with the geological–geophysical record of spreading and subduction in the Alps. *Earth-Science Reviews, 102*(3–4), 121–158. https://doi.org/10.1016/j.earscirev.2010.06.002
Henry, C., Michard, A., & Chopin, C. (1993). Geometry and structural evolution of ultra-high-pressure and highpressure rocks from the Dora-Maira massif, Western Alps, Italy. *Journal of Structural Geology, XV*(8), 965–981. https://doi.org/10.1016/0191-8141(93)90170-F
Herviou, C., Agard, P., Plunder, A., Mendes, K., Verlaguet, A., Deldicque, D., & Cubas, N. (2022). Subducted fragments of the Liguro-Piemont ocean, Western Alps: Spatial correlations and offscraping mechanisms during subduction. *Tectonophysics, 827*, 229–267. https://doi.org/10.1016/j.tecto.2022.229267
ISPRA. (2022). Aggiornamento e integrazioni delle linee guida per la realizzazione della Carta Geologica d'Italia alla scala 1:50.000 Progetto CARG. *Quaderni del Servizio Geologico d'Italia, 15*, 1–261.
Jaillard, E. (1988). Une image paleogeographique de la Vanoise brianconnaise. *Eclogae Geologicae Helvetiae, 81*, 553–566.
Kerckhove, C., Bourbon, M., & Chenet, P.-Y. (1984). Alpes: Zones internes durandiennes (nappes de l'Embrunais-Ubaye et Brianconnais). Livret-guide d'Excursion du Groupe francais du Cretace, GFC 1984, Serie" Excursion", *93*, hal-00742146.
Kerckhove, C. (1969). La "zone du Flysch" dans les nappes de l'Embrunais-Ubaye (Alpes occidentales). *Géologie Alpine, 45*, 5–204.
Kerckhove, C., Gidon, M., & Pairis, J. (2005). *Notice explicative, Carte géol France (1/50 000) Embrun-Guillestre (2e édition, coupure spéciale) (871)* (p. 139). BRGM.
Lagabrielle, Y., & Cannat, M. (1990). Alpine Jurassic ophiolites resemble the modern central Atlantic basement. *Geology, 18*(4), 319–322.
Lahfid, A., Beyssac, O., Deville, E., Negro, F., Chopin, C., & Goffé, B. (2010). Evolution of the Raman spectrum of carbonaceous material in low-grade metasediments of the Glarus Alps (Switzerland). *Terra Nova, 22*(5), 354–360.
Lanari, P. (2009). *Analyse structurale et métamorphique des métasédiments de la zone Briançonnaise au SE du Pelvoux (Briançon, Guillestre, Alpes Occidentales)*. Grenoble: PhD thesis, Univ. Joseph-Fourier.

Lanari, P., Guillot, S., Schwartz, S., Vidal, O., Tricart, P., Riel, N., & Beyssac, O. (2012). Diachronous evolution of the alpine continental subduction wedge: Evidence from P-T estimates in the Briançonnais Zone houillère (France–Western Alps). *Journal of Geodynamics, 56*, 39–54.
Laubscher, H. (1988). Material balance in Alpine orogeny. *Geological Society of America Bulletin, 100*(9), 1313–1328.
Laubscher, H. (1991). The arc of the Western Alps today. *Eclogae Geoligicae Helvetiae, 84*(3), 631–659.
Laubscher, H. (1996). Shallow and deep rotations in the Miocene Alps. *Tectonics, 15*(5), 1022–1035.
Law, R. D. (2014). Deformation thermometry based on quartz c-axis fabrics and recrystallization microstructures: A review. *Journal of Structural Geology, 66*, 129–161. https://doi.org/10.1016/j.jsg.2014.05.023
Le Guernic, J. (1966). *Etude géologique des limites du Briançonnais et du Piémontais entre le Cristillan et la Maira: "zone du Roure"*. PhD thesis, Université de Grenoble, France.
Le Guernic, J. (1967). La zone du Roure: Contribution à l'étude du Briançonnais interne et du Piémontais en haute Ubaye. *Travaux du Laboratoire de Géologie de la Faculté des Sciences de Grenoble, 43*, 95–127.
Leblanc, D. (1962). *Etude géologique de la région du col du Longet (Alpes cottiennes franco-italiennes)*. PhD Thesis. France: Université de Paris.
Lefèvre, R. (1982). *Les nappes briançonnaises internes et ultrabriançonnaises dans les Alpes cottiennes méridionales*. PhD Thesis. France: Université Paris Sud-Paris XI.
Lefèvre, R. (1968). La structure et le style tectonique de la bande d'Acceglio en Val Maira (Alpes cottiennes italiennes). *Géologie Alpine, 44*, 141–151.
Lefèvre, R., & Michard, A. (1976). Les nappes briançonnaises internes et ultrabriançonnaises de la Bande d'Acceglio (Alpes franco-italiennes): Une étude structurale et pétrographique dans le faciès des Schistes bleus à jadéite. *Sciences Géologiques, Bulletins et Mémoires, 29*(3), 183–222.
Lemoine, M. (1960). Découverte d'une microfaune du Crétacé supérieur au col du Longet (sources de l'Ubaye, Basses-Alpes); conséquences tectoniques et paléogéographiques. *C. R. somm. S.G.F*, 5, 97.
Lemoine, M. (1961). Le Briançonnais interne et le bord de la zone des schistes lustrés dans les vallées du Guil et de l'Ubaye (Hautes et Basse-Alpes). *Travaux du Laboratoire de Géologie de la Faculté des Sciences de Grenoble, 37*, 97–119.
Lemoine, M. (1964). Le problème des relations des schistes lustrés piémontais avec la zone briançonnaise dans les Alpes cottiennes. *Geologische Rundschau, 54*, 113–132.
Lemoine, M. (1967). Brèches sédimentaires marines à la frontière entre les domaines briançonnais et piémontais dans les Alpes occidentales. *Geologische Rundschau, 56*(1), 320–335.
Lemoine, M., Bas, T., Arnaud-Vanneau, A., Arnaud, H., Dumont, T., Gidon, M., Bourbon, M., de Graciansky, P., Rudkiewicz, J. L., Megard-Galli, J., & Tricart, P. (1986). The continental margin of the Mesozoic Tethys in the Western Alps. *Marine and Petroleum Geology, 3*(3), 179–199.
Lemoine, M., Bourboun, M., & Tricart, P. (1978). Le Jurassique et le Crétacé prépiémontais à l'Est de Briançon (Alpes occidentales) et l'évolution de la marge européenne de la Téthys: Données nouvelles et conséquences. *Comptes Rendus de l'académie des Sciences Paris, 286*, 1237–1240.
Lemoine, M., de Graciansky, P. C., & Tricart, P. (2000). *De l'océan à la chaîne de montagnes: Tectonique des plaques dans les Alpes* (pp. 1–207). Gordon and Breach Science Publishers.
Locatelli, M., Verlaguet, A., Agard, P., Federico, L., & Angiboust, S. (2018). Intermediate-depth brecciation along the subduction plate interface (Monviso eclogite, W. Alps). *Lithos, 320*, 378–402.
Lonchampt, D. (1962). Etude géologique du volcanisme permien du Guil, de la Haute -Ubaye et Haute Maira-Alpes franco-italiennes. Faculté des Sciences de l'Université de Grenoble, France.
Loprieno, A., Bousquet, R., Bucher, S., Ceriani, S., Dalla Torre, F. H., Fügenschuh, B., & Schmid, S. M. (2011). The Valais units in Savoy (France): A key area for understanding the palaeogeography and the tectonic evolution of the Western Alps. *International Journal of Earth Sciences, 100*(5), 963–992. https://doi.org/10.1007/s00531-010-0595-1
Lualdi, A. (1985). Elementi di correlazione in serie medio triassiche del brianzonese s.s., brianzonese ligure e prepiemontese. *Rendiconti Della Società Geologica Italiana, 8*, 43–46.
Malaroda, R., Carraro, F., Dal Piaz, G., Franceschetti, B., Sturani, C., & Zanella, E. (1970). Carta geologica del Massiccio dell'Argentera alla scala 1:50.000. *Memorie della Società Geologica Italiana, 9*(4), 557–663.
Manatschal, G., Sauter, D., Karpoff, A. M., Masini, E., Mohn, G., & Lagabrielle, Y. (2011). The Chenaillet Ophiolite in the French/Italian Alps: An ancient analogue for an oceanic core complex? *Lithos, 124*(3–4), 169–184.
Manzotti, P., Ballèvre, M., & Dal Piaz, G. (2018). Pre-Alpine (Variscan) inheritance: A key for the location of the future valaisan basin (Western Alps). *Tectonics, 37*(3), 786.
Manzotti, P., Ballèvre, M., & Poujol, M. (2016). Detrital zircon geochronology in the Dora-Maira and Zone Houillère: A record of sediment travel paths in the Carboniferous. *Terra Nova, 28*(4), 279–288. https://doi.org/10.1111/ter.12219
Manzotti, P., Ballèvre, M., Zucali, M., Robyr, M., & Engi, M. (2014). The tectono-metamorphic evolution of the Sesia-Dent Blanche nappes (internal Western Alps): Review and synthesis. *Swiss Journal of Geosciences, 107*(2), 309–336.
Manzotti, P., Schiavi, F., Nosenzo, F., Pitra, P., & Ballèvre, M. (2022). A journey towards the forbidden zone: A new, cold, UHP unit in the Dora-Maira Massif (Western Alps). *Contributions to Mineralogy and Petrology, 177*(6), 1–22. https://doi.org/10.1007/s00410-022-01923-8
Marthaler, M., Fudral, S., Deville, E., & Rampnoux, J. P. (1986). Mise en évidence du Crétacé supérieur dans la couverture septentrionale de Dora Maira, région de Suse, Italie (Alpes occidentales). Conséquences paléogéographiques et structurales. *Comptes rendus de l'Académie des sciences. Série 2, Mécanique, Physique, Chimie, Sciences de l'univers, Sciences de la Terre*, 302(2), 91–96.
Marthaler, M., & Stampfli, G. M. (1989). Les Schistes lustrés à ophiolites de la nappe du Tsaté: Un ancien prisme d'accrétion issu de la marge active apulienne? *Schweizerische Mineralogische und Petrographische Mitteilungen, 69*, 211–216.
Mégard-Galli, J. (1972a). Le Norien dans la zone briançonnaise: Découverte d'un gisement fossilifère et considérations paléogéographiques. *Comptes Rendus de l'academie des Sciences de Paris, 287*, 899–902.
Mégard-Galli, J. (1972b). Données nouvelles sur le Carnien dans la zone briançonnaise entre Briançon et la vallée du Guil: Conséquences tectoniques et paléogéographiques. *Géologie Alpine, 48*, 131–142.
Mégard-Galli, J., & Baud, A. (1977). Le Trias moyen et supérieur des Alpes nord-occidentales et occidentales: Données nouvelles et corrélations stratigraphiques. *Bulletin du Bureau de Recherche Géologiques et Minières (BRGM), 2*(3), 233–250.
Merle, O., & Brun, J. P. (1984). The curved translation path of the Parpaillon Nappe (French Alps). *Journal of Structural Geology, 6*(6), 711–719.
Michard, A., Farah, A., Chabou, M. C., & Saddiqi, O. (2023). Extension of a passive margin coeval with subduction of the adjacent slab: The Western Alps and Maghrebides files. *BSGF-Earth Sciences Bulletin,* (in press).
Michard, A. (1967). *Etudes géologiques dans les zones internes des Alpes cottiennes*. CNRS édit.
Michard, A., Avigad, D., Goffé, B., & Chopin, C. (2004). The high-pressure metamorphic front of the south Western Alps (Ubaye–Maira transect, France, Italy). *Schweizerische Mineralogische und Petrographische Mitteilungen, 84*, 215–235.
Michard, A., & Henry, C. (1988). Les Nappes briançonnaises en Haute-Ubaye (Alpes franco-italiennes); contribution a la reconstitution paléogéographique du Briançonnais au Mésozoique. *Bulletin de la Société Géologique de France, 4*(4), 693–701.
Michard, A., Henry, C., & Chopin, C. (1993). Compression versus extension in the exhumation of the Dora-Maira coesite-bearing unit, Western Alps, Italy. *Tectonophysics, 221*(2), 173–193. https://doi.org/10.1016/0040-1951(93)90331-D
Michard, A., & Martinotti, G. (2002). The Eocene unconformity of the Briançonnais domain in the French—Italian Alps, revisited (Marguareis massif, Cuneo); a hint for a Late Cretaceous—Middle Eocene frontal bulge setting. *Geodinamica Acta, 15*(5), 289–301.
Michard, A., Schmid, S. M., Lahfid, A., Ballèvre, M., Manzotti, P., Chopin, C., Iaccarino, S., & Dana, D. (2022). The Maira-Sampeyre and Val Grana Allochthons (south Western Alps): Review and new data on the tectonometamorphic evolution of the Briançonnais distal margin. *Swiss Journal of Geosciences, 115*(1), 1–43. https://doi.org/10.1186/s00015-022-00419-8
Negro, F., Bousquet, R., Vils, F., Pellet, C. M., & Hänggi-Schaub, J. (2013). Thermal structure and metamorphic evolution of the Piemont-Ligurian

metasediments in the northern Western Alps. *Swiss Journal of Geosciences, 106*(1), 63–78.
Oberhänsli, R., Bousquet, R., Engi, M., et al. (2004). Metamorphic structure of the Alps. In: *Explanatory note to the map 'Metamorphic structure of the Alps'*. Commission for the Geological Map of the World, CCGM, Paris.
Pantet, A., Epard, J. L., & Masson, H. (2020). Mimicking Alpine thrusts by passive deformation of synsedimentary normal faults: A record of the Jurassic extension of the European margin (Mont Fort nappe, Pennine Alps). *Swiss Journal of Geosciences, 113*(1), 1–25. https://doi.org/10.1186/s00015-020-00366-2
Passchier, C. W., & Trouw, R. A. J. (2005). *Microtectonics* (p. 366). Springer. https://doi.org/10.1007/3-540-29359-0
Pfiffner, A. (2014). *Geology of the Alps*. Wiley-Blackwell.
Platt, J. P. (1986). Dynamics of orogenic wedges and the uplift of high-pressure metamorphic rocks. *Geological Society of America Bulletin, 97*(9), 1037–1053. https://doi.org/10.1130/0016-7606(1986)97%3c1037:DOOWAT%3e2.0.CO;2
Platt, J., Cunningham, P., Weston, P., Lister, G., Peel, F., Baudin, T., & Dondey, H. (1989). Thrusting and backthrusting in the Briançonnais domain of the western Alps. *Geological Society, London, Special Publications, 45*(1), 135–152.
Plunder, A., Agard, P., Dubacq, B., Chopin, C., & Bellanger, M. (2012). How continuous and precise is the record of P-T paths? Insights from combined thermobarometry and thermodynamic modelling into subduction dynamics (Schistes Lustrés, W. Alps). *Journal of Metamorphic Geology, 30*(3), 323–346.
Pognante, U. (1979). The Orsiera-Rocciavrè metaophiolitic complex (Italian western Alps). *Ofioliti, 4*, 183–198.
Ramsay, J. G. (1980). The crack–seal mechanism of rock deformation. *Nature, 284*(5752), 135–139.
Rubatto, D., & Hermann, J. (2001). Exhumation as fast as subduction? *Geology, 29*(1), 3–6.
Sandrone, R., Cadoppi, P., Sacchi, R., & Vialon, P. (1993). The dora-maira massif. In J. F. von Raumer & F. Neubauer (Eds.), *Pre-Mesozoic geology in the alps* (pp. 317–325). Springer. https://doi.org/10.1007/978-3-642-84640-3_18
Sanità, E., Di Rosa, M., Lardeaux, J. M., Marroni, M., & Pandolfi, L. (2022a). Metamorphic peak estimates of the Marguareis Unit (Briançonnais Domain): New constrains for the tectonic evolution of the southwestern Alps. *Terra Nova, 34*, 305–313. https://doi.org/10.1111/ter.12592
Sanità, E., Lardeaux, J. M., Marroni, M., & Pandolfi, L. (2022b). Kinematics of the Helminthoid Flysch–Marguareis Unit tectonic coupling: Consequences for the tectonic evolution of Western Ligurian Alps. *Comptes Rendus Géoscience, 354*(G1), 141–157. https://doi.org/10.5802/crgeos.124
Sartori, M., Gouffon, Y., & Marthaler, M. (2006). Harmonisation et définition des unités lithostratigraphiques briançonnaises dans les nappes penniques du Valais. *Eclogae Geologicae Helvetiae, 99*(3), 363–407.
Scheiber, T., Adrian Pfiffner, O., & Schreurs, G. (2013). Upper crustal deformation in continent-continent collision: A case study from the Bernard nappe complex (Valais, Switzerland). *Tectonics, 32*(5), 1320–1342.
Schmid, S. M., Casey, M., & Starkey, J. (1981). The microfabric of calcite tectonites from the Helvetic Nappes (Swiss Alps). *Geological Society, London, Special Publications, 9*(1), 151–158.
Schmid, S. M., Fügenschuh, B., Kissling, E., & Schuster, R. (2004). Tectonic map and over-all architecture of the Alpine orogen. *Eclogae Geologicae Helvetiae, 97*(1), 93–117. https://doi.org/10.1007/s00015-004-1113-x
Schmid, S. M., & Kissling, E. (2000). The arc of the western Alps in the light of geophysical data on deep crustal structure. *Tectonics, 19*(1), 62–85.
Schmid, S. M., Kissling, E., Dichl, T., van Hinsbergen, D. J., & Molli, G. (2017). Ivrea mantle wedge, arc of the Western Alps, and kinematic. *Swiss Journal of Geoscience, 110*, 581–612. https://doi.org/10.1007/s00015-016-0237-0
Schmid, S. M., Panozzo, R., & Bauer, S. (1987). Simple shear experiments on calcite rocks: Rheology and microfabric. *Journal of Structural Geology, 9*(5–6), 747–778.
Schwartz, S., Guillot, S., Reynard, B., Lafay, R., Debret, B., Nicollet, C., Lanari, P., & Auzende, A.-L. (2013). Pressure–temperature estimates of the lizardite/antigorite transition in high pressure serpentinites. *Lithos, 178*, 197–210.
Schwartz, S., Lardeaux, J. M., & Tricart, P. (2000). La zone d'Acceglio (Alpes cottiennes): Un nouvel exemple de croûte continentale éclogitisée dans les Alpes occidentales. *Comptes Rendus de l'académie des Sciences-Series IIA-Earth and Planetary Science, 330*(12), 859–866.
Schwartz, S., Lardeaux, J. M., Tricart, P., Guillot, S., & Labrin, E. (2007). Diachronous exhumation of HP–LT metamorphic rocks from south-western Alps: Evidence from fission-track analysis. *Terra Nova, 19*(2), 133–140.
Seyrig, N. (1972). *Etude géologique des massifs Rocciavre-Orsiera (Alpes piémontaises; sud du val de Susa)* (Doctoral dissertation, Université Scientifique et Médicale de Grenoble).
Simon-Labric, T., Rolland, Y., Dumont, T., Heymes, T., Authemayou, C., Corsini, M., & Fornari, M. (2009). 40Ar/39Ar dating of Penninic Front tectonic displacement (W Alps) during the Lower Oligocene (31–34 Ma). *Terra Nova, 21*(2), 127–136.
Stampfli, G. M. (1993). Le Briançonnais, terrain exotique dans les Alpes? *Eclogae Geologicae Helvetiae, 86*(1), 1–45.
Stampfli, G. M., Mosar, J., Marquer, D., Marchant, R., Baudin, T., & Borel, G. (1998). Sub-duction and obduction processes in the Swiss Alps. *Tectonophysics, 296*(1–2), 159–204.
Steck, A., Masson, H., & Robyr, M. (2015). Tectonics of the Monte Rosa and surrounding nappes (Switzerland and Italy): Tertiary phases of subduction, thrusting and folding in the Pennine Alps. *Swiss Journal of Geosciences, 108*(1), 3–34. https://doi.org/10.1007/s00015-015-0188-x
Stipp, M., & Kunze, K. (2008). Dynamic recrystallization near the brittle-plastic transition in naturally and experimentally deformed quartz aggregates. *Tectonophysics, 448*(1–4), 77–97.
Stipp, M., Stunitz, H., Heilbronner, R., & Schmid, S. (2002a). Dynamic recrystallization of quartz: Correlation between natural and experimental conditions. *Geological Society, London, Special Publications, 2001*(1), 171–190. https://doi.org/10.1144/GSL.SP.2001.200.01.11
Stipp, M., Stunitz, H., Heilbronner, R., & Schmid, S. M. (2002b). The eastern Tonale fault zone: A 'natural laboratory'for crystal plastic deformation of quartz over a temperature range from 250 to 700 C. *Journal of Structural Geology, 24*(12), 1861–1884. https://doi.org/10.1016/S0191-8141(02)00035-4
Sue, C., Delacou, B., Champagnac, J. D., Allanic, C., Tricart, P., & Burkhard, M. (2007). Extensional neotectonics around the bend of the Western/Central Alps: An overview. *International Journal of Earth Sciences, 96*, 1101–1129.
Sue, C., & Tricart, P. (2003). Neogene to ongoing normal faulting in the inner western Alps: a major evolution of the late alpine tectonics. *Tectonics, 22*(5).
Tavani, S., Bertok, C., Granado, P., Piana, F., Salas, R., Vigna, B., & Muñoz, J. A. (2018). The Iberia-Eurasia plate boundary east of the Pyrenees. *Earth-Science Reviews, 187*, 314–337. https://doi.org/10.1016/j.earscirev.2018.10.008
Thélin, P., Sartori, M., Burri, M., Gouffon, Y., & Chessex, R. (1993). The pre-Alpine basement of the briançonnais (Wallis, Switzerland). In J. F. von Raumer & F. Neubauer (Eds.), *Pre-mesozoic geology in the alps* (pp. 297–315). Springer.
Thomas, J. C., Claudel, M. E., Collombet, M., Tricart, P., Chauvin, A., & Dumont, T. (1999). First paleomagnetic data from the sedimentary cover of the French Penninic Alps: Evidence for Tertiary counterclockwise rotations in the Western Alps. *Earth and Planetary Science Letters, 171*(4), 561–574.
Tissot, B. (1955). Etudes geologiques des massifs du Grand Galibier et des Cerces (zone brianconnaise, Hautes-Alpes et Savoie). *Géologie Alpine, 32*, 111–193.
Tricart, P. (1980). *Tectoniques superposées dans les Alpes occidentales, au sud du Pelvoux: évolution structurale d'une chaîne de collision*. PhD Thesis. Université Louis Pasteur-Strasbourg I.
Tricart, P. (1984). From passive margin to continental collision; a tectonic scenario for the Western Alps. *American Journal of Science, 284*(2), 97–120.
Tricart, P., Bourbon, M., Chenet, P., Cros, P., De Lorme, M., Dumont, T., de Graciansky, P. C., Lemoine, M., Megard-Galli, J., & Richez, M. (1988). Tectonique synsédimentaire triasico-jurassique et rifting téthysien dans la nappe briançonnaise de Peyre-Haute (Alpes occidentales). *Bulletin de la Société Géologique de France, 4*, 669–680. https://doi.org/10.2113/gssgfbull.IV.4.669
Tricart, P., & Schwartz, S. (2003). *Notice explicative, Carte géologique. France (1/50 000), feuille Aiguilles-Col Saint-Martin (848)*. BRGM.
Tricart, P., & Schwartz, S. (2006). A north-south section across the Queyras Schistes lustrés (Piedmont zone, Western Alps): Syn-collision refolding of a subduction wedge. *Eclogae Geologicae Helvetiae, 9*, 429–442. https://doi.org/10.1007/s00015-006-1197-6

Tricart, P., & Sue, C. (2006). Faulted backfold versus reactivated backthrust: The role of inherited structures during late extension in the frontal Piémont nappes east of Pelvoux (Western Alps). *International Journal of Earth Sciences, 95*(5), 827–840. https://doi.org/10.1007/s00531-006-0074-x

Van Hinsbergen, D. J., Torsvik, T. H., Schmid, S. M., Maţenco, L. C., Maffione, M., Vissers, R. L., Gurer, D., & Spakman, W. (2020). Orogenic architecture of the Mediterranean region and kinematic reconstruction of its tectonic evolution since the Triassic. *Gondwana Research, 81*, 79–229.

Van Hinsbergen, D. J., Vissers, R. L., & Spakman, W. (2014). Origin and consequences of western Mediterranean subduction, rollback, and slab segmentation. *Tectonics, 33*(4), 393–419.

Vialon, P. (1966). *Etude géologique du massif cristallin Dora-Maira: Alpes cottiennes internes: Italie.* PhD Thesis. Université de Grenoble.

Whitney, D. L., & Evans, B. W. (2010). Abbreviations for names of rock-forming minerals. *American Mineralogist, 95*, 185–187. https://doi.org/10.2138/am.2010.3371

Whitney, D. L., Teyssier, C., Seaton, N., & Fornash, K. (2014). Petrofabrics of high-pressure rocks exhumed at the slab-mantle interface from the "point of no return" in a subduction zone (Sivrihisar, Turkey). *Tectonics, 33*(12), 2315–2341. https://doi.org/10.1002/2014TC003677

Xiong, J. W., Chen, Y. X., Zhou, K., Schertl, H. P., Zheng, Y. F., Huang, F., Xia, X. P., & Chen, Z. W. (2021). Fe and O isotopes in coesite-bearing jadeite quartzite from the Western Alps record multistage fluid-rock interactions in a continental subduction zone. *Geochimica et Cosmochimica Acta, 312*, 1–24.

Publisher's Note